# STUDIES ON THE DYNAMICS AND OPERATION OF INTEGRATED PLANTS

**by**

**John Morud**

A Thesis Submitted for the Degree of Dr. Ing.

University of Trondheim

The Norwegian Institute of Technology

Submitted December 1995

# ABSTRACT

As chemical process plants become more efficient, they tend to become more tightly integrated; for example, raw materials are recycled and hot process streams are heat exchanged with cold process streams. This integration introduces tight couplings between processing units, which in some cases may make the dynamic and steady state behavior of the plant more complex, and lead to plants which are more difficult to operate and control.

This thesis is concerned with different aspects of dynamics and operation of integrated plants. Specifically, the following topics are treated:

- The effects of the interconnection structure of the plant flowsheet on the dynamic behavior and controllability of the plant. By analogy to Linear Systems Theory, the relation between the plant flowsheet structure and the dynamic behavior of the plant is discussed.

- The dynamic behavior of process units. By analogy to Linear Systems Theory, it is argued how couplings between phenomena within a process unit affect the dynamic behavior of that unit.

- The dynamic behavior of cascade processes. Many chemical engineering systems, such as the countercurrent separation processes, consist of many subsystems (trays) interconnected in a cascade like manner. The relation between the subsystem dynamics and the overall system behavior is analyzed.

- The effect of feed-effluent preheating on the stability of an industrial fixed-bed ammonia synthesis reactor. A fixed bed ammonia synthesis reactor in Germany, which became unstable in 1991, is examined. It is shown that the reactor may exhibit limit cycle behavior (oscillations) at certain operating points. During such limit cycle behavior, the reactor temperatures oscillate with amplitudes up to $160^{o}C$, which is large enough to pose a potential threat to the reactor.

- The effects of strong integration of distillation columns on their steady state behavior. A distillation column arrangement known as the Petlyuk column is analyzed. This column arrangement is known to have a strange steady state behavior, with multiple steady states and "holes" in the operating range, i.e. regions where no steady states exist. Using a combination of physical and geometrical arguments, this strange steady state behavior is explained.

- Optimizing control of process plants. A topic concerning hierarchical optimizing control systems is discussed; specifically, the choice of controlled outputs at the regulatory control level a plant. It is discussed how one can choose controlled outputs, whose optimal set points are as insensitive as possible to disturbances at steady state.

# ACKNOWLEDGEMENTS

I would like to thank my supervisor Sigurd Skogestad for excellent help during my four year Dr.ing.-study. His insights in Linear Systems Theory as well as his knowledge in oral and written communication has been invaluable.

I would also like to thank my fellow Dr.ing.-students during my stay here in Trondheim; in particular Håvard Moe and Sverre Støren for many fruitful discussions, and for their enthusiasm and willingness to organize social as well as technical activities. Thanks also to the students of the process control group for making my stay here at NTH a good time; especially Pål Flatby for many technical–as well as nontechnical–discussions.

Last, but not least, I would like to thank Elin Bø for many things that has no relation to the work in this thesis.

Financial support from the Research Council of Norway (NFR) is gratefully acknowledged.

# Contents

# Chapter 1

# Introduction

## 1.1 Motivation

As chemical processing plants become more efficient, they tend to become more tightly integrated; raw materials are recycled and hot process streams are heat exchanged with cold process streams. In this manner, resources are used more economically.

However, tight integration may lead to plants with a more complex dynamic and steady state behavior, and lead to plants which are more difficult to operate and control. A few decades ago, many plants could be thought of as composed of essentially independent processing units, and their behavior could be predicted from the behavior of the processing units individually. As integration become tighter, the behavior of the plant is modified, and may become very different from what could be expected by looking at the individual processing units by themselves. Integration may thus in some cases lead to instability, poor controllability or qualitative changes in dynamic behavior—introducing new steady states, limit cycles or even chaotic behavior. Thus, there is an incentive for investigating the effects of integration on plant behavior and operation.

Such investigations may be performed in various ways, ranging from the study of specific cases to the formulation of general theories. Studies of specific cases are performed by many authors (e.g. Luyben, 1992), and have the advantage that it is possible to examine quite realistic situations. Thus, case studies yield valuable input to more general investigations, which usually are more simplistic, and therefore need to be supported by such case studies. In addition, case studies give valuable inspiration for the formulation of general theories. The back side of the coin is that case studies have a limited scope, which means that their results are not general.

General investigations have a much broader scope, which increases their range of applicability. Unfortunately, there is a price to be paid for larger generality. As many chemical process plants are nonlinear, they may exhibit behavior that is in a sense unique; that is, a result of a specific combinations of nonlinearities. Thus, in order to

obtain general results, one has to disregard the unique aspects of individual cases, and focus on what they have in common. Thus, general results are in a sense incomplete when applied to nonlinear plants. However, this is not to say that general results are useless, but rather that their application has to be supported by more detailed investigations when applied to specific cases.

This thesis adopts the view that case studies and general theories complement each other; that there is a need for both. Thus, if one is to investigate, say, the possibility of limit cycle behavior in a specific plant—or in a specific class of plants—it would often be difficult, and a waste of resources, to make rigorous models of the plant and to do numerous numerical simulations. Without any *a priori* idea of where to look, this is like finding the needle in the haystack. Rather, it seems reasonable to use more general considerations and insights in order to provide plausible candidates, which can then be analyzed in more detail by more rigorous methods, such as bifurcation analysis or numerical simulations. Work in this thesis range from general considerations of the effects of the plant flowsheet structure on the dynamics and controllability of the plant, to the investigation of specific cases where such effects are in action.

## 1.2 Relations to other work

The purpose of this section is to put the thesis into perspective and to relate it to other work.

The main theme of the thesis is about the effects of couplings between process units—or between parts of such units—on the dynamic and steady state behavior of the overall system. In addition, the effects of such couplings on plant controllability is considered. When talking about couplings between units, we refer to the way the units are interconnected; for instant, unreacted reactant from a reactor may be recycled in order to be reprocessed, or heat in the effluent stream from the reactor may be used to heat the feed stream. The question is thus how such couplings affect the plant behavior.

The basic ideas in the thesis are inspired by the work of Gilliland *et al.* (1964) who studied the effects of material recycle on the dynamic behavior of a reactor/separator system. They found that the plant with recycle had a much slower behavior than any of its parts, and that the recycle led to a system that was very sensitive at steady state; for example, small changes in feed conditions could cause large changes in the state of the system. Moreover, in some cases, the recycle could lead to plant instability, even though the reactor and the separator were stable by themselves.

Such behavior seems to be very common in systems with recycle of mass and energy. These systems often tend to be very slow when there is much recycling, and to be sensitive to slow disturbances (e.g. Denn and Lavie 1982). However, as will be seen in later chapters, this is not always the case; sometimes the recycle causes other types of behavior, such as multiple steady states or oscillatory (limit cycle) behavior. Such behavior has been observed by previous authors; a recent example is the work by Recke and Jørgensen (1994).

## 1.3 Thesis overview

The thesis consists of seven independent articles, which may be read independently. The chapter sequence for the first six articles is organized from the general to the specific, starting from general considerations on the effects of plant flowsheet structure on the dynamic behavior of the plant, and ending with the analysis of specific cases. The last article is concerned with control aspects; specifically, with the choice of controlled outputs at the regulatory control level.

**Chapter 2** discusses the effects of the plant interconnection structure on the plant dynamics, using concepts from Linear Systems Theory. Such concepts are, for example, **feedback** and **parallel paths** in the plant. The basic idea is to extract some information about possible dynamic behavior by looking at the structure of the process flowsheet. Such information may provide input for more detailed studies of the plant—using more rigorous methods, such as bifurcation analysis or simulation studies.

Whereas Chapter 2 has its focus on the overall plant, **chapter 3** has its focus on the individual process units. The effects of the **internal** structure of the process units on their dynamics is examined—still borrowing concepts from Linear Systems Theory. An attempt is made to classify the effects of physical phenomena on the behavior of the processing units. The classification is far from exhaustive and is restricted to simple first order dynamics.

In **chapter 4** we study the dynamics of cascade processes. Examples of such processes could be distillation or other countercurrent separation processes, but could also be other systems consisting of similar subsystems placed after one another. A main topic in the chapter is the slow behavior often observed in such systems; in particular in high purity distillation columns. By using Laplace transform techniques, we show how the simplest case—scalar cascades of identical subsystems—may be analyzed.

In **chapter 5**, we still consider cascade processes. Specifically, we study the concentration dynamics of binary distillation columns. However, whereas the analysis in the previous chapter is performed by means of Laplace transform techniques, the approach in this chapter is by analogy to diffusion in plug flow. Using concepts from the analogy, we explain qualitatively how the column behaves.

In **chapter 6** a case is investigated in more detail. An industrial fixed bed ammonia synthesis reactor in Germany, which became unstable in 1991, is examined. The system is modeled using a simple system of partial differential equations based on mass and energy balances. The analysis shows that the system may undergo a Hopf bifurcation and enter a stable limit cycle for a certain change in operating parameters. The limit cycle behavior of the model is consistent with what has been observed in the industrial plant.

In **chapter 7** complex steady state behavior of an integrated distillation arrangement known as the Petlyuk column is analyzed in considerable detail. This complex steady state behavior may be interpreted using the same concepts as used for interpreting dynamic behavior in previous chapters, most notably the concept of **parallel** or **competing** effects. The incentive for studying Petlyuk columns is that they have the potential of combining low investment costs with low energy consumption. However, the energy savings are dependent upon proper operation of the column—possibly by

using some sort of optimizing control schemes in order to minimize energy consumption.

**Chapter 8** discusses optimizing control of process plants. Specifically, we study the choice of controlled outputs at the regulatory control level. The basic idea is to select controlled outputs in such a way that their optimal set points are as insensitive as possible to disturbances entering the process.

**Chapter 9** contains a discussion and conclusion and tries to point out some possible directions for further work.

Preliminary versions of the chapters have been presented at the following conferences:

| | |
|---|---|
| Chapter 2: | PSE'94, Kyongju, Korea, May 30-June3 1994 (Proceedings, p. 913-918) |
| Chapter 3: | Escape-3, Graz, Austria, July 5-7 1993 (Comp. Chem. Eng. Suppl. S529-534) |
| Chapter 4 and 5: | AIChE Annual Meeting, Miami Beach, USA, Nov. 12-17 1995 (Paper 189b) |
| Chapter 6: | AIChE Annual Meeting, St. Louis, USA, Nov. 1993 (Paper 26e) |
| | European Control Conference, ECC95, Rome, Sept. 5-8 1995 (session TM-8) |
| Chapter 7: | AIChE Annual Meeting, San Francisco, USA, Nov. 13-18 1994 (Paper 131d) |

# References

[1] Denn, M.M. and Lavie, R. (1982). Dynamics of Plants with Recycle. The Chem. Eng. J., 24, pp 55-59.

[2] Gilliland, E.R., Gould, L.A. and Boyle, T.J. (1964). Dynamic effects of material recycle. Preprints JACC, Stanford, California pp 140-146.

[3] Luyben, W.L. (1992) Dynamics and Control of Recycle Systems. Part 2 - Comparison of Alternative Process Designs. Paper submitted to IEC Research.

[4] Recke, B. and S. B. Jorgensen (1994). Bifurcations in Fixed Bed Reactors as a Consequence of Recycle. Presented at AIChE Annual Meeting 1994, Area 1b, San Francisco, USA, Nov. 13-18, 1994.

# Chapter 2

# The Dynamic Behavior of Integrated Plants

John Morud and Sigurd Skogestad*
Chemical Engineering
University of Trondheim - NTH
N-7034 Trondheim, Norway

Presented at
PSE'94, Kyongju, Korea, May 30-June 3 1994

**Abstract**

The effect of material recycle and heat integration on the dynamics and control of chemical processing plants is considered. In analogy to linear control theory, one may consider how plant interconnections affect the fundamental properties of the dynamics, such as the poles and zeros. This implies that recycle of mass and energy, which are feedback mechanisms, affect the poles and thus possibly the plant stability, whereas parallel interconnections in a plant affect the zeros and thus the achievable performance of the plant under feedback control.

*Address correspondence to this author. Fax: 47-73594080, E-mail: skoge@kjemi.unit.no

## 2.1 Introduction

It is known that the overall dynamics of chemical processing plants with material recycle or heat integration can be very different from the dynamics of the individual processing units (e.g. Gilliland *et al.*,1964, Denn and Lavie, 1982). Material recycle and heat integration may dramatically alter the time constants of the plant, and may give rise to instability or oscillatory behavior (limit cycles), even when the individual processing units are stable by themselves. Moreover, plant interconnections may introduce fundamental limitations in the achievable performance of any control system. The knowledge of such phenomena is important for controller design, and their effects may even pose a threat to plant safety if not foreseen.

Unfortunately, even with a model of the system in terms of its nonlinear differential equations, the analysis of the possible behavior of the system is very difficult. Although there exist mathematical tools such as bifurcation analysis, which in principle could be used to analyze a plant, the systems of equations describing whole plants are so large that a complete analysis by such tools is impractical if not impossible. Moreover, even if such an analysis were possible, there would still be a need for some "rules of thumb", or indicators, which could be used to warn us when complex behavior is plausible.

The main problem at hand is that even though we may have a thorough understanding of the dynamic behavior of the individual units, it may be extremely difficult to predict the behavior, even qualitatively, of an interconnected system. A well-known example is a distillation column which in most cases is well modelled as a number of interconnected flash tanks. Even though we may easily predict the response of the individual subsystems (the flash tanks), it is very difficult to predict the response of the overall system (the column).

The main reason for the change in behavior is the recycle of vapor and liquid (reflux). The strong effect recycle (feedback) may have on the dynamic response of a system is not appreciated by most engineers. In addition, for distillation columns the vapor-liquid relationship is nonlinear, and for persons familiar with nonlinear dynamics it is well known that this combination of nonlinearity and feedback may lead to very complex dynamic behavior. For example, a simple nonlinear function, $y = u \cdot (1 - u)$, may when combined with dynamic feedback, for example, a simple gain and delay, $u(t) = k \cdot y(t-1)$, yield a very complicated dynamic response, including chaos (try $k = 3.7$ with initial value $y(0) \in < 0, 1 >$, see e.g. Seydel 1988). For linear systems the effects are not quite as drastic, although small changes in the feedback gain can also in this case drastically change the characteristics of the response.

In most cases recycle leads to *positive feedback* effects. For example, increasing the concentration of a chemical species in a process stream will normally increase the amount of this species in the recycle streams, and thus lead to a reinforcement of the original increase. In other words, there is a self-reinforcing mechanism associated with the recycle. This positive feedback will usually increase the plant time constant, and also increase the sensitivity to slow disturbances. This is because recycle will tend to "store" material or energy within some part of the plant. An example is high purity distillation columns, where extremely long time constants have been observed (e.g., Kapoor *et al*, -86).

From a linear systems point of view, the increased time constant corresponds to a pole (system eigenvalue) being moved closer to the origin in the complex plane (approaching a pure integrator). In some cases the positive feedback may move the pole past the origin and yield instability. One example is for distillation columns where the use of mass reflux may lead to instability in some cases (Jacobsen and Skogestad, 1991, 1994). In other cases positive feedback may result in limit cycle behavior. One example is the ammonia synthesis reactor with energy recycle studied by Morud and Skogestad (1993). Finally, it should be noted that there are a few cases where recycle may yield negative feedback. All of these issues are discussed in more detail in the paper.

General work in the area of the dynamics of integrated plants is rather scarce even though issues like the effect of energy integration on reactor stability were discussed as early as 1953 by van Heerden (1953). Aris and Amundson (1957) analyzed the effect of feedback (control) on the dynamic characteristics of the continuous stirred tank reactor. Gilliland *et al.* (1964) studied the now classic example of a reactor connected to a distillation column with total recycle of the column bottom product. They reported an increased sensitivity of the plant to feed disturbances compared to the case without recycle, and that the plant may become unstable even though the reactor itself is stable. Denn and Lavie (1982) argued that a recycle system may be considered analoguous to a closed loop feedback control system with positive feedback. Hence, recycle may increase the overall response time of the plant and make the steady state gain large. They also considered the effect of time delays in the recycle path on plant dynamics. Other related work that may be mentioned is Verykios and Luyben (1978), Luyben (1992), Papadourakis *et al.* (1987, 1989), and Uppal and Ray (1974).

The main objective of this paper is to obtain qualitative insight into what dynamic behavior can be expected for processing systems, and in particular to gain insight into the effect of various plant interconnections. For a given plant such insight can then provide a starting point for a more detailed analysis. Most of our analysis is based on linear systems theory, as this theory is well developed, and because it is difficult to obtain general results for nonlinear systems.

## 2.2 Classification of Interconnections

An interconnection refers to the way the subsystems are interconnected to form the overall system. We shall classify interconnections into external or internal interconnections, and into feedback, parallel or series interconnections.

**External interconnections**. In this case the subsystems are the individual processing units, and the term external interconnections refers to how these subsystems are connected together, that is, it refers to the structure of process flowsheet. One very important interconnection of units is *recycle*. A recycle loop may be due to mass recycling, but may also in a more general sense be due to heat recycling, for example, when a reactor feed is preheated by the reactor effluent. Other common ways to arrange units, are in series and in parallel.

**Internal interconnections**. This is a somewhat more loosely defined concept. The "subsystems" in this case usually refer to the dynamics of important state variables, such as the temperature dynamics (energy balance), the component dynamics (mass balance) and the pressure dynamics (momentum balance). The interconnection then refers to the coupling between these variables (balances). The term "internal" is used because these couplings occur inside the individual processing units.

A given interconnection, be it external or internal, may be subdivided into the following three broad classes:

1. **Feedback**. A recycle loop is a special case of feedback, but the term "feedback" is often used for dynamical systems in a more general sense to include any secondary effect that modifies the original dynamic change, and includes also "internal" feedbacks within the units. For example, in some cases a dynamic model of a unit may be formulated as

$$\frac{dy}{dt} = g(y,u) + f_1(y) + f_2(y) + \cdots \tag{2.1}$$

Here, $f_1(y), f_2(y), \ldots$ may be thought of as feedback effects modifying the "original" behavior given by $\frac{dy}{dt} = g(y,u)$. If $a_i = \partial f_i/\partial y$ is positive (negative), then the feedback for effect $i$ is positive (negative).

2. **Parallel paths (Feedforward)**. Two processing units in parallel is a special case of a parallel interconnection. However, here the term "parallel path" is used in a general sense to include any system where an input affects an output through several independent subsystems or mechanisms. One specific example is the following system:

$$\frac{dy_1}{dt} = g_1(y_1,u) \tag{2.2}$$

$$\frac{dy_2}{dt} = g_2(y_2,u) \tag{2.3}$$

$$y = f(y_1,y_2) \tag{2.4}$$

Often the effect of the various subsystems $(g_1, g_2, \ldots)$ on the output, $y$, have different signs, in which case they are denoted *competing effects*. This is important as it may yield unstable zero dynamics, corresponding to inverse responses for linear systems.

3. **Series interconnections**. By a series interconnection of subsystems we mean that the output of one subsystem is the input to the next, that is, there is a one-way flow without feedback between subsystems. One example is the following system

$$\frac{dy_1}{dt} = g_1(y_1,u) \tag{2.5}$$

$$\frac{dy}{dt} = g_2(y,y_1) \tag{2.6}$$

An example could be processing units in series, but in general we would allow series connections of any concrete or abstract systems, not only processing units.

**Remarks**

1. As already mentioned, feedback may drastically change the dynamics of the system as compared to that of the subsystems. This is because feedback moves the poles of the system, and may, for example, yield instability.

2. Parallel interconnections do not generally yield responses which in themselves are drastically different from those of the subsystems. However, the presence of competing effects may lead to inverse responses and unstable zero dynamics (RHP-zeros in the linear case), which may lead to instability when feedback is applied to the system (for example, feedback control).

3. Series interconnections often yield responses that may be well predicted from those of the subsystems. It is therefore usually the simplest interconnection from a system point of view.

4. In many cases the responses within a unit may be described well by considering several "internal" parallel paths. For example, changing a valve position may at the same time change the pressure (and thus flowrate), temperature and concentration at that location. The effect of the change in these three variables will propagate downstream with different speeds in a parallel manner (often pressure effects are the fastest and temperature effects the slowest). In this sense, we may also get parallel paths through processing units in series. In some cases these effects may be competing and very complex dynamic behavior may be observed when feedback is applied to the unit.

These issues are discussed in detail for linear systems below, and are illustrated with process examples in subsequent sections.

## 2.3 Linear systems

For small deviations from the steady state, a processing unit may be well described by a linear transfer function. Before attacking the nonlinear complexities of a plant, it is therefore reasonable to review some basic results from linear systems theory.

The dynamic behavior of a linear system is determined by its poles and zeros. For an uncontrolled system, the poles are the main issue, as they determine the stability of the plant (The plant is stable if and only if all the poles are in the complex left half plane).

However, plant instability may not necessarily be a problem, since an unstable process may be stabilized by feedback control. Essentially, control involves finding a way of inverting the process: one specifies the plant output, $y$, and the controller computes the necessary input, $u$, which (approximately) achieves this. With feedback control, as the bandwidth increases, the transfer function from the reference to the

plant input approaches the inverse of the plant. This means that right half plane zeros in a plant would eventually end up as unstable poles in the closed loop system if the bandwidth were too high. Right half plane zeros in a plant therefore pose an upper limit to the achievable performance of any control system.

An important issue is therefore to understand how the poles and zeros of a plant are affected by plant integration. Here our insight from linear systems proves useful: Poles are changed by feedback, which in a processing plant will correspond to mechanisms that recycle mass or energy. On the other hand, zeros are changed or added by parallel interconnections.

We elaborate the effect of *feedback*, *parallel* and *series* interconnections for scalar linear systems to illustrate their effect.

**Feedback interconnection**. Consider a plant described by $y = g(s)u$ where $u$ and $y$ are the plant input and output respectively. Assume there is a feedback mechanism $k(s)$ as illustrated in Figure 2.1, such that $u = k(s)y + r$. The poles of the system are then the roots of $1 - g(s)k(s)$. The steady-state behavior is found by setting $s = 0$. We distinguish between the following two cases:

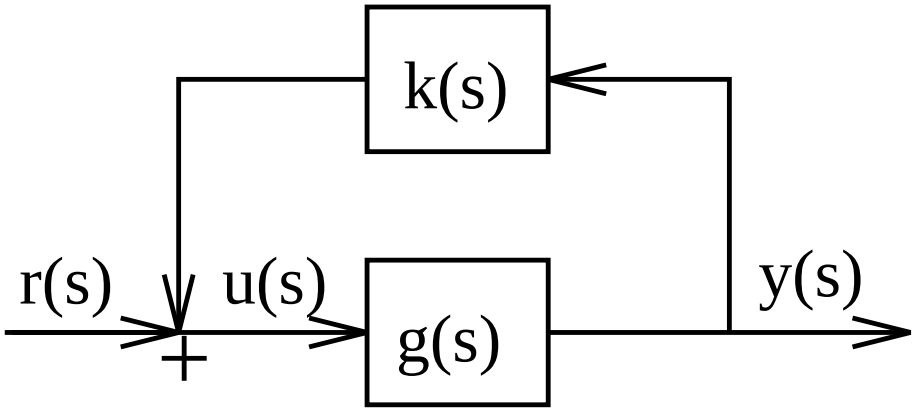


Figure 2.1: Feedback interconnection

*Case 1.* $g(0)k(0) < 0$ *(negative feedback).* This is the most common case in feedback control, but it is less likely to occur for a recycle loop. If the magnitude of the loop gain, $g(0)k(0)$, is increased, this will eventually yield instability where a pair of complex conjugate poles cross the imaginary axis (as long as there is at least $180^0$ phase lag in $g(j\omega)k(j\omega)$ at high frequencies, $\omega$).

*Case 2.* $g(0)k(0) > 0$ *(positive feedback).* If $k(0)$ is varied from zero towards $1/g(0)$, $1 - g(0)k(0)$ approaches zero. This means that a pole goes through the origin as $k(0)$ passes $1/g(0)$. A pole near the origin means that the response of the plant is slow and that the sensitivity to slow disturbances is high.

As the gain, $|k(0)|$, is increased, the zeros of the loop gain $g(s)k(s)$ attract system poles. It should be noted that because of this, complex conjugate poles may cross the imaginary axis for values of $k(0)$ less than $1/g(0)$. One specific example is an industrial fixed bed ammonia synthesis reactor studied by Morud and Skogestad (1993). In the ammonia synthesis case, complex conjugate poles approaching Right Half Plane zeros

of the reactor transfer function crossed the imaginary axis for a loop gain $g(0)k(0)$ less than one (Hopf bifurcation). This made the reactor enter a stable limit cycle. Thus, it is not always true that positive feedback leads to slow responses and high sensitivity to disturbances, it may just as well lead to e.g. limit cycle behavior. For this to happen, two conditions must be met. First, there must be at least $360^0$ phase lag in $g(j\omega)k(j\omega)$ at high frequencies. Second, the magnitude of the loop gain $|g(j\omega_{360})k(j\omega_{360})|$ at the critical frequency $\omega_{360}$ where this happens must be larger than the loop gain at steady state $g(0)k(0)$.

While the feedback, $k(s)$, moves the plant poles, it does not affect the zeros of $g(s)$, and may only introduce new zeros at the locations of the poles of $k(s)$. To see this, assume $g$ and $k$ to be rational, i.e. that they may be written as $g(s) = \frac{n_g(s)}{d_g(s)}$ and $k(s) = \frac{n_k(s)}{d_k(s)}$ where $n_g$, $n_k$, $d_g$ and $d_k$ are polynomials in $s$. This gives an expression for the transfer function from $r$ to $y$ (Fig. 2.1):

$$y = \frac{g}{1 - gk} r = \frac{d_k n_g}{d_k d_g - n_k n_g} r \tag{2.7}$$

The zeros of the closed loop system thus consist of the poles of $k(s)$ and the zeros of $g(s)$. As long as k(s) is stable (i.e. $d_k$ does not have roots in the right half plane), the closed loop system has the same right half plane zeros as $g(s)$.

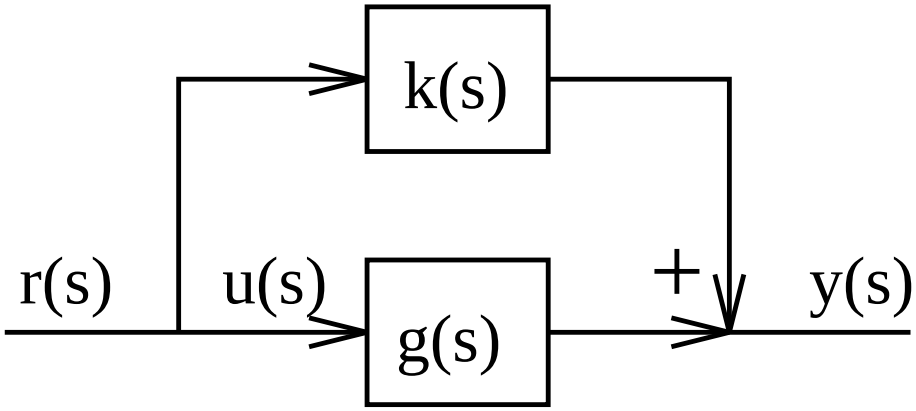


Figure 2.2: Parallel interconnection

**Parallel interconnection**. Now consider parallel interconnection of two transfer functions, as shown in Fig 2.2. For rational transfer functions, the overall transfer function from $r$ to $y$ becomes:

$$y = (g + k)r = (\frac{n_g}{d_g} + \frac{n_k}{d_k})r = \frac{n_g d_k + n_k d_g}{d_g d_k} r \tag{2.8}$$

As can be seen, the poles are the poles of $g$ and $k$, while the zeros are changed.

Right half plane zeros (often denoted "unstable zeros", since the inverse is unstable) are often associated with *competing effects*, i.e. when $g(s)$ and $k(s)$ have opposite effects on the output $y$. In terms of time responses, right half plane zeros cause an inverse

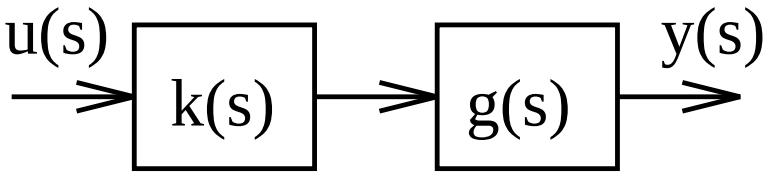


Figure 2.3: Series interconnection

response (undershoot) in the step response. Left Half Plane zeros close to the origin yield large overshoots in the step response.

**Series interconnection**. The series interconnection is shown in Fig 2.3. The overall transfer function becomes:

$$y = g(s)k(s)u \tag{2.9}$$

The poles and zeros of the combined transfer function, $g(s)k(s)$, are the poles and zeros of the individual transfer functions, $g(s)$, and $k(s)$. Thus there are really no surprises. Note however, that right half plane zeros may yield a peak in the frequency response and at the same time yield a large phase lag. In a series connection of a large number of transfer functions with Right Half Plane zeros (think of a distributed parameter system) there may therefore be peaks at very large phase lags.

In summary, feedback effects move poles, which affect the plant time constants and determine its stability, while parallel paths change or add zeros, which affect the plant behavior under feedback, whether it be a controller or feedback due to a recycle loop.

With the linear theory in mind, we now turn to the plant, and give some examples to illustrate the effect of interconnections on the dynamic behavior of plants. We will discuss separately the effects of feedback and parallel paths in integrated plants.

## 2.4 Models used for the examples

In the examples we make use of some very simple models to illustrate the dynamics. Since they are used repeatedly, we have given the models a unified treatment in the Appendix. Here, we only present their essential features. For numerical calculations we have used standard MATLAB functions (ode45, rlocus) with numerical values as listed in the Appendix.

**The CSTR**. The CSTR model used has constant molar holdup and at most three chemical species, $A, B, C$. The reaction is a simple reaction $A \rightarrow B$ (or $B \rightarrow C$) of the Arrhenius type. We allow the presence of a catalyst in the reactor, yielding a larger time constant for the energy balance than for the mass balance. For simplicity we have assumed constant heat capacities of the fluid and the catalyst.

**Heat exchanger without dynamics**. The model used is a standard $\epsilon$-NTU model with no dynamics. For constant flow rates this reduces to a linear relation between inlet and outlet temperatures when the fluid heat capacity is assumed to be a constant.

Cases involving dynamic heat exchanger models are taken from the thesis by Mathiesen (1994).

**The perfect separation unit**. The perfect separation unit with no dynamics splits a mixture of components A, B, C into pure B at the bottom and a mixture of A and C at the top.

## 2.5 Examples of recycle causing positive feedback

Material recycle and heat integration in plants usually lead to *positive feedback*. We therefore present some examples to illustrate their effects on plant dynamics.

### Example 1 Material recycle

Consider the somewhat simplified system shown in Fig 2.4a, consisting of a mixer, an isothermal continuous stirred tank reactor (CSTR) and a separation unit. There are two feed streams to the mixer, $F$ and $R$, consisting of a reactant, A, and an inert, C. In the reactor, a first order reaction $A \rightarrow B$ takes place. The separation unit separates the reactor effluent into pure product, B, at the bottom and a mixture of reactant, A, and inert, C, at the top.

Now, in order to reprocess unreacted A, one might consider material recycling, as shown in Fig 2.4b. Assuming that the two systems operate at the same steady state, we ask how the material recycle affects the dynamic behavior of this system.

For the sake of an example, assume that the separator is perfect, with no dynamics. The model and the numerical values used are listed in the Appendix.

Fig 2.5 shows the time responses to a very small step disturbance in $z_F$, the mole fraction of the reactant in the feed stream. As can be seen, the positive feedback due to the recycle has in this case made the response slower, and the steady state sensitivity higher.

### Example 2 Feedback from heat integration

Consider the system shown in Fig 2.6a showing a CSTR where a simple first order reaction $A \rightarrow B$ is taken place. The feed, $F$, is preheated in a preheater before entering the reactor.

In order to save energy, one might consider preheating the feed by the effluent, as shown in Fig 2.6b. The two systems are supposed to operate at the same steady state. For the example, we neglect the dynamics of the heat exchanger. The models and numerical values are described in the Appendix.

Fig 2.7 shows the time response of the two systems when they are given a one degree K step disturbance in the feed temperature, $T_F$. Like in the previous example, the feedback due to heat integration has increased the time constant and the steady state gain.

### Example 3 Heat exchanger network example

As an other example of positive feedback from heat integration, take the heat exchanger network shown in Fig 2.8 (Mathiesen and Skogestad, -92). Consider the

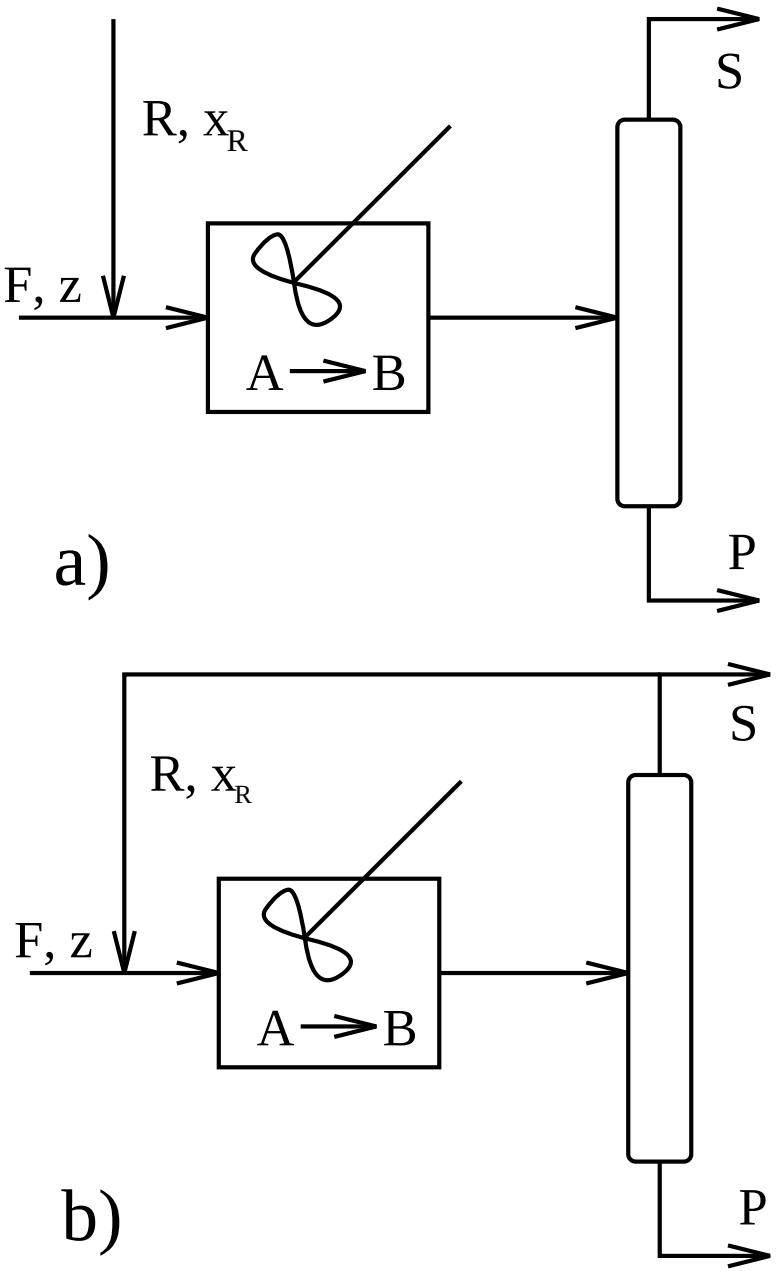


Figure 2.4: Reactor with mass recycle (positive feedback)

effect of temperature disturbances in the hot stream (H1) on the outlet temperature $y_1$. As can be seen, heat exchangers 1a and 1b form a positive feedback loop. In this case, this leads to a higher sensitivity and a slower response than if the heat exchangers were independent coolers working at the same steady state.

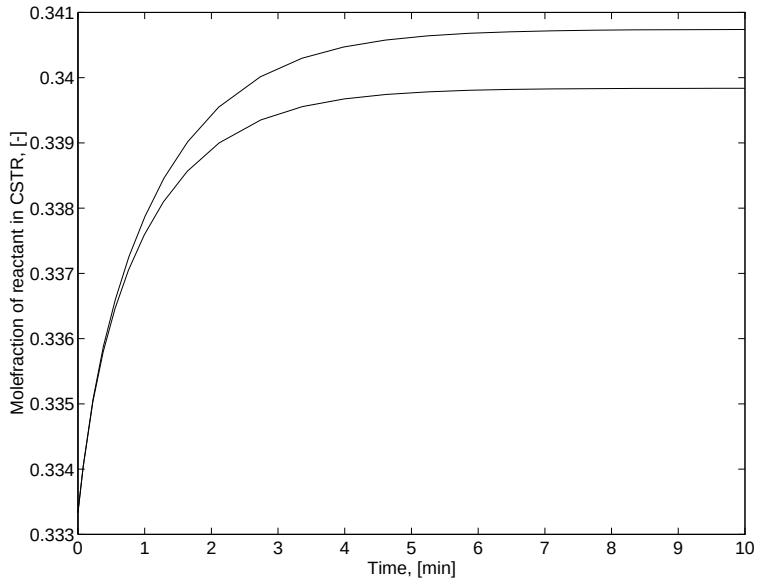


Figure 2.5: Step response of recycle system (upper curve: with recycle, lower curve: without recycle)

## 2.6 Examples of recycle causing negative feedback

Material recycle and heat integration may also lead to *negative feedback effects*. This is less common, but it is nevertheless important to be aware of the possibility. It is rare because units in a plant usually have a positive gain: Increasing an inlet temperature of an heat exchanger or a reactor normally leads to an increase in outlet temperatures. For example, as shown by Mathiesen (1994) this is always the case for heat exchanger networks. Similarly, increasing the inlet concentration of a chemical species to a system usually leads to an increase of outlet concentration of the species.

However, there are exceptions: take for instant a distillation column where the distillate flow and the boilup are the independent variables (DV configuration). Increasing the temperature of the boiler medium increases the boilup, which leads to higher purity, and hence a lower temperature, in the top of the column. The column is therefore a negative gain element from the boiler medium temperature to the top temperature. With heat integration, the column can therefore act as a negative gain element and lead to negative feedback if contained in a loop.

### Example 4 A reactor example

Another example where a loop yields negative feedback is the system shown in Fig. 2.9. Feed is preheated with the product, further heated in a second heater, and sent through two reactors. In the first reactor, a reaction $A \rightarrow B$ with negligible heat of reaction takes place (i.e. $T_3 = T_2$). In the second reactor, an endothermic reaction takes place, with total conversion of component B to component C. The temperature

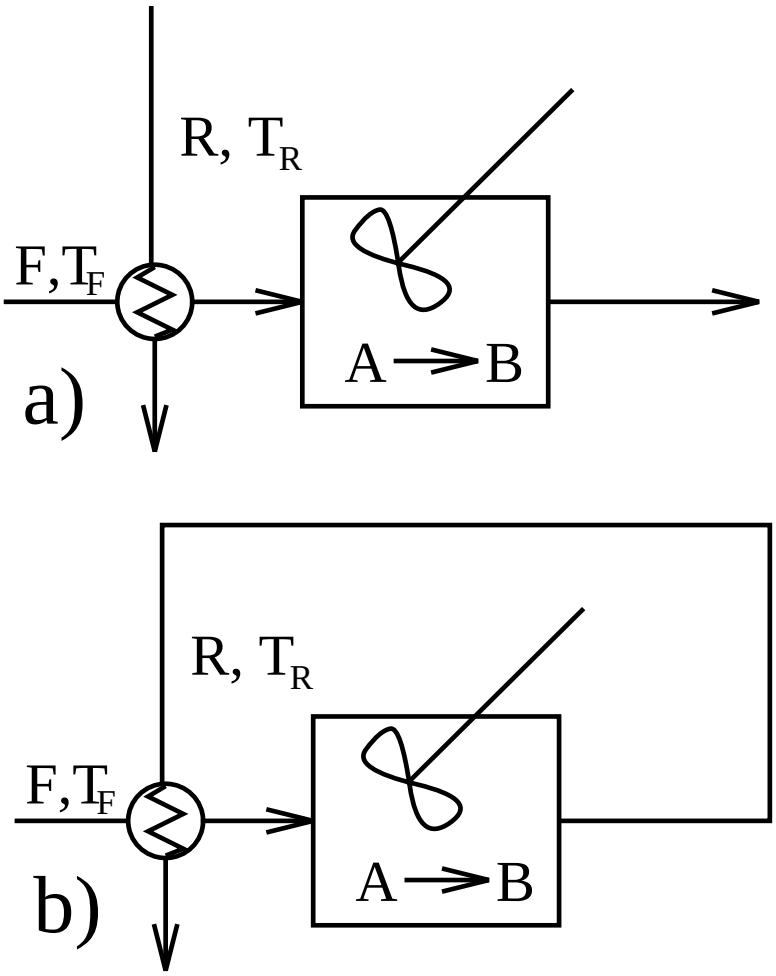


Figure 2.6: Reactor with feed/effluent preheating (positive feedback)

drop over the two reactors taken together is therefore proportional to the reaction rate, r, of the first reactor (Assuming constant heat capacity). Details in the mathematics are given in the Appendix. Consider an increase in $T_2$, the inlet temperature of the first reactor. With a proper choice of numerical values (Appendix), the outlet temperature of the second reactor, $T_4$, will decrease, that is $\frac{dT_4}{dT_2} < 0$. This is then an example of a *negative feedback effect*. Negative feedback will usually have a stabilizing effect on the system and make it faster, but may cause instability if the loop gain is large enough.

## 2.7 More complex feedback effects caused by recycle

**Flow/Heat transfer interactions**. The effects mentioned above are either pure temperature effects or pure recycle effects. Introduction of heat integration in plants may sometimes provide a coupling between temperatures and flows, and destabilize a plant. Take for example the reactor example analyzed in the previous section (Fig 2.9),

Figure 2.8: Heat exchanger network with energy recycle (positive feedback)

and assume that the feed is liquid which is partially evaporated in the preheater, such that the flow between the preheater and the second heater is two-phase. The pressure drop of the system is now affected by the heat transfer in the preheater, which is influenced by the outlet temperature of the reactors. The outlet temperature of the reactors is affected by the flow rates, which are affected by the pressure drop. With the resulting coupling between temperature and flows, one should be concerned about the stability of the plant, as it could easily be unstable. Such instabilities are discussed thoroughly by Eigenberger (1985).

**Example 5 Industrial example**

An industrial example of a flow/heat transfer interaction was given by Anderson (1966). A reactor/preheater system in a new plant turned out to be unstable for large

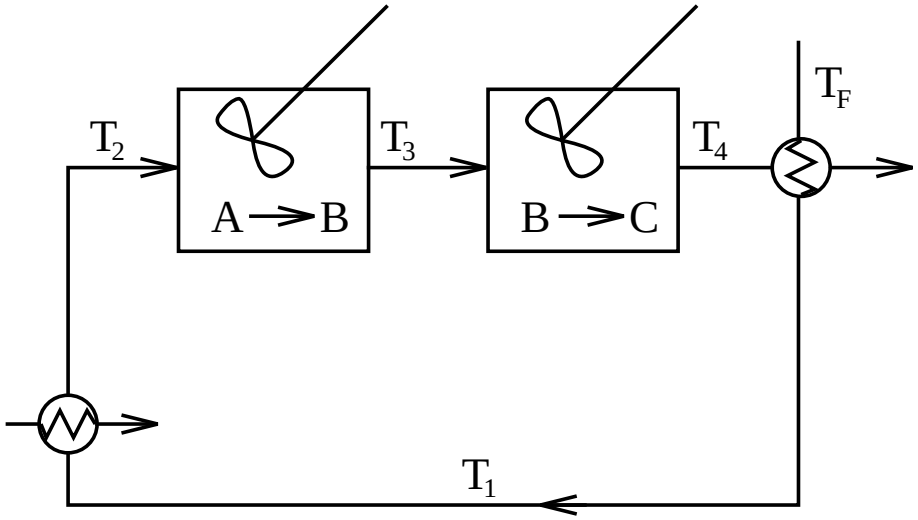


Figure 2.9: Endothermic reaction system with energy recycle (negative feedback)

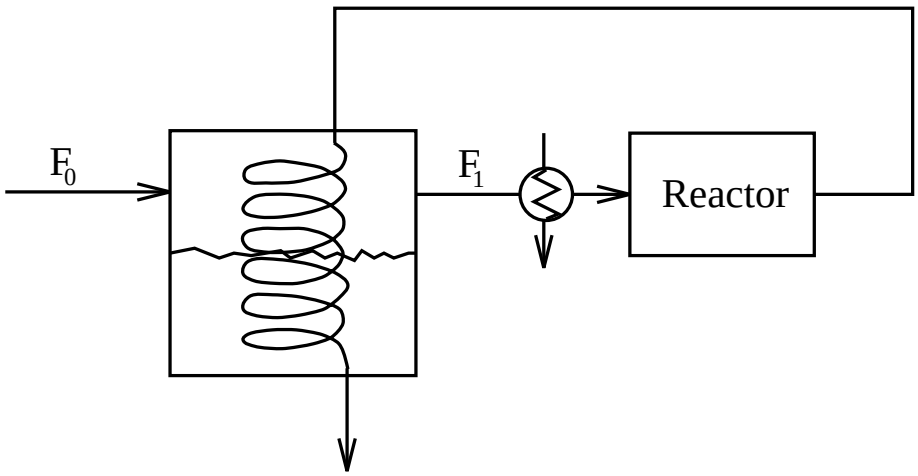


Figure 2.10: Reactor with feed preheating

throughputs. Figure 2.10 shows a simplified sketch of the system. The saturated liquid feed, $F_0$, was vaporized in an evaporator using the reactor effluent and superheated in a superheater before entering the reactor. The pressures and temperatures in the system were tightly controlled. To understand the instability, assume that the flow rate, $F_1$, through the reactor increase (due to some disturbance) while the feed flow rate, $F_0$ is kept constant. The resulting increase in the hot stream flow rate (inside the "coil" in the figure) in the boiler has two effects on the evaporator. In the long run, the liquid holdup in the evaporator will decrease, reducing the heat transfer area and thus eventually reducing the flow rate $F_1$ (*negative feedback effect*). Initially however, the liquid level in the evaporator will increase due to swelling of the boiling liquid and thus *increase* the heat transfer and thus tend to increase the vapor production, $F_1$, i.e. there is a *positive feedback effect*. In the industrial case, the loop gain due to this

positive feedback was larger than one, resulting in instability of the steady state. As the the flow, $F_1$, is constrained by the mass balance to be equal to $F_0$ on the average, the phenomenon manifests itself as limit cycles.

## 2.8 Parallel paths in plants

Manipulating an actuator in an integrated plant often has more than one effect on the plant. First, different parts of the plant may be affected, several of which may influence a given measurement. This may correspond to e.g. having units in parallel or when there are several downstream paths in a heat exchanger network. Second, several different physical effects, such as pressure, flow rate, temperature and concentration may be affected. The influence of these effects on a measurement may vary in strength and speed, and the measurement will often be the sum of several such effects. In both cases there exist *parallel paths* between the actuator and the measurement. Often the parallel paths have an opposing influence on the measurement, i.e. they are *competing effects*. We present some examples of parallel paths in plants.

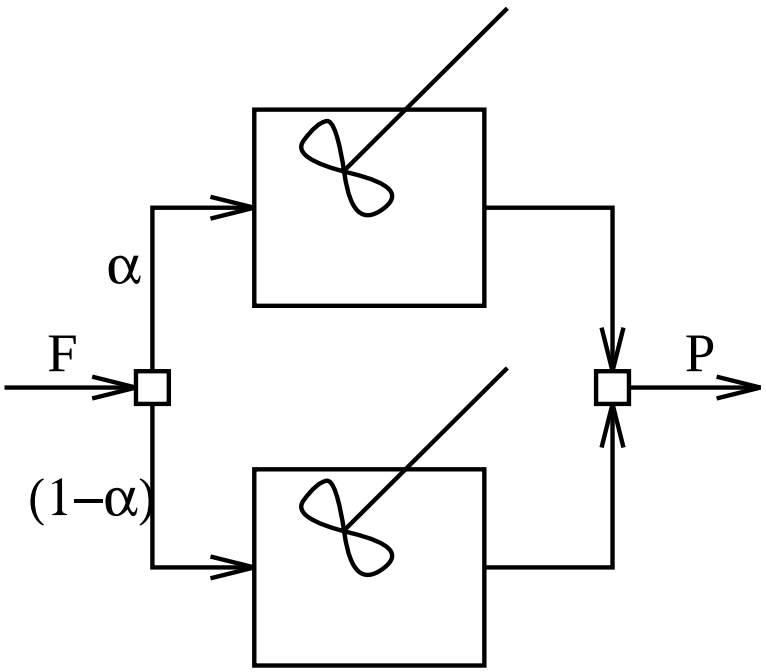


Figure 2.11: Reactors in parallel (parallel path)

**Example 6 Units in parallel**

As an example of parallel units, consider the system shown in Fig. 2.11, showing two CSTR's in parallel. The feed stream, F, consisting of pure reactant, A, is divided equally in a splitter (split fraction $\alpha = 0.5$), and fed to the reactors, where a simple reaction $A \rightarrow B$ takes place. The outlet streams from the reactors are mixed to form a product, $P$.

Figure 2.13: Heat exchanger network with parallel downstream paths (from inlet temperature of stream H2 to outlet temperature of stream C2)

**Example 7 Different downstream paths**

Consider the heat exchanger network shown in Fig 2.13. A disturbance in the hot

Figure 2.14: Heat exchanger network with "internal" parallel paths (flow rate and temperature)

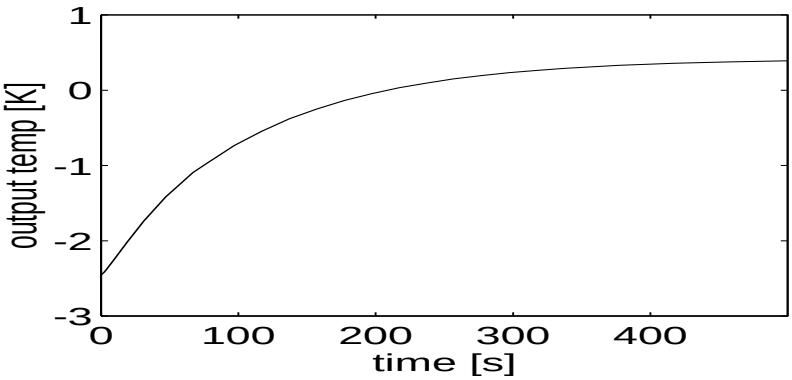


Figure 2.15: Step response to change in flow rate, $u_1$

**Example 8 Heat exchanger network**

As an example, take the simple heat exchanger network shown in Fig. 2.14 (Mathiesen, 1994). The temperature, $T_2$, is supposed to be lower than $T_1$. Manipulating the valve position, $u$, affects the outlet temperature, $T = y$, by two different effects:

through the change in the flowrate of the stream H2, and by a change in the operation of the heat exchanger. The two effects are *competing*, the former tends to decrease $T$ in response to an increase in the flow rate H2, the latter to increase $T$. As shown in the thesis by Mathiesen (Fig 2.15), this may cause inverse response behavior, reflecting the existence of Right Half Plane zeros.

## 2.9 Effects of combining recycle with parallel paths

In the heat recycle example in section 2.5, the result of the feedback was to make the system slower. We now give a similar example where the positive feedback due to the heat recycle leads to oscillatory instability due to Right Half Plane zeros introduced by "internal" parallel paths.

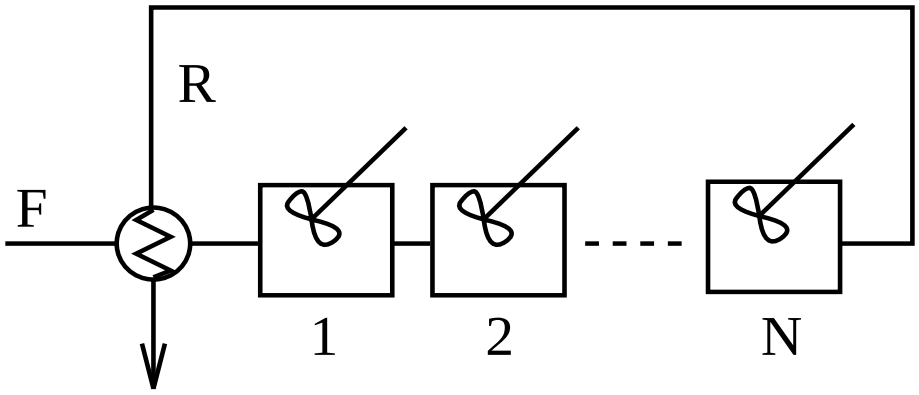


Figure 2.16: Reactors in series with feedback of heat (positive feedback)

**Example 9 CSTR's in series with heat integration**

Consider the system shown in Fig 2.16, which might represent a crude model of a fixed bed autothermal reactor. Feed gas, consisting of pure reactant, A, is preheated in a feed/effluent heat exchanger and fed into a train of CSTR's filled with catalyst before it leaves the system through the feed/effluent heat exchanger. The reaction is a simple $A \rightarrow B$ of the Arrhenius type.

As a specific numerical example, we take a system with 15 CSTR's in series. The numerical values used for the parameters are listed in the Appendix. The time constant for the energy balance is chosen an order of magnitude larger than the residence time, reflecting a large heat capacity of the catalyst. As a basis of comparison, we use a similar system with an independent preheater.

Fig 2.17 shows the responses to a small step disturbance in the feed temperature, $T_F$. As can be seen, the system with preheating is unstable. Moreover, the instability manifests itself as oscillations of growing amplitude, indicating that the instability is due to a pair of complex conjugate poles, and not the pole approaching the origin. This is confirmed in figure 2.18, showing a numerically computed pole/zero map of

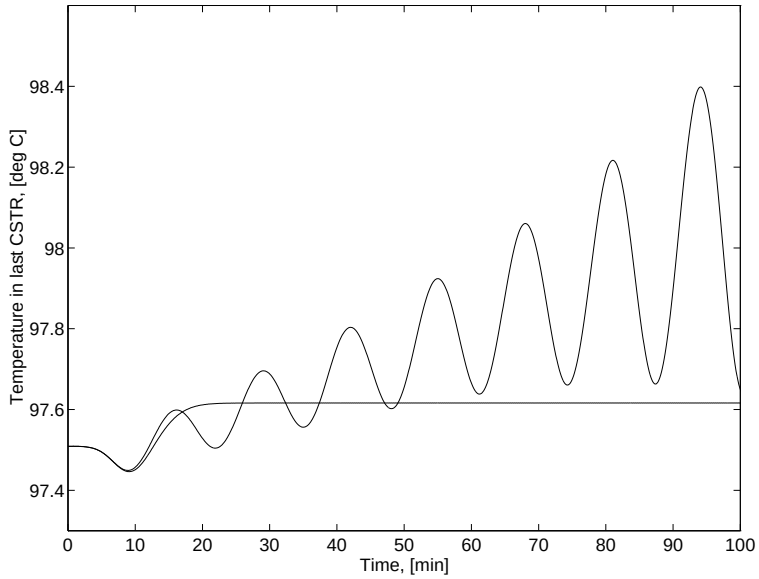


Figure 2.17: Step response of CSTR's in series with preheating (wavy curve: with feed/effluent preheating, other curve: independent preheater)

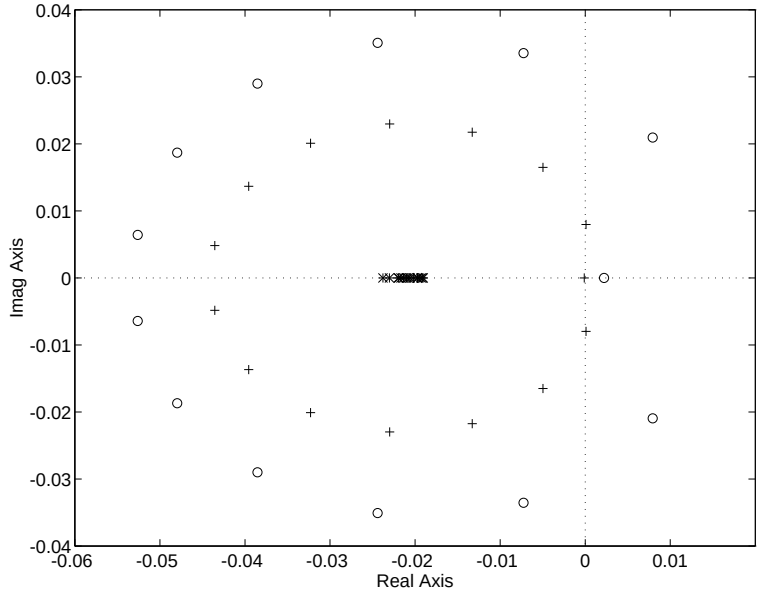


Figure 2.18: Pole and zero locations of reactor systems ('0'-zeros, 'X'-poles when independent preheater, '+'- poles with heat recycle)

the linearized system. As can be seen, there are Right Half Plane zeros in the system. These may be explained by the existence of "internal" parallel paths in the reactor train, since there are changes in both reactant concentration and temperature. Consider for instant an increase in the inlet temperature of the first bed. This has two effects on the last reactor in the train. First, as the reaction rate in the first reactor increases, there

is less reactant left to the last reactor, which tends to decrease its outlet temperature. This is the fast effect. Second, the heat produced in the first reactor will eventually reach the last reactor, tending to increase its outlet temperature. This is a slow effect due to the heat capacity of the catalyst. However, the second effect is the strongest, yielding Right Half Plane zeros. Now, the feedback gain from the heat recycle makes these Right Half Plane zeros attract a pair of complex conjugate poles, as may be seen from the figure. This makes a pair of complex conjugate poles cross the imaginary axis, yielding the instability.

This kind of behavior is more likely the larger the number of CSTR's in series. With right half plane zeros in the individual CSTR transfer functions there will typically be a peak in the frequency response and at the same time a phase lag. By compounding a large number of such units, the peak in the frequency response of the reactor train may easily extend to phase lags beyond $360^0$. As explained in the Linear Systems section this implies that a pair of complex conjugate poles cross the imaginary axis before the real pole passing the origin.

Limit cycle behavior due to such effects has been observed in industrial fixed bed reactor systems. A particular industrial example was studied by Morud and Skogestad (1993), based on an incident in an ammonia synthesis plant. References to several other examples are given by Eigenberger (1985).

## 2.10 Discussion

Plant integration has an impact on the control aspects of the plant. Feedback effects due to e.g. mass recycle may make the plant unstable or more sensitive to disturbances and increase the need for control, while parallel paths may introduce fundamental limitations in the performance of the plant under feedback control.

Consider a system with recycle, where a fraction $\alpha$ of the outlet is recycled. For a step disturbance in e.g. the feed concentration, the output, e.g. the outlet concentration of some chemical, has to stay within some acceptable limits. The response, for different values of the fraction recycled, $\alpha$, may typically look something like the plot illustrated in Fig 2.19. For high values of the fraction recycled, $\alpha$, the outlet concentration is sensitive to disturbances in the input stream, and will typically exceed its allowable limit. For low values of the amount recycled, there is in this case no need for control, as long as the output keeps within the specified limits. The recycle will typically make the sensitivity high for *slow* disturbances, such that the recycle does not necessarily introduce a need for fast control, but it introduces a need for control where it otherwise might not have been needed. With control, disturbances may be rejected, or the plant response may be speeded up if necessary, as long as the plant does not have inherent limitations in achievable control performance.

It is known that *right half plane zeros* in a plant limit the achievable control performance obtainable by any controller. Hence, if there are parallel paths between the manipulated variables and the controlled variables, this may lead to inherent limitations in what can be achieved by the control system. Hence, it is important to be aware of this when doing e.g. heat integration, as it may introduce many parallel paths in

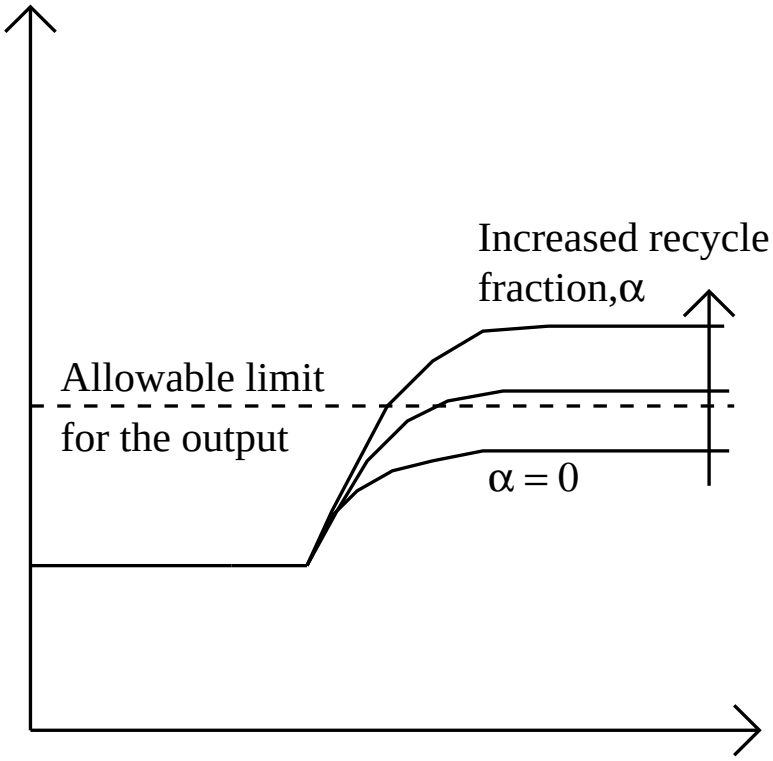


Figure 2.19: Response in output to step disturbance

the plant, some of which may lead to poor control of the resulting plant.

In this paper we have only discussed linear systems. However, many of the concepts involved may be generalized to nonlinear systems. Instead of poles, one may study the internal dynamics of the plant, i.e. the evolution of the states of the plant when the input follows a given trajectory. Instead of zeros, one may study the zero dynamics of the plant, which is the evolution of the states of the plant when the output is forced to be zero by the input. Unstable zero dynamics means that there are Right Half Plane zeros if the plant is linear, and may be thought of as a generalization of Right Half Plane zeros for nonlinear plants. Unfortunately, nonlinearities make the analysis of possible dynamic behavior much more difficult. Nonlinear systems may exhibit other types of behavior, such as chaos, which may never occur in a linear system.

## 2.11 Conclusion/proposition for further work

The dynamics of plants with material recycle or heat integration may be very different from the dynamics of the individual processing units. The effect of material recycle or heat integration may be thought of as moving the plant poles and zeros. Feedback effects due to recycle of material or energy are typically *positive*, which often leads to slow responses and high steady state sensitivity, and in some cases to instability. This will lead to an increased need for control. Parallel paths caused by e.g. heat integration change the *zero* locations of the plant, and may introduce limititations to

the achievable performance of the plant control system. In addition, combinations of these effects may lead to instability, reactor runaway, limit cycles etc. in the plant if not foreseen.

There is a need for a systematic classification of the effects of integration on the plant dynamics, as tight integration may lead to plants which are almost impossible to control. Some simple indicators which could be used to tell us when problems are probable, would be of great help.

# References

[1] Anderson, J.S. (1966). A practical problem in dynamic heat transfer. The Chemical Engineer, May, 1966, pp. CE97-CE103.

[2] Aris,R. and Amundson, N.R.(1958). An analysis of chemical reactor stability and control. Ch.Eng.Sci, vol 7,no 3, pp 121-155.

[3] Denn, M.M. and Lavie, R. (1982). Dynamics of Plants with Recycle. The Chem. Eng. J., 24, pp 55-59.

[4] Eigenberger, G. (1985). Dynamics and stability of chemical engineering processes. Int. Chem. Eng., vol 25, no. 4, pp 595-610

[5] Gilliland, E.R., Gould, L.A. and Boyle, T.J. (1964). Dynamic effects of material recycle. Preprints JACC, Stanford, California pp 140-146.

[6] Gray, P. and Scott, S.K. (1990). Chemical Oscillations and Instabilities. Nonlinear Chemical Kinetics. Clarendon Press, Oxford, ISBN 0198556462

[7] Jacobsen, E.W. and Skogestad, S. (1991). Multiple Steady States in Ideal Two Product Distillation. AIChE Journal, vol 37, No. 4., pp 499-511.

[8] Jacobsen, E.W. (1994). Dynamics of systems with input multiplicity with binary distillation as an example, Lecture at Chem. Eng. Dept, NTH, Trondheim, March 11, 1994.

[9] Jacobsen, E.W. and Skogestad, S. (1994). Instability in Distillation Columns. AIChE Journal. In press.

[10] Kapoor, N., McAvoy, T.J, Marlin, T.E. (1986). Effect of Recycle Structure on Distillation Tower Time Constants. AIChE J. vol. 32, no. 3, pp 411-418

[11] Luyben, W.L. (1992) Dynamics and Control of Recycle Systems. Part 2 - Comparison of Alternative Process Designs. Paper submitted to IEC Research.

[12] Mathiesen, K. W., and Skogestad, S. Design, Operation and Control of Resilient Heat Exchanger Networks. AIChE Annual Meeting, Miami Beach, Nov 1-6, 1992, Session: Design and Control.

[13] Mathiesen, K. W. (1994). Integrated Design and Control of Heat Exchanger Networks. PhD thesis, University of Trondheim, NTH, Norway, 1994

[14] Morud, J.C. and Skogestad, S. (1993). The Dynamics of Chemical Reactors with Heat Integration. Paper 26e at AIChE Annual meeting, St. Louis, USA, Nov. 8-12, 1993.

[15] Morud, J.C. and Skogestad, S. (1994). Effects of Recycle on Dynamics and Control of Chemical Processing Plants. Computers and Chemical Engng 18, Suppl S529-S534

[16] Papadourakis, A., Doherty, M.F. and Douglas, J.M. (1989). Approximate Dynamic Models for Chemical Process Systems. Ind. Eng. Chem. Res. 28, No. 5, 546-552

[17] Papadourakis. A, Doherty, M.F. and Douglas, J.M. (1987). Relative Gain Array for Units in Plants with Recycle. Ind. Eng. Chem. Res., Vol 26, 1259-1262.

[18] Pareja, G. and Reilly, M.J. (1969). Dynamic Effects of Recycle Elements in Tubular Reactor Systems. IEC Fund. 8, 442.

[19] Seydel, R., (1988). "From equilibrium to chaos. Practical bifurcation and stability analysis". Elsevier Science Publishing Co. 1988.

[20] Uppal, A., Ray, W.H. and Poore, A.B (1974). On the dynamic behavior of continuous stirred tank reactors. Ch.Eng.Sci. vol 29, pp 967-985

[21] Uppal, A., Ray, W.H. and Poore, A.B. (1976). The classification of the dynamic behavior of continuous stirred tank reactors-Influence of reactor residence time. Ch.Eng.Sci, vol 31, pp 205-214.

[22] van Heerden, C. (1953). Autothermic Processes. Properties and Reactor design. Industr. Engng. Chem. (Industr.), 45, 1242

[23] Verykios, X.E. and Luyben, W.L. (1978). Steady-state Sensitivity and Dynamics of a Reactor/Distillation Column System with Recycle. ISA Transactions, vol 17, no. 2. pp 31-41.

## Nomenclature

| | |
|---|---|
| $C_{p,fluid}$ | fluid heat capacity (J/mole.K) |
| $C_{p,solid}$ | catalyst heat capacity (J/kg.K) |
| $E$ | activation energy (J/mole) |
| $F$ | flow rate (mole/sec) |
| $k(T)$ | reaction rate constant ($sec^{-1}$) |
| $k_0$ | Arrhenius constant ($sec^{-1}$) |
| $M_{fluid}$ | fluid holdup in CSTR (mole) |
| $M_{solid}$ | amount of catalyst in CSTR (kg) |
| $r$ | reaction rate ($sec^{-1}$) |
| $R$ | universal gas constant ($8.31 J/mole.K$) |
| $T$ | temperature (K) |
| $T_0$ | reference temperature (K) |
| $x$ | mole fraction of chemical species (-) |
| $z$ | mole fraction of chemical species in the feed (-) |

Greek

| | |
|---|---|
| $\alpha$ | flow split fraction in splitter $F_{out}/\sum_{out} F_{out}$ (-) |
| $-\Delta H_{rx}$ | heat of reaction (J/mole) |
| $\epsilon$ | heat exchanger efficiency (-) |
| $\tau$ | fluid residence time in CSTR (sec) |
| $\tau_T$ | time constant of energy equation (sec) |

Subscripts

| | |
|---|---|
| $A$, $B$, $C$ | chemical species |
| $F$ | feed stream |
| $i$ | index taking the values A, B, C |
| $in$ | index over all inlet streams |
| $out$ | index over all outlet streams |
| $R$ | recycle stream |

## Appendix A. Models for the examples

The models used for the examples are:

**The CSTR**. The CSTR model used has constant molar holdup, $M_{fluid}$, and at most three chemical species, $A, B, C$. The reaction is a simple reaction of the Arrhenius type $A \rightarrow B$ (or $B \rightarrow C$). The reaction rates, $r_i$, $i = A, B, C$ are given by ($r_C = 0$ when $C$ is an inert):

$$r_A = -r_B = k(T) \cdot x_A, \quad k(T) = k_0 e^{-\frac{E}{R}(\frac{1}{T}-\frac{1}{T_0})} \tag{2.10}$$

Mass balance for component $i$, $i = A, B, C$:

$$\dot{x}_i = \frac{1}{\tau}(x_{in,i} - x_i) - r_i \tag{2.11}$$

Energy balance (constant heat capacity):

$$\dot{T} = \frac{1}{\tau_T}(T_{in} - T) + \frac{-\Delta H_{rx}}{C_p} \cdot r_A \tag{2.12}$$

The time constants in these equations are given by:

$$\tau = M_{fluid}/F, \quad \tau_T = \frac{C_{p,fluid}M_{fluid} + C_{p,solid}M_{solid}}{C_{p,fluid}F} \tag{2.13}$$

**Heat exchanger without dynamics**. The model used is a standard $\epsilon$-NTU model (Two streams, 1 and 2):

$$T_{1,out} = \epsilon_1 T_{2,in} + (1 - \epsilon_1)T_{1,in} \tag{2.14}$$

where the heat exchanger efficiency, $\epsilon_1 \in [0 \quad 1]$, is a function of the flow rates only. In the examples where it is used, it is just a constant, as the flow rates are constant in these examples.

**The perfect separation unit**. The perfect separation unit with no dynamics splits a mixture of components A, B, C into pure B at the bottom (i.e. $x_{bottom,B} = 1$, $x_{bottom,A} = x_{bottom,C} = 0$) and a mixture of A and C at the top. The mass balance for component $i$, $i = A, B, C$ becomes:

$$Fx_{in,i} = F_{top}x_{top,i} + F_{bottom}x_{bottom,i} \tag{2.15}$$

**Splitters and mixers**. The mass balances of splitters and mixers are taken as (component $i$, $i = A, B, C$):

$$\sum_{in} F_{in,i}x_{in,i} = \sum_{out} F_{out,i}x_{out,i} \tag{2.16}$$

For the mixer, the inlet streams are fully specified. For the splitter, the mole fractions of all streams are the same. The outlet flowrates are $F_1 = \alpha F$, $F_2 = (1 - \alpha)F$, where $F$ is the inlet flow rate.

## Numerical values for the examples

**Example 1**: $z_A = 0.95$, $z_C = 0.05$, $x_{R,A} = x_{R,C} = 0.33$, $F = 1 vol.units/min$, $R = 1.7 vol.units/min$, $k(T) = 2.7 min^{-1}$ (isothermal), $\tau = 1 min$, step size $\Delta z_A = 0.01$.

**Example 2**: $z_A = 1$, $z_C = 0$, $T_F = 25^0 C$, $T_0 = 60^0 C$, $T_R = 90.6^0 C$, $F = 1 vol.units/min$, $R = F$, $k_0 = 1 min^{-1}$, $\tau = M/F = 1 min$, $\frac{-\Delta H_{rx}}{C_p} = 50K$, $\frac{-E}{R} = -7693K$, $\epsilon_{feed} = 1/3$ (Feed is stream 1 in eq. 2.14), step size $\Delta T_F = 1K$

**Example 4**: $E$=60 kJ/mol, $R$=8.31 J/mol.K, $T_0 = T_2 = 573.15K$, $\frac{-\Delta H_{rx}}{C_p} = -1000K$, $k_0 = 5.76 \cdot 10^{-4} sec^{-1}$, residence time of first reactor $\tau = 300 sec$, inlet to first reactor $z_A = 1$.

**Example 6**: Feed to system: $z_A = 1$, $\alpha = 0.5$, $F = 1 vol.units/min$, Bottom reactor: feed $(1-\alpha)F$, $k(T) = 2min^{-1}$ (isothermal), $M = 0.5 vol.units$, Upper reactor: feed $\alpha F$, $k(T) = 1/2 min^{-1}$ (isothermal), $M = 1 vol.units$, step size $\Delta\alpha = 0.05$

**Example 9**: $T_0 = 60^0C$, $T_F = 2^0C$, $z_A = 1$, number of reactors 15, $\epsilon_{feed} = 0.5$, $\tau = 1min$, $\tau_T = 60min$, $\frac{-\Delta H_{rx}}{C_p} = 5K$, $k = 1min^{-1}$ (isothermal), $\frac{-E}{R} = -7693K$, $T_R = 97.5^0C$, step size $\Delta T_F = 1K$

## Details of example 4

See the example. Throughout the derivation, $\tau$, $z_A$ and $x_B$ are the residence time, the inlet mole fraction of reactant and the outlet mole fraction of the first reactor. The mole fraction at the outlet of the first reactor (isothermal) at steady state is found from the mass balance, eq. 2.11.

$$0 = \frac{1}{\tau}(z_A - x_A) - k(T_2) \cdot x_A \tag{2.17}$$

which yields:

$$x_B = 1 - x_A = 1 - \frac{z_A}{1 + k(T_2)\tau} \tag{2.18}$$

Total conversion of this in the second reactor yields the temperature difference (energy balance):

$$T_2 - T_4 = T_3 - T_4 = -\frac{-\Delta H_{rx}}{Cp} x_B \tag{2.19}$$

which yields (dropping argument of $k$, i.e $k = k(T_2)$):

$$\frac{dT_4}{dT_2} = 1 + \frac{-\Delta H_{rx}}{Cp} \frac{z_A \tau}{(1+k\tau)^2} \frac{dk}{dT_3} = 1 + \frac{-\Delta H_{rx}}{Cp} \frac{z_A \tau}{(1+k\tau)^2} \frac{E}{RT^2} k \tag{2.20}$$

With a proper choice of numerical values (listed above) this is a negative quantity.

# Chapter 3

# The Dynamic Behavior of Processing units

John Morud and Sigurd Skogestad*
Chemical Engineering
University of Trondheim - NTH
N-7034 Trondheim, Norway

Presented at
Escape-3, Graz, Austria, July 5-7 1993

**Abstract**

The effect of recycle of mass and energy on the dynamic characteristics of process units is examined. After reviewing some basic results from linear systems theory, the dynamic behavior of a simple well stirred control volume is analyzed. It is shown how the introduction of phenomena like chemical reactions, material recycle, heating/cooling etc. modify the dynamic behavior of the system. The basic idea is that such modifications may be viewed as feedback effects around the original system; and may thus change the plant eigenvalues, cause large time constants and introduce instability or complex nonlinear behavior. The effects are greatly influenced by the choice of independent variables.

*Address correspondence to this author. Fax: 47-73594080, E-mail: skoge@kjemi.unit.no

## 3.1 Introduction

It is known that recycle of mass and energy may greatly influence the dynamic behavior of chemical engineering systems. (Gilliland *et al.*,1964, Denn and Lavie, 1982). Recycle may dramatically alter the time constants of a system, and may give rise to instability or oscillatory behavior (limit cycles). Knowledge of such phenomena is important for controller design, and their effects may even pose a threat to plant safety if not foreseen.

Unfortunately, even with a model of a system in terms of its nonlinear differential equations, the analysis of the possible behavior of the system is very difficult. For example, the behavior of a set of equations depends entirely on the parameter values as well as on the specification (choice of independent variables), and even for very simple sets of equations one may get complex behavior such as instability, multiple steady states, limit cycles and even chaotic behavior.

The objective of this paper is not to analyze such systems in detail, but rather to examine what simple mechanisms that may give rise to complex behavior in chemical engineering systems, and in particular for cases with recycle of mass or energy. By analyzing very simple systems, general insight into the effects of such mechanisms are gained. Such insights prove useful when analyzing more realistic situations. The emphasis is on a process unit level rather than on a plant flowsheet level.

We give a brief outline of the paper. First, we review some basic results from Linear Systems Theory, and elaborate the implications of different interconnection structures, such as feedback, series and parallel interconnections. Then, with this linear theory in mind, we analyze in detail a simple CSTR (continuous stirred tank reactor), and investigate the effects of various modifications on its stability and speed of response. For example, we study the effects of chemical reaction, recycle of unreacted reactant, feed-effluent preheating, and vapor liquid equilibrium.

General work in the area seems rather scarce even though issues like the effect of energy integration on reactor stability were discussed as early as 1953 by van Heerden (1953). Aris and Amundson (1957) analyzed the effect of feedback (control) on the dynamic characteristics of the continuous stirred tank reactor. Gilliland *et al.* (1964) studied the classical example with a reactor connected to a distillation column and total recycle of the column bottom product. They reported an increased sensitivity of the plant to feed disturbances compared to the reactor without recycle, and that the plant may become unstable even though the reactor itself is stable. Denn and Lavie (1982) argued that a recycle system may be considered analoguous to a closed loop feedback control system with positive feedback. Hence, recycle may increase the overall response time of the plant and make the steady state gain large. They also considered the effect of time delays in the recycle path on plant dynamics. Kapoor *et al.* (1986) studied the effect of recycle structure on the time constants of distillation columns, and argued that the reflux may be viewed as a positive feedback effect which may result in very large time constants for high-purity separations. Other related work that may be mentioned is Verykios and Luyben (1978), Luyben (1992), Papadourakis *et al.* (1987, 1989) and Uppal and Ray (1974).

## 3.2 Linear systems

For small deviations from the steady state, a processing unit may be well described by a linear transfer function. Before attacking the nonlinear complexities of a plant, it is therefore reasonable to review some basic results from linear systems theory. Our main reason for studying linear systems theory is that the introduction of recycle in a plant often can be thought of as a sort of feedback mechanism.

Consider a system (or plant) with linear transfer function model $G(s)$. The response is mainly determined by the location (and possible direction) of the poles and zeros. For a scalar system the zeros $z$ correspond to $g(z) = 0$, and the poles $\lambda$ correspond to $|g(\lambda)| = \infty$. The poles are equal to the eigenvalues of the Jacobi matrix for the states and are often referred to simply as "eigenvalues". The poles determine the speed (and possible oscillations) of the response whereas the zeros determine the shape of the response (e.g., overshoot for left half plane (LHP) zeros, and inverse response for RHP zeros). Plants with poles in the right half plane are unstable. If the plant has a pole near the origin, the response time will be large.

Assume that the original plant (e.g., without recycle) has transfer function $G(s)$, and that one somehow (e.g., by a recycle) introduces a modification $C(s)$. We now want to consider the effect of such modifications.

**1. Series interconnection,** $GC$. (Fig. 3.1a). In this case the poles and zeros of the combined system $GC$ are given by the poles and zeros of the individual elements, $G$ and $C$. Thus, in this case the overall response may be predicted directly from the individual elements.

**2. Parallel interconnection,** $G + C$. (Fig. 3.1b). The combination has the same poles as the individual elements, but the zeros are different. Thus, it may be difficult to predict in detail the overall response from knowledge of the elements. However, the overall response will usually not differ drastically from that of the individual responses, since it is simply their sum.

**3. Feedback** $C$ **around** $G$. (Fig 3.1c). The overall transfer function becomes

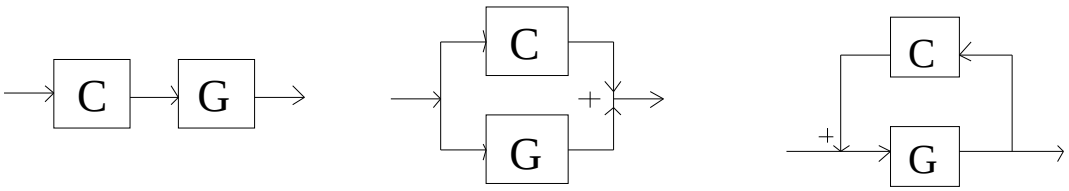


Figure 3.1: Interconnections of transfer functions

$H(s) = G(s)[I - C(s)G(s)]^{-1}$. In this case the zeros of $H(s)$ are equal to the zeros of $G(s)$, but the poles are moved by the feedback, and the resulting response may of course be drastically different from that of the individual elements $G(s)$ and $C(s)$. For example, the individual elements may be stable and the overall response unstable and *vice versa*. Even the location of the poles may be difficult to predict. For example, consider the scalar case with static feedback, $c(s) = k$ ($k > 0$ corresponds to positive

feedback). Then we know that for $k = 0$ the poles of the overall system $h(s)$ are equal to the *poles* of $g(s)$, and as $|k| \to \infty$ the poles of $h(s)$ approach the *zeros* of $g(s)$. However, as anyone with familarity with a root locus plot knows, for intermediate values of $k$ the poles may move widely about in the complex plane, and a detailed calculation is needed to obtain the location of the poles.

Of course, there are exceptions. For example, in this paper we mainly study simple first-order models such as $g(s) = 1/(s + a)$, and we get with constant gain feedback $h(s) = 1/(s+a-k)$. In this case the pole $\lambda = -a+k$ moves monotonically to the right along the real axis as $k$ increases. Eventually, for $k > a$, we get instability, but before this occurs we will observe that "the response becomes slower" (since the time constant of $h(s)$ is $\tau = -1/\lambda = 1/(a - k)$) and "the gain gets larger" (since the gain of $h(s)$ is $1/(a - k)$). However, in the general case the behavior is much more complex, and statements such as "positive feedback makes the system slower and the gain larger" may not hold.

The conclusion from the above review of linear system theory is that the effect of feedback, and thus of recycle, is generally very difficult to predict just from considering the individual elements $G(s)$ and $C(s)$. This is discouraging, and the situation of course gets much more complicated for nonlinear systems.

## 3.3 Classification of simple effects

Chemical engineering systems are usually quite accurately described by of a large number of coupled nonlinear differential equations which include a large number of feedback/recycle effects. From the above discussion of linear systems it seems almost hopeless to analyze such a system in its general case (taking into account various parameter values, specifications, etc.). Fortunately, it seems that most real chemical engineering processes behave in a relatively simple matter. In fact, most chemical engineers seem to be believe that essentially all "natural" chemical engineering systems respond in a rather simple and sluggish way (of the form first order response plus delay), and that any oscillations or instability are due to poorly tuned controllers.

In this section we will make an attempt to classify some individual effects which by themselves may cause complex behavior in chemical engineering systems, and thus demonstrate that the above belief is to some extent false.

We define a "simple" or "individual effect" as an effect involving only one differential equation (balance equation), and study below in particular the location of the pole (eigenvalue) and the possibility for instability. An ideal mixing tank is used as the basic element in this analysis. Some of these involve recycle, most of them have some sort of "positive feedback" effect.

**Notation.** In all cases we consider a simple mixing tank with feed $F$ [kmol/sec.] and constant holdup $M$ [kmol]. Let $z_A, x_A$ and $y_A$ denote mole fractions of component A in the feed, liquid and vapor, respectively. We consider a binary mixture of components A and B, and then we have $x_B = 1-x_A$. For cases with reaction we consider the reaction

A $\rightarrow$ B with rate $r(x_A, x_B, T)M$ (kmol A reacted / sec.) where for a 0'th order reaction $r = k(T)$ and for a 1st order reaction $r = kx_A$.

**Base case: Simple mixing tank.** The base case has only one phase, one product stream and no reaction. In this case a material balance for component A yields

$$M\frac{dx_A}{dt} = F(z_A - x_A); \quad \lambda = -\frac{1}{\tau_0} \tag{3.1}$$

where $\tau_0 = M/F$ is the residence time in the tank. $\lambda$ represents the eigenvalue of the linearized system and we note that the system is always stable and that the eigenvalue moves to the right and the response becomes slower as the residence time $\tau_0$ increases. Clearly, at steady-state we get $x_A = z_A$.

We will below consider the effect of introducing a reaction, adding recycle, adding preheater, considering temperature effects and evaporization, etc.

**Class 1. Reaction.** Consider an isothermal continuous stirred tank reactor (CSTR) with a 1st order reaction taking place (the reaction is assumed isothermal such that $r$ depends on $x_A$ only). We get

$$\frac{dx_A}{dt} = \frac{1}{\tau_0}(z_A - x_A) - kx_A; \quad \lambda = -\frac{1}{\tau_0} - k \tag{3.2}$$

At steady-state we get $x_A = z_A/(k\tau_0 + 1)$. We note that the reaction introduces a negative feedback which "stabilizes" the system and makes the response faster. To get instability from the reaction alone we would need an autocatalytic reaction, e.g. $r = kx_B$. With autocatalytic reactions, the number of different possible dynamic behavior is virtually endless: multiple steady states, instabilities, limit cycle behavior or even chaotic behavior. An extensive analysis of autocatalytic reactions may be found in Gray and Scott (1990). However, in this paper we restrict ourselves to simple kinetics.

**Class 2. Reaction with recycle**. Consider the same example as above, but introduce recycle of unreacted A (Fig. 3.2) such that all the reactor outlet except $(1 - \alpha)F, \alpha \in [0, 1]$ is sent to the perfect separation unit. If the dynamics of the separation unit is neglected, a component balance around the total system yields:

$$\frac{dx_A}{dt} = \frac{1}{\tau_0}(z_A - (1 - \alpha)x_A) - kx_A; \quad \lambda = -\frac{1}{\tau_0} - k + \frac{\alpha}{\tau_0} \tag{3.3}$$

As can be seen the introduction of the recycle has introduced *positive feedback* and the eigenvalue of the system is moved to the right ("slower reponse") as the recycle $\alpha$ increases.

However, the system never becomes unstable since we get $\lambda = -k$ for the limiting case with $\alpha = 1$ (*all* unreacted A is recycled). In this case the eigenvalue is independent of the residence time, but of course the actual conversion will depend on $\tau_0$, as we have at steady-state $x_A = z_A/(k\tau_0)$ (this also puts a lower limit on $\tau_0$ since we must have $x_A \leq 1$). We also note from this equation that the sensitivity ("gain") of $x_A$ to changes in $z_A$ has increased by introducing the recycle.

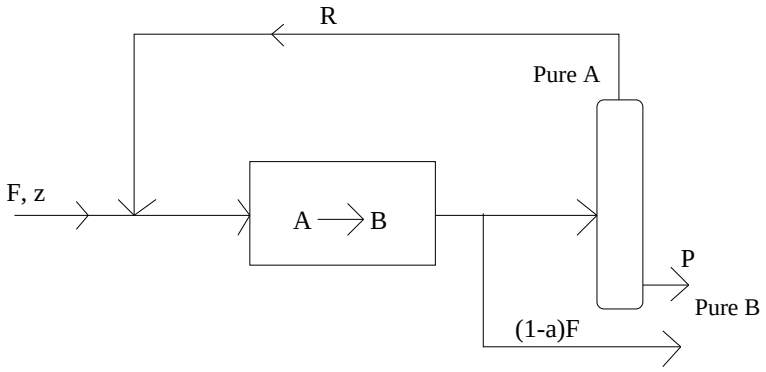


Figure 3.2: Reactor with recycle of unreacted feed

**Class 3. Temperature dependent exothermic reaction.** Consider an adiabatic CSTR with a 0'th order exothermic reaction, i.e. $r = k(T)$ (the reason for assuming a 0th order reaction is to show that we are dealing with a pure temperature effect). An energy balance assuming constant $c_P$ and $c_P = c_V$ yields:

$$\frac{dT}{dt} = \frac{1}{\tau_0}(T_{in} - T) + f(T); \quad \lambda = -\frac{1}{\tau_0} + T_{ad}k'(T) \tag{3.4}$$

where the "energy production term" is $f(T) = k(-H_{rx})/c_P = kT_{ad}$ where $T_{ad} = (-H_{rx})/c_P$ is the adiabatic temperature rise. For an Arrhenius type of rate expression we get $k'(T) = dk(T)/dT = kE/(RT^2)$ where $E$ [J/kmol] is the activation energy. Hence, the temperature dependency of the reaction has introduced *positive feedback* which moves the eigenvalue to the right and makes the response slower or even unstable. The positive feedback may be explained as follows: increasing the temperature causes an increased reaction rate, which again increases the energy production due to the exothermic reaction.

**Class 4. Recycle of energy by preheating.** Consider a mixing tank where the feed is preheated with the product (Fig.3.3). To isolate the effect of the preheating we assume no reaction. Energy balances yield: Tank by itself:

$$\frac{dT}{dt} = \frac{1}{\tau_0}(T_1 - T); \quad \lambda = -\frac{1}{\tau_0} \tag{3.5}$$

Heat exchanger:

$$T_1 = \alpha T + (1 - \alpha)T_{in}; \quad \alpha \in [0, 1) \tag{3.6}$$

where $\alpha$ is independent of temperature. The overall model then becomes:

$$\frac{dT}{dt} = \frac{1 - \alpha}{\tau_0}(T_{in} - T); \quad \lambda = -\frac{1}{\tau_0} + \frac{\alpha}{\tau_0} \tag{3.7}$$

The preheating introduces *positive feedback* which moves the eigenvalue towards the right, and thus makes the response slower. The system gets increasingly slower as the

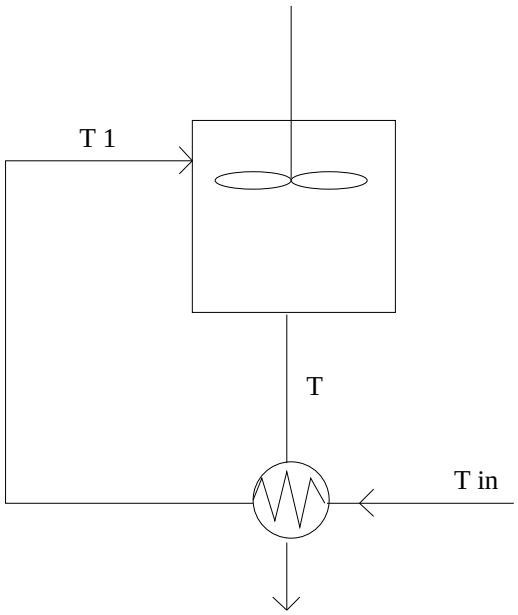


Figure 3.3: Preheating the feed with the product

exchanger becomes more effective, but it never becomes unstable as $\alpha < 1$. Also note that (7) is identical to the recycle example in (3) with no reaction.

**Class 5. Heating or cooling.** Consider a mixing tank with heating or cooling and no reaction. An energy balance yields:

$$\frac{dT}{dt} = \frac{1}{\tau_0}(T_{in} - T) - \beta(T - T_{cool}); \quad \lambda = -\frac{1}{\tau_0} - \beta \tag{3.8}$$

where $\beta = UA/Mc_p$ is a parameter (inverse of thermal time constant) , $T_{in}$ the feed temperature, and $T_{cool}$ the cooling (or heating) water temperature. The heating or cooling thus introduces negative feedback which makes the response faster, which is the opposite of the preheating considered above.

**Class 6. Flash tank with heating**. Consider a flash tank where products are withdrawn both as vapor $V$ and liquid $L$. The material balance for component A yields

$$M\frac{dx_A}{dt} = Fz_A - Lx_A - Vy_A \tag{3.9}$$

If we assume that $V$ (or $L = F - V$) is an independent variable (and specifically does not depend on composition) then the pole (eigenvalue) becomes

$$\lambda = -\frac{1}{\tau_0}(K\frac{V}{F} + \frac{L}{F}) \tag{3.10}$$

where $K = dy_A/dx_A$ is the local slope of the equilibrium line. In most cases $K$ is reasonably close to 1 and we find that $\lambda$ is close to $-1/\tau_0$, but in theory it may take on any negative real value.

Now consider the case where *the heat input $Q$ is the independent variable*, and where $V$ indirectly depends on composition because $H_{vap}$ depends on composition. In this case rather surprising effects may occur. By neglecting heat capacity terms in the energy balance we get

$$V = Q/H_{vap}; \quad H_{vap} = y_A H_{vap,A} + y_B H_{vap,B} \tag{3.11}$$

Here we have assumed that the heat of vaporization depends linearly on composition. Introducing this into (3.9) and using $L = F - V$ results in the eigenvalue

$$\lambda = -\frac{1}{\tau_0}(K\frac{V}{F} + \frac{L}{F}) + \frac{1}{\tau_0}K\frac{V}{F}\frac{x_A - y_A}{\frac{H_{vap,B}}{H_{vap,B}-H_{vap,A}} - y_A} \tag{3.12}$$

Assume that component A is the least volatile component such that $x_A > y_A$ and at the same time has the smallest heat of vaporization such that $H_{vap,B} > H_{vap,A}$ (this is not very common but does happen). In this case we find that the composition dependency of $V$ has introduced *positive feedback* in the system, but the response may never become unstable.

**Class 7. Exothermic reaction with evaporization**. Next consider an example which is quite similar to the one above in that $V$ depends on composition.

First consider the material balance for a flash tank with a 1st order reaction A $\rightarrow$ B. The temperature is assumed constant (e.g., by adjusting the pressure). The material balance for component A yields

$$M\frac{dx_A}{dt} = Fz_A - Lx_A - Vy_A - kx_A M \tag{3.13}$$

If we assume that $V$ (or alternatively $L = V - F$) is an independent variable then the eigenvalue becomes

$$\lambda = -\frac{1}{\tau_0}(K\frac{V}{F} + \frac{L}{F}) - k \tag{3.14}$$

and we note as found before that the reaction has introduced additional negative feedback.

Now consider the case where an exothermic adiabatic reactor is cooled by evaporization, that is, the vapor flow $V$ is caused by the heat released by the reaction and thus *$V$ depends on composition*. This may change the dynamics drastically as is shown next. By neglecting heat capacity terms in the energy balance we get

$$V = Mkx_A(-H_{rx})/H_{vap} \tag{3.15}$$

where $rM = kx_A M$ [kmol/s] is the reaction rate. Introducing this into (3.13) and using $L = F - V$ results in the eigenvalue

$$\lambda = -\frac{1}{\tau_0}(K\frac{V}{F} + \frac{L}{F}) - k + \frac{1}{\tau_0}\frac{V}{F}(1 - \frac{y_A}{x_A}) \tag{3.16}$$

Assume that A is the heavy component such that $x_A > y_A$. Then we find that the composition dependency of $V$ has introduced *positive feedback* in the system, and the

response becomes slow, and even unstable in some cases. The positive feedback can be explained as follows: An increase in $x_A$ yields an increased reaction rate, which increases $V$, which removes relatively more of light component B from the liquid, which increases $x_A$ even more, etc.

**Class 8. Composition dependent recycle: Mass reflux in distillation.** It was recently recognized by Jacobsen and Skogestad (1991) that one may get instability and multiple steady states in ideal two-product distillation if the liquid reflux is specified on a mass (or volume) basis, $R_w$ [kg/s], instead of on a molar basis, $R$ [kmol/s]. The motivation for this specification is that the liquid flow rate in pumps or valves rarely can be said to be specified on a molar basis. The instability may even occur for cases with a single equlibrium stage. Consider for example the two staged system in Fig 3.4. Assuming negligible holdup in the top stage and equilibrium between the two

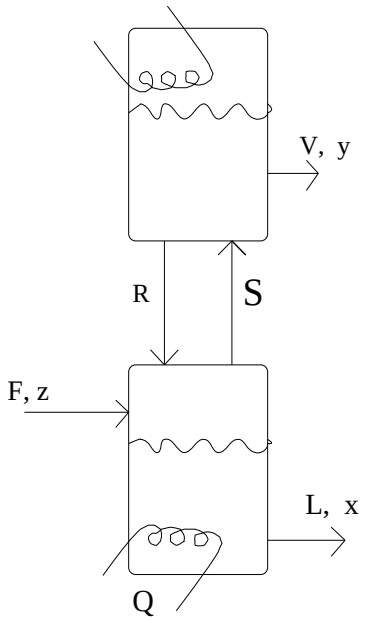


Figure 3.4: Simple distillation-like system

stages, the material balance for the system becomes as before:

$$M\frac{dx_A}{dt} = Fz_A - Lx_A - Vy_A \tag{3.17}$$

If R and S are independent variables specified on a molar basis, the eigenvalue becomes:

$$\lambda = -\frac{1}{\tau_0}(K\frac{V}{F} + \frac{L}{F}) \tag{3.18}$$

Consider now the effect of specifying the boilup, S, on a molar basis, and the liquid reflux, R, on a *mass basis*. The vapor flow from the system is the difference of these:

$$V = S - \frac{R_w}{M_w}, \quad M_w = y_A M_{wA} + (1 - y_A)M_{wB} \tag{3.19}$$

where $M_{wA}$, $M_{wB}$ and $M_w$ are the molar weights of component A, B and the mixture respectively. The eigenvalue now becomes:

$$\lambda = -\frac{1}{\tau_0}(K\frac{V}{F} + \frac{L}{F}) + \frac{1}{\tau_0}K(\frac{S}{F} - \frac{V}{F})\frac{x_A - y_A}{y_A + \frac{M_B}{M_A - M_B}} \tag{3.20}$$

Hence, we have introduced *positive feedback*, and the system may easily go unstable.

## 3.4 Discussion

By combining a few simple effects like the ones above one may easily get very complex behavior. Consider for example the CSTR with a 1. order reaction and an Arrhenius type rate expression. For the adiabatic case (combined class 1 and 3) there may be several steady states (van Heerden, 1953), and if heating or cooling is introduced, the system may behave in a number of qualitatively different ways, including limit cycle behavior (Uppal *et al.*, 1974).

The analysis of a system is further complicated by the fact that there are a number of ways of choosing the controlled (specified) variables of a plant, and because this choice may have a large impact on the dynamic characteristics. Even the choice of specification of a flow on mass or volume basis instead of on molar basis, as in class 8 above, may change a system from having a unique stable steady state to having multiple steady states or instability. In addition, there are normally many different ways of choosing which variables should be the independent ones.

## 3.5 Conclusion/Proposition for further work

A system with recycle of mass or energy may sometimes be considered analoguous to a closed loop feedback control system with positive feedback. Hence, the system eigenvalues may be shifted closer to the right half plane, and yield longer response times and greater sensitivity to disturbances. The positive feedback effect may also cause instability or nonlinear behavior such as limit cycles or even chaotic behavior.

In the general case the positive feedback analogy may not hold. The feedback effect caused by e.g. recycle may in general move the poles of the plant to almost any point in the complex plane, complicating any unified approach to analyzing recycle systems.

A further complication arize from the fact that the choice of specified (independent) variables has a large impact on the plant behavior. The number of possible set of specified variables for a given plant is usually very large.

There is a need for a systematic classification of effects which may introduce complex behavior in a plant. By labelling and analyzing different effects, it should be possible to increase the understanding of different phenomena, and to provide some indicators as to when they occur.

# References

[1] Aris,R. and Amundson, N.R.(1958). An analysis of chemical reactor stability and control. Ch.Eng.Sci, vol 7,no 3, pp 121-155.

[2] Denn, M.M. and Lavie, R. (1982). Dynamics of Plants with Recycle. The Chem. Eng. J., 24, pp 55-59.

[3] Gilliland, E.R., Gould, L.A. and Boyle, T.J. (1964). Dynamic effects of material recycle. Preprints JACC, Stanford, California pp 140-146.

[4] Gray, P. and Scott, S.K. (1990). Chemical Oscillations and Instabilities. Nonlinear Chemical Kinetics. Clarendon Press, Oxford, ISBN 0198556462

[5] Jacobsen, E.W. and Skogestad, S. (1991). Multiple Steady States in Ideal Two Product Distillation. AIChE Journal, vol 37, No. 4., pp 499-511.

[6] Kapoor, N., McAvoy, T.J, Marlin, T.E. (1986). Effect of Recycle Structure on Distillation Tower Time Constants. AIChE J. vol. 32, no. 3, pp 411-418

[7] Luyben, W.L. (1992) Dynamics and Control of Recycle Systems. Part 2 - Comparison of Alternative Process Designs. Paper submitted to IEC Research.

[8] Papadourakis, A., Doherty, M.F. and Douglas, J.M. (1989). Approximate Dynamic Models for Chemical Process Systems. Ind. Eng. Chem. Res. 28, No. 5, 546-552

[9] Papadourakis. A, Doherty, M.F. and Douglas, J.M. (1987). Relative Gain Array for Units in Plants with Recycle. Ind. Eng. Chem. Res., Vol 26, 1259-1262.

[10] Pareja, G. and Reilly, M.J. (1969). Dynamic Effects of Recycle Elements in Tubular Reactor Systems. IEC Fund. 8, 442.

[11] Uppal, A., Ray, W.H. and Poore, A.B (1974). On the dynamic behavior of continuous stirred tank reactors. Ch.Eng.Sci. vol 29, pp 967-985

[12] Uppal, A., Ray, W.H. and Poore, A.B. (1976). The classification of the dynamic behavior of continuous stirred tank reactors-Influence of reactor residence time. Ch.Eng.Sci, vol 31, pp 205-214.

[13] van Heerden, C. (1953). Autothermic Processes. Properties and Reactor design. Industr. Engng. Chem. (Industr.), 45, 1242

[14] Verykios, X.E. and Luyben, W.L. (1978). Steady-state Sensitivity and Dynamics of a Reactor/Distillation Column System with Recycle. ISA Transactions, vol 17, no. 2. pp 31-41.

# Chapter 4

# The Dynamic Behavior of Cascades. Part 1: A transfer function approach

John Morud and Sigurd Skogestad*
Chemical Engineering
University of Trondheim - NTH
N-7034 Trondheim, Norway

A preliminary version was presented at
AIChE Annual Meeting, Miami Beach, USA, Nov. 12-17 1995

**Abstract**

The dynamic behavior of cascade processes is examined. By a cascade process, we here refer to an interconnected system consisting of many similar subsystems placed after one another, in such a way that a subsystem is influenced only by its nabor subsystems. An example of such a process is a distillation column, which is essentially a cascade interconnection of its individual trays.

By using Laplace transform techniques, we first show how the poles of simple cascades may be determined from the knowledge of the subsystem transfer functions. Knowing these pole locations, it is then straightforward to obtain, for example, a time response of the cascade. We then proceed to show how positive feedback interconnections of such cascade sections may result in very long time constants. Such long time constants have been observed in high purity distillation columns; in fact, the magnitude of these time constants may increase exponentially with the number of stages in the column.

*Address correspondence to this author. Fax: 47-73594080, E-mail: skoge@kjemi.unit.no

## 4.1 Introduction

Although most chemical processing plants consist of rather simple elements—such as flash tanks and pipes—their overall behavior can be rather complex, and very different from the behavior of the individual elements. An example is a distillation column, which is essentially a cascade interconnection of many simple flash tanks (trays). Even though the dynamic behavior of the individual elements—the trays—is easy to understand, it is not obvious without prior knowledge how the overall column behaves.

The purpose of this paper is to analyze the behavior of such cascaded processes. With a cascade we here refer to an interconnected system consisting of many similar subsystems placed after one another, in such a way that a subsystem is influenced only by its nabor subsystems. The obvious examples of cascades would be the countercurrent separation processes (such as distillation), or countercurrent heat exchangers. Many series connections of processing units also fall within this class, as the units in a series interconnection of processing units are often influenced by its *downstream* as well as its upstream neigbor. For example, the flow rate from a unit is often influenced by the pressure in the downstream unit.

We emphasize that it is not our purpose to develop accurate models for computer simulation of cascade processes. Such simulation models are well established, and it is straightforward to do numerical simulations of, for instant, a distillation column. Our main purpose is qualitative insight into cascade behavior.

In the paper, we treat cascades from a general point of view, using Laplace transform techniques. We first define what we mean with a cascade, and give an expression for the pole locations of cascades consisting of identical scalar subsystems. We then specialize on conservative systems, which typically arise from conservation equations for mass and energy. We proceed by giving several examples, i.e. by analyzing the concentration dynamics of a stripping column; the pressure dynamics of a train of vessels; and the dynamics of heat conduction in plug flow. Finally, we explain why the interconnection of two linear cascades may result in very long time constants. In fact, these time constants may increase exponentially with the number of stages in the cascade sections.

The rest of this introduction is devoted to reviewing previous work.

Lapidus and Amundson (1950) consider the transient behavior of adsorbtion and extraction equipment. By analytical treatment, they solve simple models of such columns, and find expressions for the step responses. Their treatment is rather involved, but contains many insights.

Montroll and Newell (1952) approximate multistaged cascade processes by nonlinear partial differential equations, and find analytical solutions for such equations.

Rosenbrock (1960) discusses a "conservation property" of distillation columns. He shows how a particular measure of deviation from steady state operation may be thought of as a "conserved" property in the column.

Rosenbrock (1962) reviews previous work on the transient behavior of distillation columns and heat exchangers. He discusses approximation of distillation column models by means of partial differential equations.

Williams (1963) reviews the status of results on the dynamic behavior of mass

transfer processes at that time (1963), and lists some problems that require further investigation (per 1963).

Haagensen and Lees (1966) compare experimental frequency responses with theoretical models for a gas absorbtion column, and obtain fair agreement between the experiments and their model. The theoretical model consists of simple transfer function models derived from mass and energy balances.

Levy *et. al.* (1969) perform modal decompositions of some models for binary distillation. They conclude that the composition dynamics is much slower than the hydraulics, which means that these phenomena tend to be decoupled; that is, the hydraulics may be considered quasi-stationary compared to the composition dynamics.

Osborne (1971) develops approximate models for multicomponent distillation columns by using partial differential equations. Simulations indicate that his approach yields accurate results.

Kim and Friedly (1974) study countercurrent cascades of equilibrium stages, and develop simple low-order-plus-delay transfer functions for such cascades. They refer to Lapidus and Amundson (1950) as being the first to obtain analytical expressions for the eigenvalues of countercurrent cascades.

The lecture notes by Asbjørnsen (1974) contain analytical derivations of transfer functions for simple cascades (among other things). The lecture notes also contain derivations of eigenvalues of simple cascades.

Wong and Luus (1980) consider model reduction of multistage systems by means of orthogonal collocation. They obtain good agreement between step responses of their reduced order models with the original high order models.

Cho and Joseph (1983) use partial differential equations approximations of separation processes together with orthogonal collocation in order to obtain reduced order models of such processes.

Fuentes and Luyben (1983) consider control of high-purity distillation columns. By computer simulations of columns, they show that such columns may be controlled effectively despite the large linearized time constants of high-purity distillation columns.

Celebi and Chimowitz (1985) continue the work by Kim and Friedly, and derive simple second-order-plus-delay transfer functions for cascades.

Kapoor and McAvoy (1986a) study the effect of distillation column recycle structure on distillation column time constants, and present a method for estimating time constants of such columns.

Kapoor and McAvoy (1986b) present analytical expressions for predicting distillate and bottoms composition transient responses for distillation columns.

Skogestad and Morari (1987) develop simple transfer function models for binary distillation columns, and find simple expressions for the dominant time constant of such columns. For high purity columns, they found excellent agreement between the simple expressions and detailed calculation.

## 4.2 Cascade interconnections

Most of this paper is specialized to a simple type of cascades, namely scalar cascades consisting of identical subsystems. However, we will first present what we mean by a cascade *in general*.

### 4.2.1 Distinctions and definitions

We distinguish between cascades with **identical** and **non-identical** subsystems and between **linear** and **nonlinear** cascades.

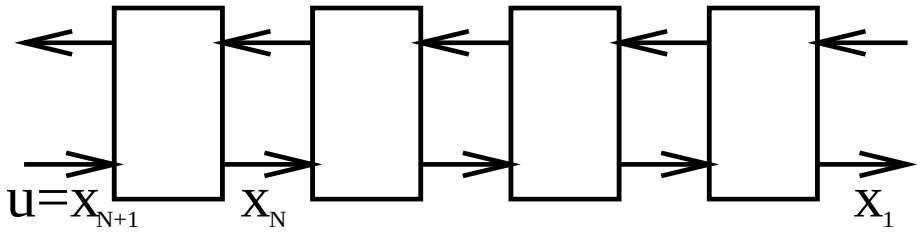


Figure 4.1: General cascade interconnection

#### Nonlinear cascades

By a **cascade**, we mean a system of N similar subsystems placed after one another, such that the state of subsystem $j$ is determined by the subsystem preceding and following that subsystem (see Fig. 4.1). Formally, we may write $x_j = \mathcal{N}_j(x_{j+1}, x_{j-1})$, where $x_j$ is a vector that determines the state of subsystem $j$ ($j = 1, 2, \cdots, N$), and $\mathcal{N}_j$ is an (in general nonlinear) operator. This definition is fairly general—perhaps too general to yield much insight into cascade behavior. For insight, it is thus convenient to study linear cascades.

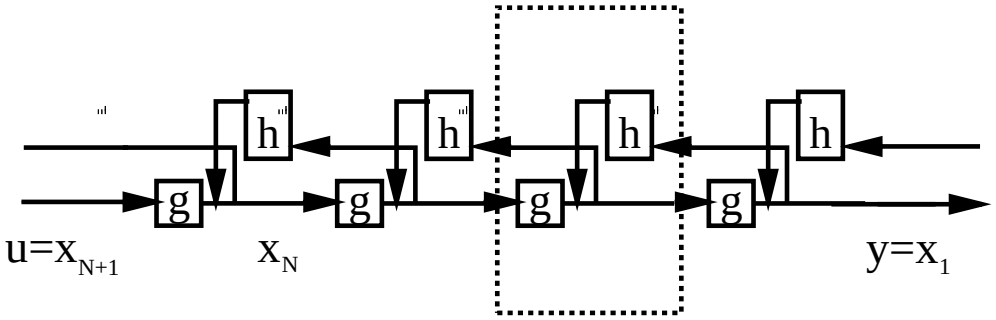


Figure 4.2: Linear cascade interconnection

### Linear cascades

By a **linear** cascade, we mean a system on the form:

$$x_j(s) = G_j(s)x_{j+1}(s) + H_j(s)x_{j-1}(s) \tag{4.1}$$

Here, $G_j$ and $H_j$ are transfer matrixes. This interconnection structure is shown in Fig 4.2. A special case applies to scalar systems, in which case we will use lower case letters, $g_j$ and $h_j$. In the case where $g_j$ and $h_j$ are the same for all stages, we drop the subscript $j$.

## 4.3 Linear cascades of identical subsystems

### 4.3.1 Theoretical results

It is straightforward to do numerical simulations of such systems, even in the nonlinear case. For example, one may use a standard state space model. However, there are other computational forms, which may be convenient for analytical purposes. The aim of the present section is to find analytical expressions for the pole and zero locations of scalar cascades.

#### A recursion formula

Consider a linear cascade with N stages—described by eq. 4.1. Suppose that we want to find the overall transfer function, say $T_N$, between $u$ ($\equiv x_{N+1}$) and $x_1$ (see Fig. 4.2). To do this, consider factorizing $T_N$ into

$$T_N = \Pi_{j=1}^{N} S_j \tag{4.2}$$

where $S_j$ is the transfer function between two consecutive stages, $x_j = S_j x_{j+1}$. By inserting this expression into equation 4.1 and collecting terms, one obtains the following recursion formula for $S_j$:

$$S_j = (I - H_j S_{j-1})^{-1} G_j, \quad S_0 = 0, \quad j = 1, 2 \cdots N \tag{4.3}$$

Note that the transfer function $S_0$ is a fictitious quantity; the meaningful $S_j$'s start with $j = 1$.

#### Structure of the overall transfer function.

The advantage of the recursion formula above, is that it makes it possible to analyze analytically the connection between the behavior of the subsystems and the behavior of the overall system. For scalar linear systems of identical subsystems,

$$x_j(s) = g(s)x_{j+1}(s) + h(s)x_{j-1}(s) \quad , \tag{4.4}$$

the overall transfer function, $T_N$, from one end of the cascade to the other, is (Appendix A):

$$T_N(s) = \frac{\lambda_1^N - \lambda_2^N}{\lambda_1^{N+1} - \lambda_2^{N+1}} g(s); \quad \lambda_{1,2} = \frac{1 \pm \sqrt{1 - 4g(s)h(s)}}{2} \tag{4.5}$$

In Appendix A, it is shown that this may be factorized into:

$$T_N(s) = \frac{g(s)^N}{\Pi_n(1 - k_n g(s)h(s))} \tag{4.6}$$

where:

$$k_n = 4\cos^2(\frac{n\pi}{N+1}), \quad n = 1, 2, \cdots \lfloor \frac{N+1}{2} \rfloor \tag{4.7}$$

The floor brackets $\lfloor \rfloor$ means rounded down to the nearest integer.

Also, since from eq. 4.2 :

$$T_N = \Pi_{j=1}^N S_j = S_N \Pi_{j=1}^{N-1} S_j = S_N T_{N-1} \tag{4.8}$$

it follows that the transfer function, $S_N$, from the input at one end to the output at the same end (i.e. from $x_{N+1}$ to $x_N$) is given as:

$$S_N = \frac{T_N}{T_{N-1}} \tag{4.9}$$

These expressions provide a generalization of results of previous authors (e.g. Celebi and Chimowitz 1985; Kim and Friedly 1974; Lapidus and Amundson 1950). The relevance of achieving a factorized expression for $T_N$, is that this makes the relation between the subsystems and the overall system transparent.

This means that the pole (and zero) locations of the overall system, $T_N$, may be inferred directly from the subsystem transfer functions, $g$ and $h$. The pole locations are important, as they determine the stability and speed of response of the system, and thus essentially determine its dynamic behavior.

Note that the zeros of the denominator, $\Pi_n(1 - k_n g(s)h(s))$, all lie on the root locus of $L \equiv gh$, with feedback gains as given by the $k_n$'s (equation 4.7). For simple systems, the root locus of $gh$ may easily be sketched by hand. It is thus easy to predict qualitatively the pole locations of scalar cascades of identical subsystems, and thus their dynamic behavior.

Before we turn to some specific examples of cascades, we specialize the results of this section (eqs. 4.4 and 4.6) to conservative systems.

### 4.3.2 Special case: First order systems

We consider the special case where $g(s)$ and $h(s)$ are first order transfer functions, i.e. the cascade has the form:

$$\dot{x}_j = \underbrace{\frac{\gamma}{1+\tau s}}_{g(s)} x_{j+1} + \underbrace{\frac{\beta}{1+\tau s}}_{h(s)} x_{j-1} \tag{4.10}$$

The transfer function from one end of the cascade to the other then becomes:

$$N \quad even: \quad T_N(s) = \frac{\gamma^N}{\Pi_{n=1}^{N/2}[(1+\tau s)^2 - k_n\gamma\beta]} \tag{4.11}$$

$$N \quad odd: \quad T_N(s) = \frac{\gamma^N(1+\tau s)}{\Pi_{n=1}^{(N+1)/2}[(1+\tau s)^2 - k_n\gamma\beta]} \tag{4.12}$$

Note that the pole excess is $N$ in both cases.

### Pole locations

The pole locations are given by the characteristic function (denominator of $T_N(s)$):

$$(1+\tau s)^2 - k_n\gamma\beta = 0 \tag{4.13}$$

Inserting $k_n$ from eq. 4.7 and solving for $s$ yields

$$s = \frac{1}{\tau}[-1 \pm 2\sqrt{\beta\gamma}\cos(\frac{n\pi}{N+1})]; \quad n = 1, 2\cdots\lfloor\frac{N+1}{2}\rfloor \tag{4.14}$$

which is the desired expression for the pole locations. These pole locations are distributed on the interval $-\frac{2}{\tau}$ to 0. Note that in this particular case, all eigenvalues are supposed to be simple roots of the characteristic equation; thus do not consider $\pm 0$ to mean a double eigenvalue.

### Poles of first order conservative systems

We consider an even more restricted case, first order conservative systems. Here, we define conservative to mean that the sum of coefficients $\beta$ and $\gamma$ is one, i.e.:

$$\beta + \gamma = 1 \tag{4.15}$$

The equation for the cascade may then be written:

$$\dot{x}_j = \underbrace{\frac{1-\beta}{1+\tau s}}_{g(s)} x_{j+1} + \underbrace{\frac{\beta}{1+\tau s}}_{h(s)} x_{j-1} \tag{4.16}$$

The motivation for the term "conservative" is that some cascades described by conservation equations for mass or energy has this property. This will become clear later, when we present examples of such cascades.

In this case, the expression for the pole locations, eq. 4.14 becomes:

$$s = \frac{1}{\tau}[-1 \pm 2\sqrt{\beta(1-\beta)}\cos(\frac{n\pi}{N+1})]; \quad n = 1, 2\cdots\lfloor\frac{N+1}{2}\rfloor \tag{4.17}$$

Similar expressions have been obtained by previous authors (e.g. Celebi and Chimowitz 1985; Kim and Friedly 1974; Lapidus and Amundson 1950).

We distinguish between the following two cases:

1. $\beta \in < 0, 1 >$. In this case, the poles are negative real (i.e. in the Left Half Plane).
2. $\beta \notin < 0, 1 >$. In this case, the poles are complex conjugates in the Left Half Plane.

The slowest time constant—corresponding to a pole close to zero—occurs when $\beta = 1/2$. To see this, introduce the approximation $\cos x \approx 1 - x^2/2$ into eq. 4.17, which applies when $x$ is small, i.e. when $N$ is large. The slowest pole and corresponding time constant then becomes (for $n = 1$):

$$\beta = \frac{1}{2}: \quad s \approx -\frac{1}{2\tau}(\frac{\pi}{N+1})^2 \Rightarrow \tau_1 \approx \frac{2}{\pi^2}\tau N^2 \tag{4.18}$$

Hence, the time constant may increase proportionally with the *square* of the number of stages (relative to the time constant of a single stage), which is a well known result (Lapidus and Amundson, 1950). However, if $\beta$ is not exactly equal to $1/2$, then as $N \to \infty$, the slow pole approaches

$$\beta \neq \frac{1}{2}: \quad s = \frac{1}{\tau}[-1 + 2\sqrt{\beta(1-\beta)}] \Rightarrow \tau_1 = \frac{\tau}{-1 + 2\sqrt{\beta(1-\beta)}} \tag{4.19}$$

That is, the slow pole approaches a fixed value. Hence, the time constant is asymptotically **independent** of the number of stages if $\beta \neq 1/2$.

Note that all this applies to an **open ended** column section. As will be shown below, the slowest time constant may increase **exponentially** with $N$ when two linear cascades are interconnected.

We turn to some specific examples of cascade interconnections.

### 4.3.3 Examples

The purpose of the examples below, is to illustrate the application of the above results, and to draw the attention to similarities between different physical systems. These similarities make it possible to use the examples as analogies for each other, thus enhancing the understanding of each of them individually.

#### Example 1. Concentration dynamics of a stripping or adsorbtion column

Consider the concentration dynamics of a section in a stripping or absorbtion column. It is assumed that the equilibrium line is linear in the range of compositions in the section. As a simple model, take:

$$M\frac{dx_j}{dt} = L(x_{j-1} - x_j) + V(y_{j+1} - y_j); \quad y_j = Kx_j \tag{4.20}$$

where $M$ is the molar holdup on each stage; $L$ and $V$ are the liquid and vapor molar flow rates; and $x$ and $y$ are the liquid and vapor mole fractions of light component.

Taking the Laplace transform and collecting terms we obtain:

$$x_j = \frac{1-\beta}{1+\tau s}x_{j+1} + \frac{\beta}{1+\tau s}x_{j-1} \tag{4.21}$$

where $\beta = \frac{1}{1+\frac{VK}{L}}$ and $\tau = \frac{M}{L+VK}$. The quantity $\tau$ may be interpreted as the time constant of a single tray, whereas the gain $\beta$ is a function of $\frac{VK}{L}$–the ratio between the slopes of the equilibrium- and the operating line in a McCabe-Thiele diagram.

This is seen to be a cascade on standard form. We observe the following:

1. This is a **conservative** system according to the definition given in the previous section (sum of coefficients equal 1).

2. The eigenvalues (poles) are all real in this case, since $\beta \in < 0, 1 >$.

3. The slowest eigenvalue–which is the one closest to zero–is given by eq. 4.19, except in the special case with $\beta = 1/2$. For the special case $\beta = 1/2$, which corresponds to parallel equilibrium- and operating lines in a McCabe-Thiele diagram, we get instead $s = \frac{1}{\tau}[-1 + \cos(\frac{\pi}{N+1})]$ (set $n = 1$, $\beta = 1/2$ in eq. 4.17). According to the approximation above, eq. 4.18, the time constant may then be proportional to $N^2$, the square of the number of stages.

   The next slowest eigenvalue is found for $n = 2$ ($s = \frac{1}{\tau}[-1 + \cos(\frac{2\pi}{N+1})]$ ) and is approximately a factor *four* faster than the slowest one. Again, this only applies in the special case $\beta = 1/2$.

**Example 2. Concentration dynamics of a column section with autocatalytic reaction**

Consider a cascade described by the same model as in the previous example, except that there is an autocatalytic reaction, $A \rightarrow B$, occurring. As a model, we take (mass balance for product, $B$):

$$M\frac{dx_j}{dt} = L(x_{j-1} - x_j) + V(y_{j+1} - y_j) + Mkx_j; \quad y_j = Kx_j \tag{4.22}$$

where $M$ is the molar holdup on each stage; $L$ and $V$ are the liquid and vapor molar flow rates; $k$ is the reaction rate constant; and $x$ and $y$ are the liquid and vapor mole fractions of light component—which is the product, component $B$.

Taking the Laplace transform and collecting terms we obtain:

$$x_j = \underbrace{\frac{\gamma}{1+\tau s}}_{g(s)} x_{j+1} + \underbrace{\frac{\beta}{1+\tau s}}_{h(s)} x_{j-1} \tag{4.23}$$

where $\beta = \frac{1}{1+\frac{VK}{L}-\frac{Mk}{L}}$, $\gamma = \frac{\frac{VK}{L}}{1+\frac{VK}{L}-\frac{Mk}{L}}$ and $\tau = \frac{M}{L+VK-Mk}$. As in the previous example, the quantity $\tau$ may be interpreted as the time constant of a single tray.

This is on the standard form, and the poles are given by eq. 4.14. For the cascade to be stable, we demand that all poles stay in the Left Half Plane, which means that (set $Re(s) < 0$ into the equation and solve for $\frac{Mk}{L}$):

$$\frac{Mk}{L} < 1 + \frac{VK}{L} - 2\cos(\frac{\pi}{N+1})\sqrt{\frac{VK}{L}} \tag{4.24}$$

This is thus a necessary and sufficient criterion for stability of the cascade with autocatalytic reaction. Note that the system tends to become less stable as the number of stages, $N$, increases.

**Example 3. Pressure dynamics of a train of vessels**

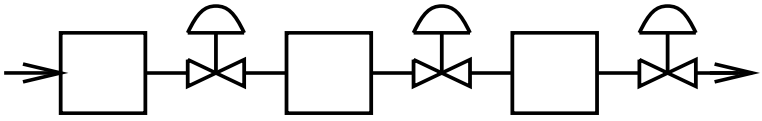

Figure 4.3: Pressure vessels in series

Consider the pressure dynamics of a train of vessels, as depicted in Fig 4.3. The pressure is specified at both sides. This has sometimes been proposed as a conceptual model of the vapor dynamics of distillation columns, where the valves represent the pressure drop due to flow of vapor through the trays (e.g. Rademaker *et. al.*, 1975). Inertia effects are assumed negligible, and the pressure drop between the vessels is assumed to be proportional to the square of the volume flow rate, and the same for all vessels. A simple model for the system may then be written as an equation for the pressure, $p_j$ (deviation variable), in vessel $j$ (derived in Appendix B):

$$2\tau \frac{dp_j}{dt} = p_{j+1} - 2p_j + p_{j-1} \tag{4.25}$$

Here, the time constant of a single vessel, $\tau = \frac{\Delta p}{nP} \cdot \tau_{res}$, is a function of the pressure drop between vessels, $\Delta p$; the absolute pressure in the vessels, $P$; the polytropic coefficient, $n$; and the vessel residence time, $\tau_{res}$.

The model may be written in the standard form as:

$$p_j = \frac{1/2}{1+\tau s} p_{j+1} + \frac{1/2}{1+\tau s} p_{j-1} \tag{4.26}$$

so

$$g(s) = h(s) = \frac{1/2}{1+\tau s} \tag{4.27}$$

which is a special case of eq. 4.16 with $\beta = 1/2$. The dominant time constant for $N$ vessels in series is then:

$$\tau_1 \approx \frac{2}{\pi^2} \tau N^2 \approx 0.2 \tau N^2 \tag{4.28}$$

Note that this time constant apply to constant pressure boundary conditions, and not flow rate boundary conditions. It turns out that the case of fixed inlet flow rate and fixed outlet pressure still has a time constant proportional to $N^2$, as will be discussed below.

**Example 4. A distributed parameter system: Heat conduction in plug flow**

Consider plug flow of a conducting fluid in an insulated pipe. The temperature, $T$, of the fluid is governed by the equation:

$$\frac{\partial T}{\partial t} + u\frac{\partial T}{\partial z} = \nu\frac{\partial^2 T}{\partial z^2} \tag{4.29}$$

where $u$ and $\nu$ are the fluid velocity and thermal diffusivity; and $z$ is the position in the pipe.

The purpose of presenting this example is threefold: First, to exemplify the application of the above results on a distributed parameter system; second, to show how the stability of finite difference schemes for numerical calculations may be analyzed in this framework; and third, to provide a physical analogy for the other examples. This analogy will be exploited in a later section.

By discretizing using central differences with $h = L/N$ this becomes:

$$\frac{dT_j}{dt} + u\frac{T_{j+1} - T_{j-1}}{2h} = \nu\frac{T_{j+1} - 2T_j + T_{j-1}}{h^2} \tag{4.30}$$

which may be recast into the standard form by taking Laplace transforms and collecting terms:

$$T_j = \frac{1/2 - Pe/4}{1 + \tau s}T_{j+1} + \frac{1/2 + Pe/4}{1 + \tau s}T_{j-1} \tag{4.31}$$

where $Pe = \frac{uh}{\nu}$ is a Peclet number and $\tau = \frac{h^2}{2\nu}$ is a (conduction) time constant.

This is again a special case of eq. 4.16 with $\beta = 1/2 + Pe/4$. In this case the parameter $\beta$ is not bounded between zero and one, which means that we may get complex conjugate poles for values of $\beta$ outside this range, i.e. for $|Pe| > 2$.

It is well known that one may get numerical difficulties applying central differences in this example when $|Pe| > 2$. This is seen to be caused by very lightly damped complex conjugate poles introduced by the discretization scheme. Integration of this system would therefore be rather difficult by most higher order numerical methods, and it's stability might depend on the way the boundary conditions are implemented.

### 4.3.4 Discussion of examples

**Discussion of example 3: Vapor flow response in column section**

In example 3 we showed that the slow time constant of a number of pressure vessels in series increases as $N^2$—the square of the number of stages—when the pressure is specified at both ends of the cascade. In this subsection we argue that this is the case also for fixed inlet flow rate. For example, this may describe the pressure and vapor flow in response to a change in the heat input (reboiler vapor flow). The argument is similar to that of Skogestad and Morari (1987).

We consider the whole cascade as one black box, with one inlet and one outlet. Consider the response of the outlet flow rate from the cascade, $F_o(t)$, when there is a small step change, $\Delta F_i$ in the inlet flow rate:

$$\Delta F_o(t) = \Delta F_i \cdot s(t) \tag{4.32}$$

Here, $s(t)$ is the output flow response to a unit step in the inlet flow rate.

The total mass balance for the whole cascade is given by:

$$\dot{M} = F_i - F_o(t) \tag{4.33}$$

which may be time integrated from zero to to $\infty$ to yield the total change in holdup between the initial and final steady state:

$$\Delta M = \int_0^\infty (\Delta F_i - \Delta F_o(t))dt = \Delta F_i \int_0^\infty (1 - s(t))dt \tag{4.34}$$

This may be rewritten as:

$$\tau_I = \frac{\Delta M}{\Delta F_i}; \qquad \tau_I \equiv \int_0^\infty (1 - s(t))dt \tag{4.35}$$

Here, we have introduced a new time constant, $\tau_I$, which may be denoted an integral time constant (or time scale), and may be considered to be some sort of lumped time constant of the system. We argue that $\tau_I$ increases as $N^2$ for the cascade, because an increase in the number of vessels in the cascade has two effects on the change in overall holdup, $\Delta M$, in the system at steady state:

1. The total pressure drop increases. This means that a small change in flow rate produces a larger change in pressures when there are many vessels than if there are few. Averaged over all vessels, the average change in pressure, and thus in average holdup per vessel, say $(\Delta M_i)_{av}$, is proportional to the number of vessels, $N$.

2. There are more vessels. This means that the change in holdup, $\Delta M = \sum_1^N \Delta M_i \sim N \cdot (\Delta M_i)_{av}$, increases as $N^2$.

Since the change in holdup in response to a small step in inlet flow rate increases as $N^2$, it follows that $\tau_I = \frac{\Delta M}{\Delta F_i}$ also increases as $N^2$.

Numerical calculations confirm this finding. However, for this case—fixed inlet flow rate to the cascade—the time constant $\tau_1$ (inverse of smallest eigenvalue) is larger than the corresponding time constant, $\tau_1 \approx 0.2\tau N^2$, found for the case of fixed pressure at both ends (In fact, it is larger by a factor four).

### Discussion of example 4

There are several things to be learned from the plug flow example:

1. The example contains the case of pure conduction (heat conduction in a slab) as a special case when $Pe = 0$ and $\beta = 1/2$. This is when the largest time constants occur.

2. The example provides an analogy for both example 1 (composition dynamics of stripping column) and example 2 (pressure dynamics of a train of vessels).

   For stripping columns, the largest time constant occurs when the operating line and the equilibrium line are parallel. The phenomenon may then be interpreted as

caused by diffusion like—or random walk—behavior. In practice, the equilibrium line and the operating line are not parallel, and the column then behaves much more like plug flow, with short time constants.

The second example, pressure dynamics in a train of vessels, is seen to be analoguous to pure heat conduction in a slab. It is important to note, however, the assumption of negligible inertia effects of the gas.

3. The example shows the effect of using central differences for the convection term in convection-diffusion equations (not advisable when convection dominates conduction/diffusion).

### 4.3.5 Time constants of interconnected cascades

So far, we have only considered open ended cascades. In the cases studied, the longest time constant approaches a limit as $N \to \infty$ (An exception occurs when $\beta = 1/2$, in which case the longest time constant increases as the square of the number of stages). However, as we show in this section, the interconnection of two such linear cascades (with finite time constants) may result in very large time constants.

We start by explaining how positive feedback between two general transfer functions may result in very large time constants, and proceed by using this to explain why the interconnection of two cascades may result in such long time constants. In fact, the slowest time constant of such an interconnection may increase exponentially with the number of stages in the cascade.

#### Positive feedback may result in very long time constants

We give a simplified argument why positive feedback may result in very long time constants. The arguments are similar to those of Kapoor and McAvoy (1986).

Consider the feedback interconnection of two transfer functions, $c_1(s)$ and $c_2(s)$, as shown in Fig. 4.4. Each of the two transfer functions may be thought of as representing a column section in, for instant, a distillation column. We assume that the transfer functions $c_i(s)$, $i = 1, 2$, are rational, with a gain **very close to one**, i.e. with a transfer function on the form:

$$c_i(s) = (1 - \epsilon)\frac{\Pi_{zeros}(1 + \tau_z s)}{\Pi_{poles}(1 + \tau_p s)} \tag{4.36}$$

Close to the origin of the complex plane, each transfer function may be approximated as first order transfer functions:

$$c_i(s) \approx \frac{1 - \epsilon}{1 + T_i s} + O(s^2) \quad where \quad T_i = \sum_{poles} \tau_p - \sum_{zeros} \tau_z \tag{4.37}$$

To find the closed loop poles of the interconnected system, we form the return difference:

$$0 = 1 - c_1(s)c_2(s) \approx 1 - \frac{1 - \epsilon_1}{1 + T_1 s} \cdot \frac{1 - \epsilon_1}{1 + T_2 s} \tag{4.38}$$

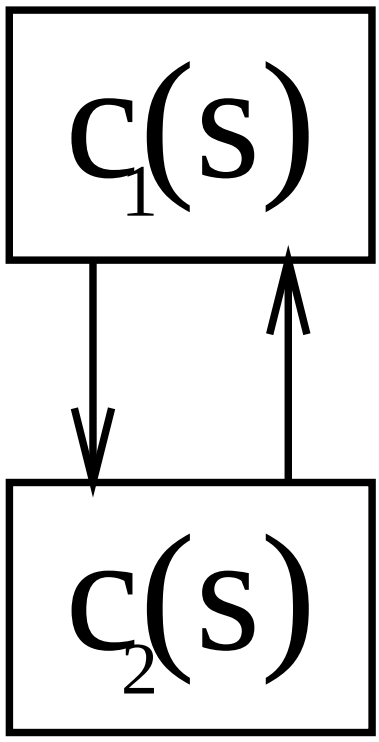


Figure 4.4: Feedback interconnection of transfer functions

Neglecting second order terms, we may solve for the pole closest to the origin:

$$s = -\frac{\epsilon_1 + \epsilon_2}{T_1 + T_2} + O(\epsilon_1^2, \epsilon_2^2) \tag{4.39}$$

Hence, the slowest time constant has been magnified by a factor $\frac{1}{\epsilon_1+\epsilon_1}$ compared to the individual transfer functions, and if the $\epsilon$'s are sufficiently small, the closed loop time constant will be very large. This is seen to be an effect of **positive feedback** between the two transfer functions.

As we will see below, the corresponding $\epsilon$'s may be exponentially small (in $N$) for interconnected cascades.

### A simple distillation model

We discuss a simplified model for binary distillation, as shown in Fig. 4.5. The equivalents to the transfer functions $c_1(s)$ and $c_2(s)$ are shown as dotted boxes. As a simple model, we take (mass balance for light component):

$$M\frac{dx_j}{dt} = L(x_{j-1} - x_j) + V(y_{j+1} - y_j); \quad y_j = Kx_j \tag{4.40}$$

where the notation is as before. We assume that the parameters are constant within each of the two column sections; however, they are different for the two sections. Specifically, we assume that the absorbtion factor in the lower column section, $a_2 = \frac{L}{VK}$,

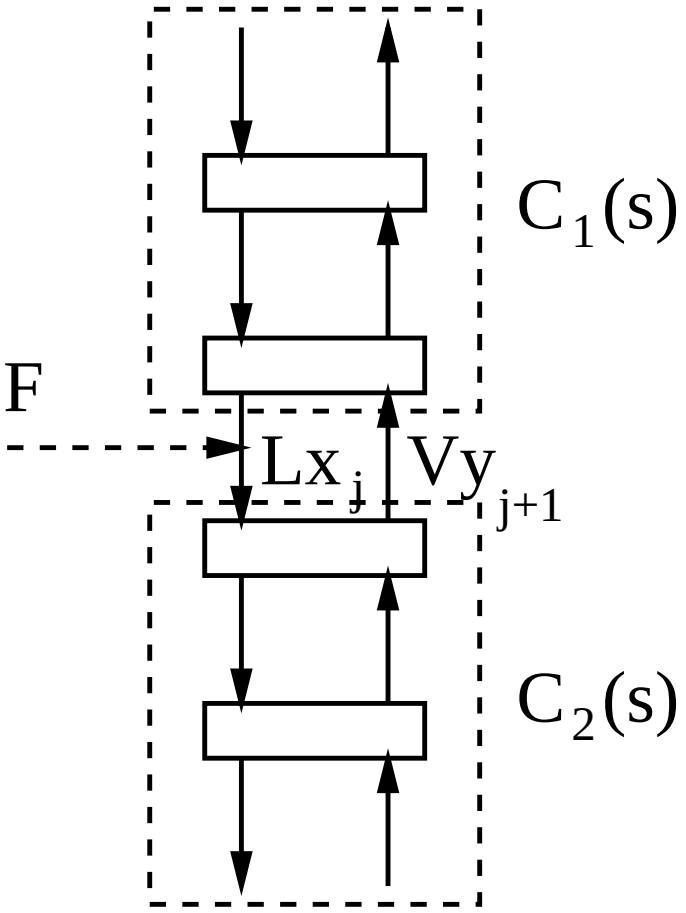


Figure 4.5: Simplified distillation model

is constant and smaller than one in magnitude. Similarly, we assume that the stripping factor in the upper column section, $s_1 = \frac{VK}{L}$, is constant and smaller than one in magnitude. To assume that these are constant within each column section corresponds to approximating the vapor-liquid equilibrium by two straight lines, as shown in Fig. 4.6.

In Appendix C and D, we show that the transfer function from $Vy_{j+1}$ to $Lx_j$ for the upper column section—the transfer function $c_1(s)$—may be approximated at low frequencies as:

$$c_1(s) \approx \frac{1-\epsilon_1}{1+T_1 s} \tag{4.41}$$

where

$$\epsilon_1 \approx s_1^{N_1}(1-s_1); \quad T_1 = \frac{1+s_1}{1-s_1}\tau_1 \tag{4.42}$$

and $s_1 \equiv \frac{V_1 K_1}{L_1}$ is the stripping factor; $\tau_1 = \frac{M}{L_1+V_1K_1}$ is the time constant of a single tray; and $N_1$ is the number of stages in the upper column section.

Similarly, the transfer function $c_2(s)$ for the lower column section may be approxi-

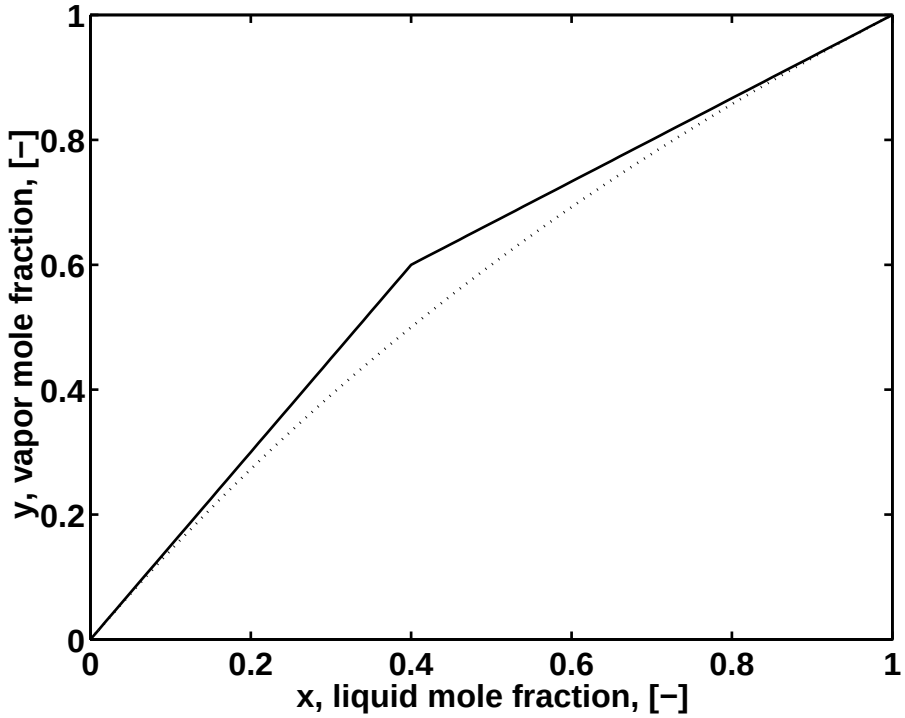


Figure 4.6: Simplified vapor-liquid equilibrium, consisting of two linear segments

mated at low frequencies if we take (Appendix C and D):

$$\epsilon_2 \approx a_2^{N_2}(1-a_2); \quad T_2 = \frac{1+a_2}{1-a_2}\tau_2 \tag{4.43}$$

where $a_2 \equiv \frac{L_2}{V_2 K_2}$ is the absorbtion factor; $\tau_2 = \frac{M}{L_2+V_2K_2}$ is the time constant of a single tray; and $N_2$ is the number of stages in the lower column section.

Using these transfer functions, we then get the desired estimate of the slow time constant of the interconnected column:

$$T = \frac{T_1+T_2}{\epsilon_1+\epsilon_2} = \frac{\frac{1+s_1}{1-s_1}\tau_1 + \frac{1+a_2}{1-a_2}\tau_2}{s_1^{N_1}(1-s_1)+a_2^{N_2}(1-a_2)} \tag{4.44}$$

Now, observe that $\epsilon_1 \to 0$ as $N_1 \to \infty$ (assuming $s_1 < 1$) and $\epsilon_2 \to 0$ as $N_2 \to \infty$ (assuming $a_2 < 1$).

Thus, the longest time constant of the interconnected cascade, $T$, increases **exponentially** with the number of stages in the column. Moreover, observe that it is the larger of $\epsilon_1$ and $\epsilon_2$ that dominates; that is, the column section with the poorest separation determines the dynamics.

### Numerical sample calculation

The estimate of eq. 4.44 has been compared numerically with the smallest eigenvalue found from a linear column model, and it has been established that it yields very

accurate results. For application to distillation columns, the main source of error does not seem to be the simplifications made in the derivation of the estimate, but rather the approximation of the liquid-vapor equlibrium line by two linear segments.

To give an indication of the magnitudes of these errors, consider a case with 82 stages (41 in each section), and constant relative volatility $\alpha = 1.5$. The rest of the assumptions are given in Table 4.1. There is no condenser, and no reboiler.

| Assumption | Numerical value |
|---|---|
| Constant relative volatility | $\alpha = 1.5$ |
| Constant molar holdup | $M = 1$, on each stage |
| Constant molar flows | $L = 2.635$, $V = 3.135$, distillate flow rate $D = 0.5$ |
| Feed flow rate and mole fraction at the middle of the column | $F = 1$ and $z = 0.5$ |

Table 4.1: Assumptions made for cascade model

We compare the three following cases:

1. Numerical calculation of the nonlinear model above. Linearizing the model about the steady state, and calculating the eigenvalues numerically (using MATLAB), yields $\tau = 0.22 \cdot 10^5$.

2. Numerical calculation when the equlibrium line is approximated with two straight lines (yielding $K = 1/\alpha$ in the top section and $K = \alpha$ in the lower section). This yields $\tau = 1.296 \cdot 10^5$.

3. Analytical calculation using the estimate, eq. 4.44. This yields $\tau = 1.295 \cdot 10^5$.

For this many stages, the estimate yields almost the same results as the numerical calculation when the equilibrium lines are the same for the two cases (linear segments). However, the numerical calculation using constant relative volatility yields a time constant that is a factor six lower, indicating that the time constant is sensitive to changes in the vapor-liquid equilibrium line.

## 4.4 Discussion

### Extensions and generalizations

The framework presented in this paper could be extended to more complex situations. For example, nonlinear scalar cascades may in some cases be considered to be piecewise linear, and thought of as an interconnection of several small linear cascades. In order for this patching to be practical, further work is needed for making derivations of overall transfer functions. Remember, however, that the purpose of such derivations is qualitative insight—not numerical computations—as it is hard to compete with state space models when it comes to computer simulations.

It might also be possible to generalize the results to multivariable systems. However, how one might translate insight into subsystem behavior to insight into the behavior of the overall system is not known to the authors. Again, it is straightforward to make numerical computations on a computer.

### "All trays have the same response"

Having realized that one mode is slow, Skogestad and Morari (1987) derived very accurate formulaes for the slow time constant of binary distillation columns based on the assumption that all trays in a column have the same response. That is, they assumed that the change in mole fraction of light component at tray $j$ may be expressed as $\Delta x_j(t) = a_j f(t)$, where $a_j$ represents the amplitude at tray $j$ and $f(t)$ is the response– the same for all stages.

In essence, this is an assumption of one-dimensional (linear) behavior. In the light of the previous subsection, the good results obtained by Skogestad and Morari may therefore not come as a great surprise.

### Ways of understanding the dynamics of cascades

In this paper (Part 1), we have analyzed cascades from a transfer function point of view. We emphasize that this is not the only possible way of understanding the dynamics of such cascades. Another approach, which is used in Part 2 of the paper, is by analogy to other systems. For example, in Part 2, we analyze binary distillation by analogy to diffusion in plug flow. A third approach to analyzing cascades, is by making certain *ad hoc* assumptions, and to derive the consequences of these assumptions. An example is the assumption "All trays have the same response", made by Skogestad and Morari.

### Accuracy of time constant estimates

In the paper, we derived estimates of the slow time constant of a simplified model of binary distillation. The purpose of the derivation was qualitative insight—not to derive more accurate formulas than previous authors.

These estimates—although accurate compared to rigorous calculations on the same model—are not expected to yield accurate results when applied directly to a real life situation. The reason is rather fundamental: small errors at each stage multiply from stage to stage and yield order of magnitude errors when there are many stages.

A remedy is to follow Morari and Skogestad (1987) and express the results in terms of outputs—in this case the product purities—instead of inputs—in this case the number of stages, internal flow rates, etc. This remedy may be thought of as reducing uncertainty by using feedback, and the results then become much more accurate. In practice, product purities are known, so there is no need for making uncertain estimates of these.

## 4.5 Conclusion

In this paper, we have shown how simple cascade systems may be analyzed; first by showing how the poles of scalar cascades may be determined from the subsystem transfer functions. Knowing the pole locations, it is then straightforward to find, for example, time responses of such systems.

Application of the results to stripping or adsorbtion columns with linear equilibrium lines, shows that the slowest time constant of these columns approaches a fixed value when the number of stages becomes large, i.e. when $N \to \infty$ (equation 4.19). An exception occurs when the equilibrium- and the operating lines are parallel, in which case the slowest time constant increases as $N^2$—the square of the number of stages.

We then showed that the interconnection of scalar cascades may result in very long time constants, and that this may be thought of as an effect of **positive feedback** between the cascades. A distillation column may be thought of as such an interconnection of two cascades. In fact, the slow time constant of binary distillation increases exponentially with the number of stages when all other quantities are kept constant.

## Notation

| | |
|---|---|
| $a$ | absorbtion factor, $a = \frac{L}{VK}$ |
| $D$ | distillate flow rate |
| $F$ | feed flow rate |
| $g(s)$ | transfer function in scalar cascade (eq. 4.4) |
| $G(s)$ | transfer function in multivariable cascade (eq. 4.1) |
| $h$ | discretization length in eq. 4.29 |
| $h(s)$ | transfer function in scalar cascade (eq. 4.4) |
| $H(s)$ | transfer function in multivariable cascade (eq. 4.1) |
| $k_n$ | factor defined by eq. 4.7 |
| $K$ | slope of vapor-liquid equilibrium line |
| $L$ | liquid molar flow rate |
| $L(s) = G(s)H(s)$ | "loop" transfer function in cascade |
| $M$ | molar holdup on tray |
| $N$ | number of trays in column |
| $\mathcal{N}$ | nonlinear operator |
| $p$ | pressure (deviation variable) |
| $P$ | absolute pressure |
| $Pe = \frac{uh}{\nu}$ | Peclet number |
| $s$ | Laplace variable; or stripping factor $s = \frac{VK}{L}$ |
| $S(s)$ | transfer function between two consecutive stages |
| $t$ | time |
| $T$ | temperature; or lumped time constant |
| $T(s)$ | overall transfer function for cascade |
| $u$ | equivalent velocity |
| $V$ | vapor molar flow rate |
| $x$ | liquid mole fraction of light component |

| | |
|---|---|
| $y$ | vapor mole fraction of light component |
| $z$ | space coordinate; or feed mole fraction of light component |

Greek

| | |
|---|---|
| $\alpha$ | constant relative volatility |
| $\beta$ | Parameter in eq. 4.16 |
| $\nu$ | diffusivity |
| $\tau$ | time constant |

Subscripts

| | |
|---|---|
| $i$ | index over stages in column |
| $j$ | index over stages in column |
| $N$ | last stage in column |

# References

[1] Asbjørnsen, O. A., 1974. Process Dynamics (Lecture notes). University of Trondheim, Chem. Eng. Laboratory, N7034 Trondheim, Norway

[2] Celebi, C and E.H. Chimowitz, 1985. Analytic Reduced-Order Dynamic Models for Large Equilibrium Staged Cascades. AIChE J., 31, 12, pp. 2039-2051

[3] Cho, Y.S and B. Joseph, 1983. Reduced-Order Steady State and Dynamic Models for Separation Processes. AIChE J., 29, 2, p. 261-276

[4] Croockewit, P., C. C. Honig and H. Cramers, 1955. Chem Eng Sci, 1955, 4, p 111

[5] Fuentes, C. and W.L. Luyben, 1983. Control of High-Purity Distillation Columns. Ind. Eng. Chem. Proc. Des. Dev., 22, pp. 361-366

[6] Haagensen, A.J and F.P. Lees, 1966. The Frequency Response of a Plate Gas Absorbtion Column. Chem. Eng. Sci., 21, pp. 77-86

[7] Hwang,Y.L., 1990. Dynamics of continuous countercurrent mass-transfer processes - IV. Multicomponent waves and assymetric dynamics.Chem. Eng. Sci., 45, pp. 2907-2915

[8] Hwang,Y.L., 1991. Nonlinear Wave Theory for Dynamics of Binary Distillation Columns. AIChE J. 37, pp. 705-723

[9] Kapoor, N. and T.J. McAvoy, 1986a. An Analytical Approach to Approximate Dynamic Modeling of Distillation Towers. Ind. Eng. Chem. Res., 26, 12, pp. 2473-2482.

[10] Kapoor, N. and T.J. McAvoy, 1986b. Effect of Recycle Structure on Distillation Tower Time Constants. AIChE J., 32, 3, pp. 411-418

[11] Kienle A. and W. Marquardt, 1992. Nonlinear Waves in Counter-Current Separation Processes Involving Highly Nonideal Multicomponent Mixtures. AIChE J., 1992

[12] Kim, C. and J.C. Friedly, 1974. Approximate Dynamic Modeling of Large Staged Systems. Ind. Eng. Chem. Proc. Des. Dev., 13, 2, pp. 177-181

[13] Lapidus, L. and N.R. Amundson, 1950. Ind. Eng. Chem., 42, p. 1071

[14] Levy, R.E., A.S. Foss and E.A. Grens, 1969. Response Modes of a Binary Distillation Column. IEC Fund., 8, 4, pp. 765-776

[15] Marquardt, W., 1990. Traveling waves in chemical processes. Ind.Chem.Eng., 30, pp. 585-606

[16] Montroll, E.W and G.F. Newell, 1952. Unsteady-State Separation Performance of Cascades. J. of Appl. Physics, 23, 2, pp. 184-194

[17] Osborne, A., 1971. The calculation of Unsteady State Multi-component Distillation Using Partial Differential Equations. AIChE J., 17, 3, pp. 696-703

[18] Rademaker, O., J. E. Rijnsdorp and A. Maarleveld, 1975. Dynamics and Control of Continuous Distillation Units. Elsevier, Amsterdam, 1975

[19] Rosenbrock, H.H., 1960. A Theorem of "Dynamic Conservation" for Distillation Columns. Trans. Instn. Chem. Engrs. 38, pp. 279-287

[20] Rosenbrock, H.H., 1962. The Transient Behavior of Distillation Columns and Heat Exchangers. A Historical and Critical Review. Trans. Instn. Chem. Engrs. 40, pp. 376-384

[21] Skogestad, S. and M. Morari, 1987. The Dominant Time Constant for Distillation Columns. Comput. Chem. Engng., 11, 6, pp. 607-617

[22] Tabrizi, M.H.N., 1990. An investigation into the dynamics of the distillation column, Search for a wave effect. IEEE Proc., pp. 599- 602

[23] Williams, T.J., 1963. The Status of Studies of the Dynamics of Mass-transfer Operations—A review and Commentary. Chem. Eng. Progr. Symp. Ser. 59, 46, pp. 1-8.

[24] Wong, K.T. and R. Luus, 1980. Model Reduction of High-Order Multistage Systems by the Method of Orthogonal Collocation. The Canadian J. of Chem. Eng., 58, pp. 382-388

[25] Wong, S.K.P. and D.E. Seborg, 1986. Low-order Nonlinear, Dynamic Models for Distillation Columns. Proceedings ACC 86, Seattle.

## Appendix A. Derivation of $T_N$

We are deriving equation 4.6, i.e.:

$$T_N = \frac{g(s)^N}{\Pi_n(1 - k_n g(s)h(s))} \tag{4.45}$$

Consider the transfer function $S_j$ from eq. 4.3, $S_j = (1 - hS_{j-1})^{-1}g$. First pull out a factor $g$ to get a transfer function $R_j$, i.e. $S_j = R_j g$. Inserting this into the recursion formula for $S_j$, eq. 4.3, yields:

$$R_j = \frac{1}{1 - L \cdot R_{j-1}}; \quad L \equiv gh \tag{4.46}$$

Decomposing $R_j$ into its nominator and denominator polynomial (in $L$, not in $s$!), yields:

$$\frac{n_j(L)}{d_j(L)} = \frac{d_{j-1}(L)}{d_{j-1}(L) - Ln_{j-1}(L)} \tag{4.47}$$

from which we obtain recursion formulas for $n_j$ and $d_j$ (dropping the $L$-argument for convenience):

$$n_j = d_{j-1} \tag{4.48}$$

$$d_j = d_{j-1} - Ln_{j-1} = d_{j-1} - Ld_{j-2} \tag{4.49}$$

The last equation is a homogeneous linear difference equation with constant coefficients. Its characteristic equation is:

$$\lambda^2 = \lambda - L \tag{4.50}$$

with roots:

$$\lambda_{1,2} = \frac{1 \pm \sqrt{1-4L}}{2} \tag{4.51}$$

The general solution is then on the form

$$d_j = C_1\lambda_1^j + C_2\lambda_2^j, \quad d_0 = d_1 = 1 \tag{4.52}$$

Eliminating $C_1$ and $C_2$ using the boundary conditions ($d_0 = d_1 = 0$) yields:

$$d_j = \frac{\lambda_1^{j+1} - \lambda_2^{j+1}}{\lambda_1 - \lambda_2} \tag{4.53}$$

In order to obtain eq. 4.45, we have to factorize this polynomial, i.e. we have to find the roots of $d_j(L) = 0$:

$$\frac{\lambda_1^{j+1} - \lambda_2^{j+1}}{\lambda_1 - \lambda_2} = 0 \quad \Rightarrow \quad \frac{(\frac{\lambda_1}{\lambda_2})^{j+1} - 1}{\frac{\lambda_1}{\lambda_2} - 1} = 0 \tag{4.54}$$

Solving for $\frac{\lambda_1}{\lambda_2}$ (roots of unity):

$$\frac{\lambda_1}{\lambda_2} = e^{\frac{2\pi k}{j+1}}, \quad k = 1, 2 \cdots j \tag{4.55}$$

Substituting for $\frac{\lambda_1}{\lambda_2}$ using eq. 4.51, and solving for $L \equiv gh$:

$$L_k = \frac{1}{4\cos^2(\frac{k\pi}{j+1})}, \quad k = 1, 2, \cdots j \tag{4.56}$$

Noting that this expression counts the roots twice, we may now factorize $d_j$:

$$d_j = \Pi_{k=1}^{\lfloor \frac{j+1}{2} \rfloor}(1 - \frac{L}{L_k}), \quad L \equiv gh \tag{4.57}$$

Finally, we may find $T_N$:

$$T_N \quad = \Pi_{j=1}^N S_j = \Pi_{j=1}^N R_j g = \Pi_{j=1}^N \frac{n_j}{d_j} g$$

$$= g^N \Pi_{j=1}^N \frac{d_{j-1}}{d_j} = \frac{g^N}{d_N}$$
$$= \frac{g(s)^N}{\Pi_n(1 - k_n g(s)h(s))} \tag{4.58}$$

where:

$$k_n = 1/L_n = 4\cos^2(\frac{n\pi}{N+1}), \quad n = 1, 2, \cdots \lfloor \frac{N+1}{2} \rfloor \tag{4.59}$$

## Appendix B. Dynamics of a train of vessels

The model for the train of vessels are described by a mass balance, a flow relation, and a polytropic relation for each volume $j$, $j = 1, 2, \cdots N$:

$$\begin{aligned} \frac{d}{dt}(\bar{\rho}_j V) &= F_{j-1} - F_j \\ F_j = C\sqrt{\Delta p}, \quad \Delta p &\equiv p_j - p_{j+1} \\ p &= k\bar{\rho}^n \end{aligned} \tag{4.60}$$

where $F_j$ and $\bar{\rho}_j$ are molar flow and density; $V$ and $p$ are the volume of a vessel and its pressure; and $n$ is a polytropic coefficient ($n = 1$ for isothermal vessels; $n = \gamma \equiv$ *adiabatic constant* for isentropic vessels; in general $1 < n < \gamma$). It is implicitly assumed that inertia effects are unimportant, and that the pressure drops and flows are more or less the same between all vessels.

These equations may be linearized to get:

$$\begin{aligned} V\frac{d\delta\rho_j}{dt} &= \delta F_{j-1} - \delta F_j \\ \delta F_j = \frac{C}{2\sqrt{\Delta p}}(\delta p_j - \delta p_{j+1}) &= \frac{F_j}{2\Delta p}(\delta p_j - \delta p_{j+1}) \\ \delta p = kn\bar{\rho}^{n-1}\delta\bar{\rho} &= \frac{np}{\bar{\rho}}\delta\bar{\rho} \end{aligned} \tag{4.61}$$

and combined to one equation in $\delta p$:

$$2\tau\delta\dot{p}_j = \delta p_{j+1} - 2\delta p_j + \delta p_{j-1} \tag{4.62}$$

where $\tau = \frac{\Delta p\bar{\rho}V}{F_j np} = \frac{\Delta p}{np}\tau_{res}$ is the time constant of a single vessel, and $\tau_{res} = \frac{\bar{\rho}V}{F_j}$ is the residence time of one vessel.

## Appendix C. The steady state gain of column sections

The purpose of this Appendix is to derive an analytical expression for the steady state gain of a column section in the simple distillation model analyzed in section 4.3.5.

We consider the top section of the column, described by a mass balance for light component:

$$M\frac{dx_j}{dt} = L(x_{j-1} - x_j) + V(y_{j+1} - y_j); \quad y_j = Kx_j \tag{4.63}$$

The notation is as before. We assume that $\frac{VK}{L} < 1$ in this section.

The Laplace transform version of the equation is given as:

$$x_j = \underbrace{\frac{1-\beta}{1+\tau s}}_{g(s)} x_{j+1} + \underbrace{\frac{\beta}{1+\tau s}}_{h(s)} x_{j-1} \tag{4.64}$$

where $\beta \equiv \frac{1}{1+\frac{VK}{L}}$ and $\tau = \frac{M}{L+VK}$.

We consider the gain from (1) the molar flow of the component into the bottom of the column section, $Vy_{N+1}$, to (2) the molar flow of the component leaving this bottom, $Lx_N$. This gain may be derived as follows: We start by the definition of $S_N$—the transfer function between two consecutive stages, $x_{N+1}$ and $x_N$:

$$x_N \equiv S_N x_{N+1} \tag{4.65}$$

This is equivalent with:

$$Lx_N = \frac{S_N}{\frac{VK}{L}}(Vy_{N+1}); \quad where \quad y_{N+1} = Kx_{N+1} \tag{4.66}$$

hence the gain is given by:

$$gain_N = \frac{S_N(0)}{\frac{VK}{L}} = \frac{R_N(0)g(0)}{\frac{VK}{L}} \tag{4.67}$$

Here, we have introduced the quantity $R_j(s)$ from Appendix A.

This transfer function $R_j$ was derived in Appendix A, and is given by (eq. 4.53 ):

$$R_N(0) = \frac{n_N(0)}{d_N(0)} = \frac{d_{N-1}(0)}{d_N(0)} = \frac{\lambda_1^N - \lambda_2^N}{\lambda_1^{N+1} - \lambda_2^{N+1}} \tag{4.68}$$

The $\lambda(0)$'s are given by inserting $g(0) = 1-\beta$, $h(0) = \beta$ into eq. 4.51; thus we get:

$$R_N(0) = \frac{\beta^N - (1-\beta)^N}{\beta^{N+1} - (1-\beta)^{N+1}} \tag{4.69}$$

Eliminating $VK/L$ by the definition of $\beta$ (i.e. $\beta = \frac{1}{1+\frac{VK}{L}}$), we get:

$$gain_N = \beta \frac{\beta^N - (1-\beta)^N}{\beta^{N+1} - (1-\beta)^{N+1}} \tag{4.70}$$

and

$$\epsilon \equiv 1 - gain_N = \frac{(1-\beta)^N(2\beta - 1)}{\beta^{N+1} - (1-\beta)^{N+1}} \tag{4.71}$$

which is the sought expression for $\epsilon$.

An alternative form of this expression is obtained in terms of the stripping factor, $s = VK/L$, if we substitute $\beta \equiv \frac{1}{1+\frac{VK}{L}}$ and get:

$$\epsilon = \frac{s^N(s-1)}{s^{N+1}-1} \approx s^N(1-s); \quad s \equiv \frac{VK}{L} \tag{4.72}$$

This expression is valid for the upper column section. A similar expression is obtained for the lower column section by simply replacing $\beta$ by $1-\beta$ in the expression (symmetry). This corresponds to replacing the stripping factor, $s$, by the absorbtion factor $a = \frac{L}{VK}$ and we get:

$$\epsilon \approx a^N(1-a); \quad a \equiv \frac{L}{VK} \tag{4.73}$$

which is the corresponding expression valid for the lower column section.

## Appendix D. Finding lumped time constants for column sections

The purpose of this Appendix is to show how one may find the lumped time constants of a cascade section. In section 4.3.5, we claimed that a transfer function $c_1(s)$ may be approximated by

$$c_1(s) = \frac{k}{1+T_1 s} + O(s^2) \tag{4.74}$$

This equation is valid sufficiently close to the origin. The question is then how to find $T_1$. Our interest here, is the lumped time constant of the transfer function from Appendix C, namely

$$gain_N(s) \equiv \frac{S_N(s)}{\frac{VK}{L}} \tag{4.75}$$

Before we do this, we digress a moment to see how one may find the lumped time constant of an arbitrary transfer function, say $\Psi(s)$. By a Taylor series expansions about the origin, we get:

$$\Psi(s) = \Psi(0) + \Psi'(0) \cdot s + O(s^2)$$

Similarly, the transfer function given in equation 4.74 may be expanded as

$$\frac{k}{1+T_1 s} = k - kT_1 s + O(s^2) \tag{4.78}$$

If these two expressions are to be the same, we have to require

$$k = \Psi(0); \quad T_1 = -\frac{\Psi'(0)}{\Psi(0)} \tag{4.79}$$

This procedure corresponds to the well known method of moment matching.

We return to our problem of finding the lumped time constant of $gain_\infty(s)$ given by eq. 4.75; that is, for infinitely many stages. All dynamics is confined to $S_\infty(s)$, so we restrict ourselves to studying that. The quantity $S_\infty$ is the stable (in $N$) solution of the recursion equation for $S(s)$, eq. 4.3:

$$S_j(s) = (1 - h(s)S_{j-1}(s))^{-1} g(s) \tag{4.80}$$

Solving this for the stable solution, $S_\infty(s)$, yields:

$$S_\infty(s) = \frac{1 - \sqrt{1 - 4g(s)h(s)}}{2h(s)} \tag{4.81}$$

where $g(s) = \frac{1-\beta}{1+\tau s}$ and $h(s) = \frac{\beta}{1+\tau s}$ as before. We may then find the lumped time constant by differentiation:

$$T_1 = -\frac{S'_\infty(0)}{S_\infty(0)} = \frac{\tau}{2\beta - 1} \tag{4.82}$$

where $\tau = \frac{M}{L+VK}$ is the time constant of a single tray as before.

An alternative form of this expression is obtained in terms of the stripping factor, $s_1 = VK/L$, if we substitute $\beta \equiv \frac{1}{1+\frac{VK}{L}}$ and get:

$$T_1 = \frac{1 + s_1}{1 - s_1}\tau_1 \quad ; s_1 = VK/L \tag{4.83}$$

This expression was derived for the upper column section. A similar expression for the lower column section is obtained by replacing $\beta$ by $1 - \beta$ in the expression for $T_1$; or—which is equivalent—by repacing the stripping factor, $s$, by the absorbtion factor, $a_2 = \frac{L}{VK}$ and get:

$$T_2 = \frac{1 + a_2}{1 - a_2}\tau_2; \quad a_2 = \frac{L}{VK} \tag{4.84}$$

which is the corresponding expression valid for the lower column section.

# Chapter 5

# The Dynamic Behavior of Cascades. Part 2: Composition Dynamics of Binary Distillation

John Morud and Sigurd Skogestad*
Chemical Engineering
University of Trondheim - NTH
N-7034 Trondheim, Norway

A preliminary version was presented at
AIChE Annual Meeting, Miami Beach, USA, Nov. 12-17 1995

**Abstract**

The composition dynamics of a binary distillation column is considered. By using an analogy to diffusion in plug flow, we show that the slow time constant of such a column may increase exponentially with the number of stages—all other things held constant. Moreover, using the analogy, we give a qualitative description of the dynamic behavior of the column.

*Address correspondence to this author. Fax: 47-73594080, E-mail: skoge@kjemi.unit.no

## 5.1 Introduction

Although most chemical processing plants consist of rather simple elements—such as flash tanks and pipes—their overall behavior can be rather complex, and very different from the behavior of the individual elements. An example is a distillation column, which is essentially a cascade interconnection of many simple flash tanks (trays). Even though the dynamic behavior of the individual elements—the trays—is easy to understand, it is not obvious without prior knowledge how the overall column behaves.

The purpose of this paper is to analyze the behavior of such a cascaded system. Specifically, we study a model of the composition dynamics of a binary distillation column. We emphasize that the model is very simple, and it is not our purpose to develop models with great numerical accuracy. Rather, the purpose is to gain some qualitative insight into the behavior of such a cascaded system.

We first present a simple model for the composition dynamics of a binary distillation column, and proceed by proposing an analogy for this column. The analogy is based on diffusion in plug flow, and suggests that the slowest time constant of binary distillation increases exponentially with the number of stages in the column. Finally, we perform some numerical experiments in order to explore this exponential dependence, and to shed some light on the behavior of the column. We interpret the results in terms of concepts borrowed from the plug flow analogy.

The rest of this introduction is devoted to reviewing previous work.

Montroll and Newell (1952) approximate multistaged cascade processes by nonlinear partial differential equations, and find analytical solutions for such equations.

Rosenbrock (1960) discusses a "conservation property" of distillation columns. He shows how a particular measure of deviation from steady state operation may be thought of as a "conserved" property in the column.

Rosenbrock (1962) reviews previous work on the transient behavior of distillation columns and heat exchangers. He discusses approximation of distillation column models by means of partial differential equations.

Williams (1963) reviews the status of results on the dynamic behavior of mass transfer processes at that time (1963), and lists some problems that require further investigation (per 1963).

Levy *et. al.* (1969) perform modal decompositions of some models for binary distillation. They conclude that the composition dynamics is much slower than the hydraulics, which means that these phenomena tend to be decoupled; that is, the hydraulics may be considered quasi-stationary compared to the composition dynamics.

Osborne (1971) develops approximate models for multicomponent distillation columns by using partial differential equations. Simulations indicate that his approach yields accurate results.

Wong and Luus (1980) consider model reduction of multistage systems by means of orthogonal collocation. They obtain good agreement between step responses of their reduced order models with the original high order models.

Cho and Joseph (1983) use partial differential equations approximations of separation processes together with orthogonal collocation in order to obtain reduced order models of such processes.

Skogestad and Morari (1987) develop simple transfer function models for binary distillation columns, and find simple expressions for the dominant time constant of such columns. For high purity columns, they found excellent agreement between the simple expressions and detailed calculation.

Marquardt (1990) gives a general treatment of wave phenomena in chemical processes. Among his examples are regenerative heat exchangers, adsorbers and distillation columns. The basic idea is that the dynamics of many chemical engineering systems—such as the composition dynamics of distillation columns—may be described as waves travelling through the system.

Hwang and Helfferich (1990) study the countercurrent mass transfer processes. They approximate them with hyperbolic partial differential equations (PDE's), which they solve by the method of characteristics. Hyperbolic PDE's naturally lead to an interpretation of the dynamics in terms of travelling waves.

Hwang and Helfferich (1991) study the composition dynamics of binary distillation, and interpret this dynamics in terms of nonlinear travelling waves. They use an analogy to ion exchange in a fixed bed.

## 5.2 Analyzing binary distillation

Below, we will use an analogy to diffusion in plug flow in order to shed some light on the behavior of a binary distillation column. Before we present this analogy, we start with a simple column model.

### 5.2.1 A simple distillation model

We present a simple model for the concentration dynamics of a binary distillation column. The column is depicted in Fig. 5.1a.

#### Mathematical model

As a model for the column, we take (mass balance for light component at stage $j$):

$$M\frac{dx_j}{dt} = L(x_{j-1} - x_j) + V(y_{j+1} - y_j); \quad y_j = \frac{\alpha x_j}{1 + (\alpha - 1)x_j} \tag{5.1}$$

where $M$, $L$ and $V$ are the molar holdup, reflux, and vapor flow, respectively; $x_j$ and $y_j$ are the liquid and vapor mole fractions of light component; and $\alpha$ is the relative volatility.

This equation may be linearized around the steady state to get :

$$M\dot{x}_j = Lx_{j-1} - (L + VK_j)x_j + VK_{j+1}x_{j+1} \tag{5.2}$$

where $x$ is now a deviation variable. The slope of the equilibrium line, $K_j$, is given by $K_j = \frac{dy_j}{dx_j} = \frac{\alpha}{[1+(\alpha-1)x_j]^2}$.

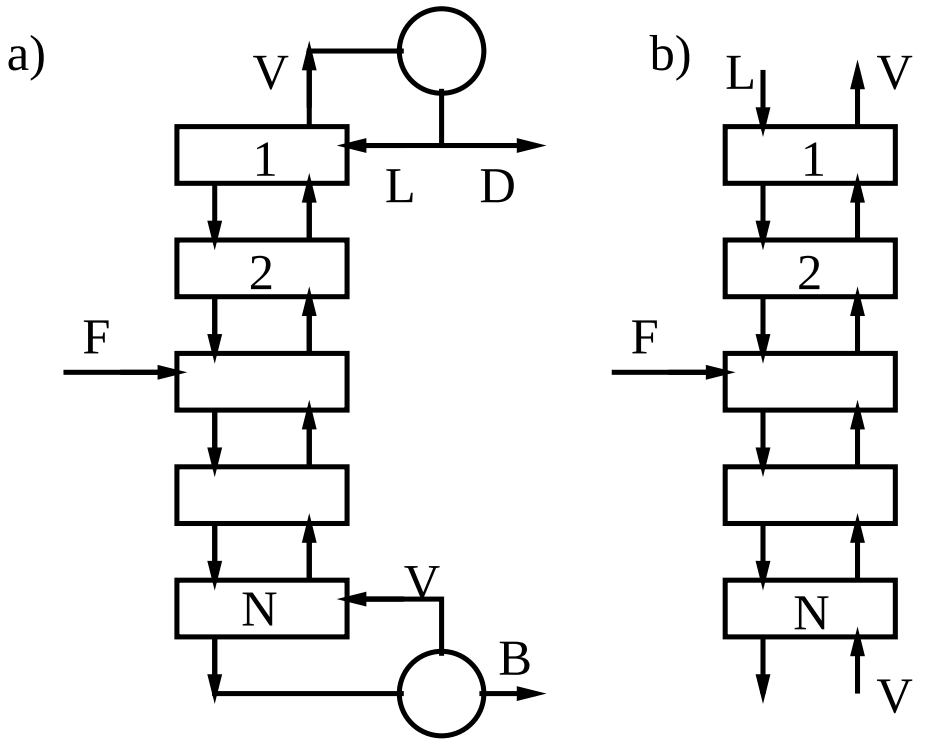


Figure 5.1: Binary distillation column (a) and a modified open end version (b).

### 5.2.2 Conceptual models for binary distillation

We now describe a very simple model—an analogy—which exhibits a dynamic behavior similar to a binary distillation column. The relation between this simple model and the binary distillation column is presented afterwards. Similar analogies have been presented previously, e.g. Rosenbrock (1962).

#### An analogy for a binary distillation column

Consider the system shown in Fig. 5.2, showing a pipe of length $2l$, initially containing a fluid with an impurity (concentration $x$). Pure fluid enters at both ends of the pipe, and flows towards the middle of the pipe, where pure fluid is removed. That is, the outlet at the middle of the pipe does not let the impurity through. This means that the only way the impurity may leave the pipe, is by diffusing through the pipes against the flowing current. As a model of this convection-diffusion process, we take:

$$\frac{\partial x}{\partial t} + \frac{\partial (ux)}{\partial z} = \frac{\partial}{\partial z}(\nu \frac{\partial x}{\partial z}) \tag{5.3}$$

where $x$ is the concentration of impurity, $u$ and $\nu$ are the fluid velocity and the diffusivity, and $z$ is the position in the pipe.

It is shown in Appendix A that the slowest time constant of this system may be

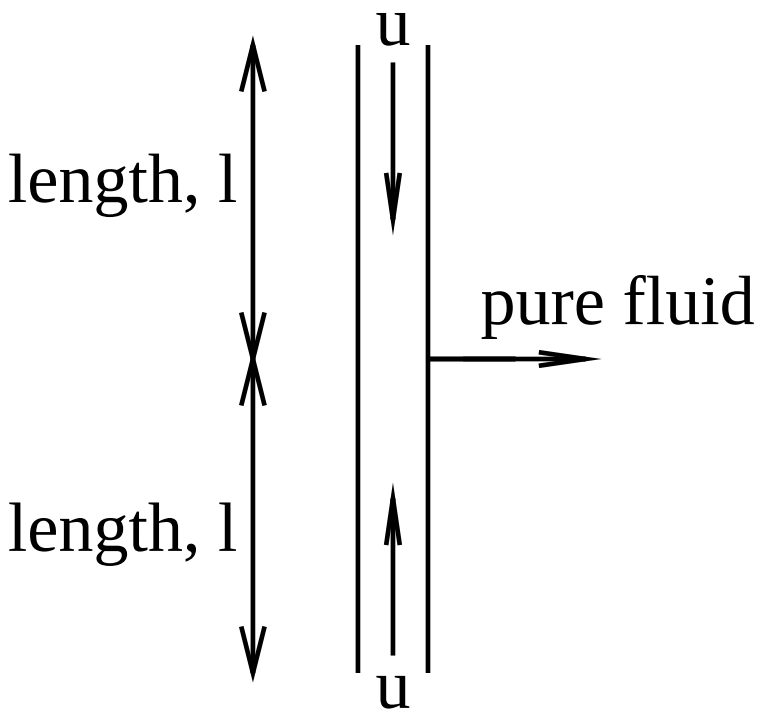


Figure 5.2: Pipe and tank analogy to binary distillation

approximated as :

$$\tau \approx \frac{\nu}{u^2} e^{\frac{ul}{\nu}}; \quad for \quad \frac{ul}{\nu} >> 1 \tag{5.4}$$

Hence, the time constant for depletion of impurity increases **exponentially** with the length of the pipe. This exponential dependence may not come as a surprise, since countercurrent diffusion is not very effective; and the pipe therefore retains the impurity quite effectively.

Note for later use that equation 5.14 may be approximated by the finite difference equation:

$$\frac{dx_i}{dt} + (\frac{u_i}{\Delta z} x_i - \frac{u_{i-1}}{\Delta z} x_{i-1}) = \frac{\nu_i}{\Delta z^2}(x_{i+1} - x_i) - \frac{\nu_{i-1}}{\Delta z^2}(x_i - x_{i-1}) \tag{5.5}$$

## Comparison of analogy and simple distillation model

We now proceed with the model for binary distillation. The overall aim is to make a comparison between the column model and the conceptual pipe model.

Consider the linearized model of the binary distillation column analyzed in the previous section, where x is the mole fraction of light component—or more correctly, the deviation of that mole fraction from steady state (eq. 5.2):

$$M\dot{x}_j = Lx_{j-1} - (L + VK_j)x_j + VK_{j+1}x_{j+1} \tag{5.6}$$

This may be rewritten as:

$$\dot{x} + (u_j x_j - u_{j-1} x_{j-1}) = \nu_j(x_{j+1} - x_j) - \nu_{j-1}(x_j - x_{j-1}) \tag{5.7}$$

where the equivalent velocity and diffusivity are expressed as:

$$u_j \equiv \frac{L - VK_{j+1}}{M}; \quad \nu_j = \frac{VK_{j+1}}{M} \tag{5.8}$$

Thus, the distillation model, eq. 5.7, is seen to be a **finite difference** analog to the pipe model, eq. 5.3. Hence, we expect their behavior to be very similar.

Thus, we may see the analogy to the pipe model:

1. First, note that the deviation variable, $x$—which is the deviation of the mole fraction from steady state—is a **conserved quantity**. This is seen if we sum up the mass balance, eq. 5.6, over several consecutive stages:

$$\frac{d}{dt}(\sum_{j=n}^{j=m} M_j x_j) = \sum_{j=n}^{j=m} \frac{d}{dt}(M_j x_j) = Lx_{n-1} - VK_n x_n - Lx_m + VK_{m+1} x_{m+1} \tag{5.9}$$

   It is seen that terms cancel, such that only terms at the summation limits remain. The interpretation is that an increase in mole fraction at one stage corresponds to a decrease at a neighboring stage. In other words, the deviation in mole fraction from steady state can not "vanish" inside the column, but has to "leave" through the column ends. This is similar to the case of the impurity in the pipe analogy, which also has to leave through the ends.

   That the deviation, $x$, from steady state operation, represents some sort of "conserved" property, has also been noted by Rosenbrock (1960).

2. The "velocity" $u_j \equiv \frac{L-VK_{j+1}}{M}$ is directed from the ends of the column towards the middle of the column. This follows from the fact that the slope of the equilibrium line, $K_j$, is larger than the slope of the operating line, $L/V$, at the bottom of the column, and smaller at the top of the column. Hence, this velocity, $u$, corresponds to the velocity in the two pipes in the simple model.

3. The effective diffusivity in the distillation column is $\nu_j = \frac{VK_{j+1}}{M}$.

4. The pipe lengths, $2l$, in the simple model corresponds to the number of stages in the distillation column.

5. The deviation variable tends to accumulate at points where the equilibrium- and operating lines are parallel, i.e. where $u_j = \frac{L-VK_{j+1}}{M} = 0$.

### Definitions

For subsequent discussion, we define some concepts:

- **Equivalent velocity**. $u_j \equiv \frac{L-VK_{j+1}}{M}$
- **Equivalent diffusivity**. $\nu_j = \frac{VK_{j+1}}{M}$.
- **Stationary point**. A point in the column—i.e. a stage—where the equivalent velocity $u_j$ is zero. This corresponds to parallel equilibrium and operating lines.

- **Accumulation points**. A stationary point where the equivalent velocities on each side are pointing **towards** the stationary point—not **from** the stationary point. The reason for the term "accumulation point" is that the deviation variable, $x$, tends to "flow" towards it, which means that it tends to accumulate at such points.

## 5.3 Numerical observations

According to the plug flow analogy presented above, we expect the slow time constant of binary distillation to increase exponentially with the number of stages in the column—all other quantities being the same (internal flow rates etc). We present some numerical experiments exploring this exponential dependence. The starting point—the base case—is the column model described above. We then do various modifications in order to test the sensitivity of the results to some of the assumptions. These assumptions are listed in Table 5.1.

| Assumption | Numerical value |
|---|---|
| Constant relative volatility | $\alpha = 1.5$ |
| Constant molar holdup | $M = 1$, on each stage |
| Constant molar flows | $L = 2.635$, $V = 3.135$, distillate flow rate $D = 0.5$ |
| Feed flow rate and mole fraction at the middle of the column | $F = 1$ and $z = 0.5$ |
| Total condenser | holdup $M = 1$ |
| Reboiler as one equilibrium stage | |

Table 5.1: Assumptions made for the distillation model

### Cases studied

We compare the following cases:

- **Base case.** This is the real column model described above.
- **Case 1.** As the base case, but with the equilibrium line approximated by two straight segments, as shown in Fig. 5.3. The slopes of the segments are $\alpha$ and $1/\alpha$, where $\alpha = 1.5$ is the relative volatility. Thus, this is an approximation to the equilibrium line for high and low values of $x$—the mole fraction of light component.
- **Case 2.** As the base case, but with the reboiler and condenser removed, as shown in Fig. 5.1b. Instead, there is a feed, $L$, of pure light component at the top of the column, and a feed, $V$, of pure heavy component at the bottom. The purpose of the arrangement is to see the effect of the reflux from the reboiler and the condenser; one would, of course, never build such an arrangement.

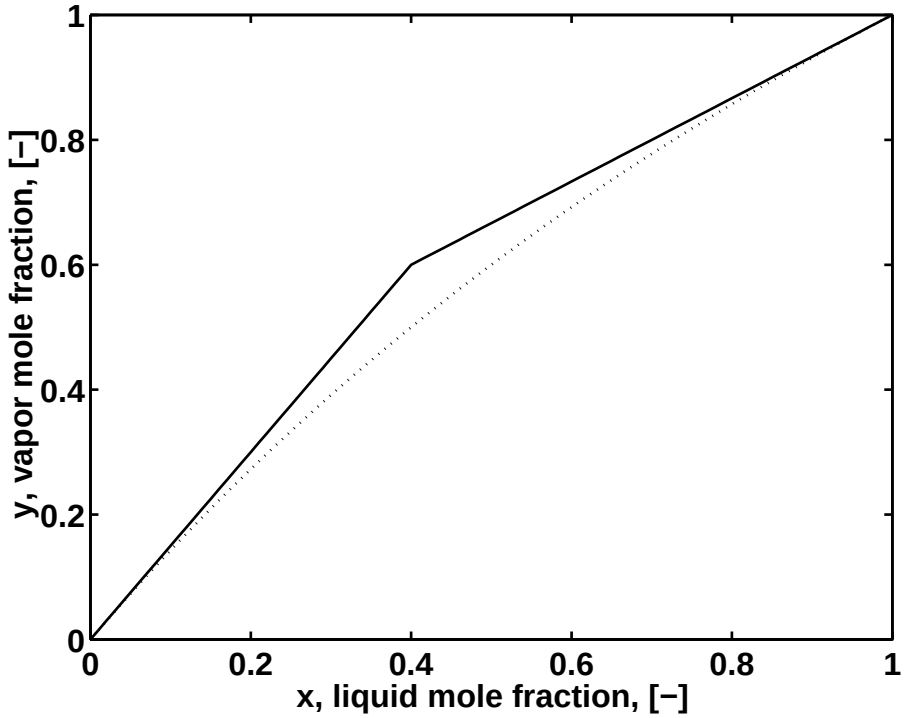


Figure 5.3: Simplified vapor-liquid equilibrium, consisting of two linear segments

- **Case 3.** As case 2, but with **impure** feeds $L$ and $V$. The impurities are $x = 0.95$ at the top and $y = 0.05$ at the bottom.

### The slow time constant

Figure 5.4 shows the dependence of the slow time constant (resiprocal of the smallest eigenvalue) as a function of the number of stages in the column—all other parameters kept constant. As can be seen, for all cases except case 3, the results are straight lines in a semi-logarithmic plot, which means that the time constant increases **exponentially** with the number of stages in the column. For case 3—impure feeds $L$ and $V$ at the top and bottom—the time constant approaches a limit as $N \to \infty$.

### A numerical experiment

In order to illustrate the relation between the distillation column and the pipe analogy, consider the following thought experiment: Assume that we inject some extra light component into tray 20 (counted from the top of the column) at time $t = 0$ in a column with 82 stages—the base case above. This corresponds to an impulse response with input at tray 20.

**Remark:** The reason for showing a case where the injection of extra light component is at tray 20—and not, for example, the feed tray, which would be more realistic in practice—is that it makes it easier to see the nature of the column behavior. In

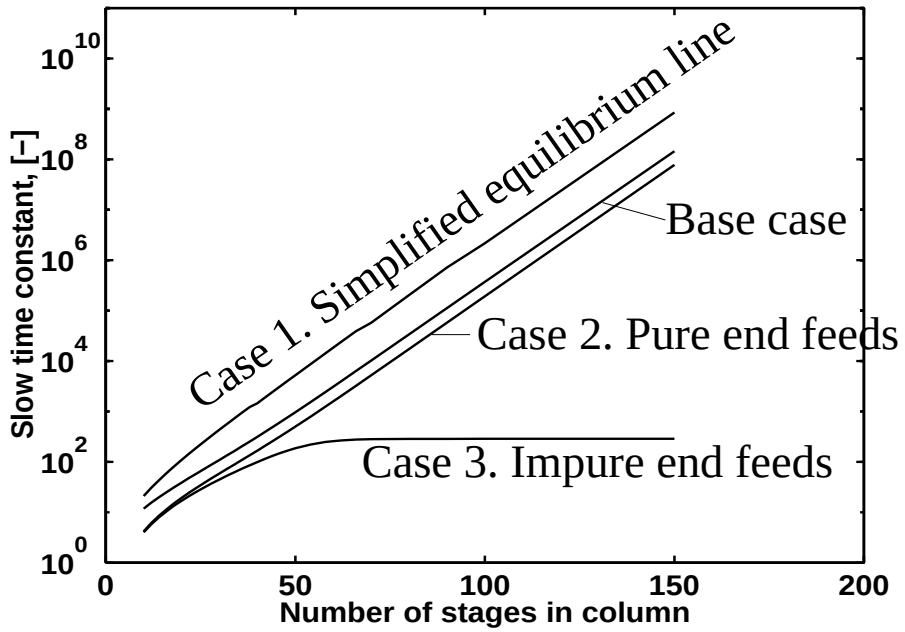


Figure 5.4: Slow time constant as a function of number of stages

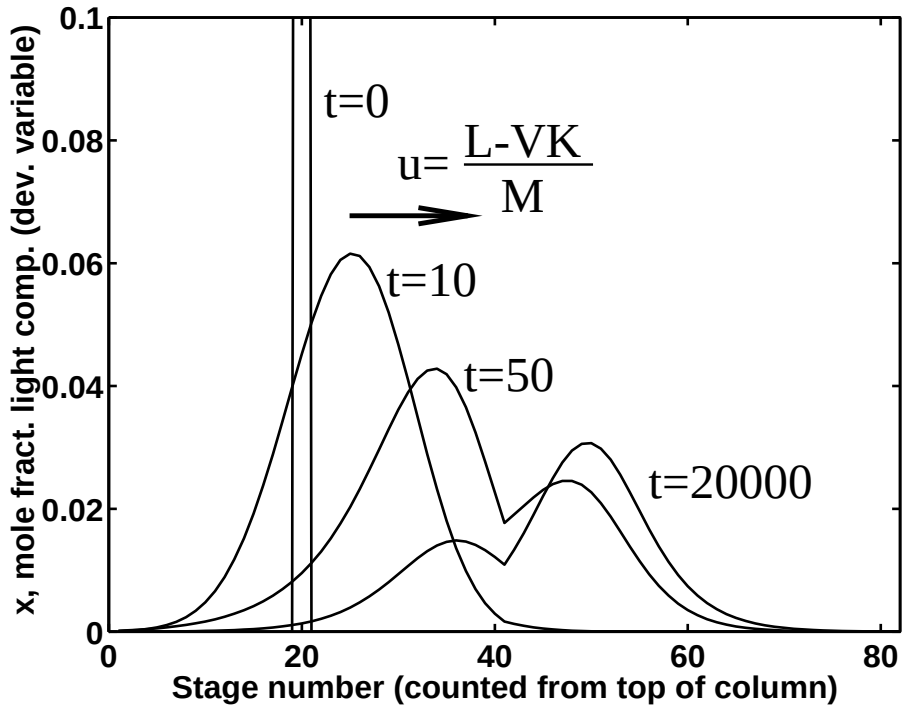


Figure 5.5: Impulse in light component at stage 20.

particular, it makes it easier to see the effect of the equivalent velocity, which is rather small near the feed tray.

Fig. 5.5 shows the resulting column concentration profiles (deviation variable) through the column for different times. As can be seen, the excess amount of light component is first located at tray 20. It then moves towards the center of the column with velocity $u_j \approx \frac{L-VK_{j+1}}{M}$, spreading according to a diffusivity $\nu_j \approx \frac{VK_{j+1}}{M}$. In the long run, it tends to accumulate at tray 35 and 49—the accumulation points—where the operating- and equilibrium lines are approximately parallel, i.e. where the velocity is zero, $u_j \approx \frac{L-VK_{j+1}}{M} = 0$. The concentration profile relatively quickly assumes the shape of the slow eigenvector of the linearized system, and then vanishes very slowly, keeping the shape of the slow eigenvector as it vanishes.

That the operating- and equilibrium lines are parallel at the accumulation points–stage 35 and 49–may be seen in the McCabe-Thiele diagram shown in Fig. 5.6.

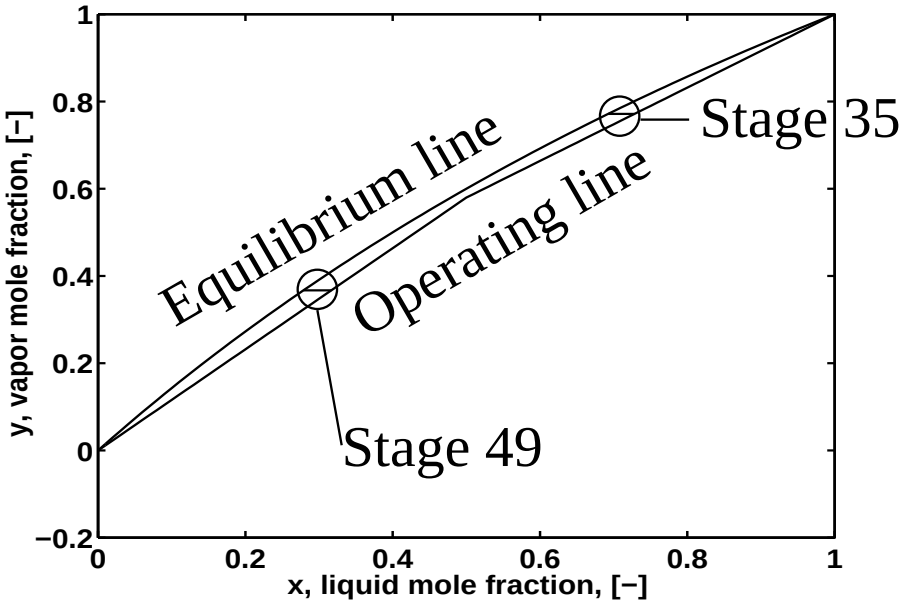


Figure 5.6: McCabe-Thiele diagram. Accumulation points, stage 35 and stage 49 are shown

Fig 5.7 shows the **equivalent velocity profile** in the column. As can be seen, there are three stationary points ($u = 0$), of which stage 35 and 49 are accumulation points. Note that there is a region, between stage 35 and 49, where the "flow" is **outwards** from the feed tray towards the column ends. In the rest of the column the "flow" is from the ends towards the feed tray.

This sheds some light on the dynamic behavior of the binary distillation column. However, we have not explained why the open ended column with impure feeds at the column ends—case 3 above—has a time constant that approaches a fixed value as $N \to \infty$ rather than increasing exponentially as was the case for the other cases.

Coincidentally, Hwang (1991) presents a similar analysis.

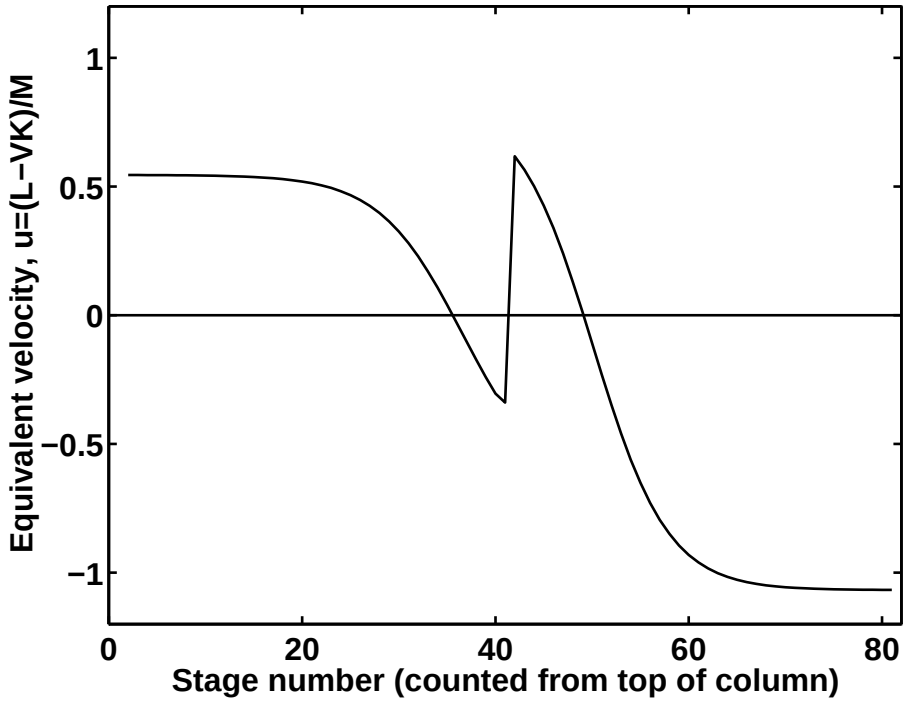


Figure 5.7: Velocity profile in column

### Open ended column with impure feeds

Figure 5.8 compares concentration profiles (absolute values, not deviation variables) through the column for the base case, case 2 (open ends, pure feeds) and case 3 (open ends, impure feeds). It can be seen that the concentration profiles are similar, except that in case 3 (impure feeds), there is a flat region below the feed tray. The current plot applies to impurities $x = 0.95$ at the top and $y = 0.05$ at the bottom of the column. Similar flat concentration profiles are obtained with other values of the impurities; however, sometimes the flat region close to the feed tray is at the **upper** side of the feed tray.

This flat region in case 3 implies that one of the accumulation points stays close to the column end as we increase the number of stages. In fact, the distance between the accumulation point and the column end approaches a fixed value as the total number of stages is increased. This distance corresponds to the equivalent length of pipe in the pipe-and-tank analogy; thus, the corresponding time constant approaches a fixed value as $N \to \infty$.

### Steady state sensitivity

To complete the numerical experiment, we show that the steady state sensitivity of the column is also very high. Fig. 5.9 shows the concentration profile of light component in the column (absolute value, not deviation variable) for three different values of $z$—the mole fraction of light component in the feed. As can be seen, very small changes in $z$

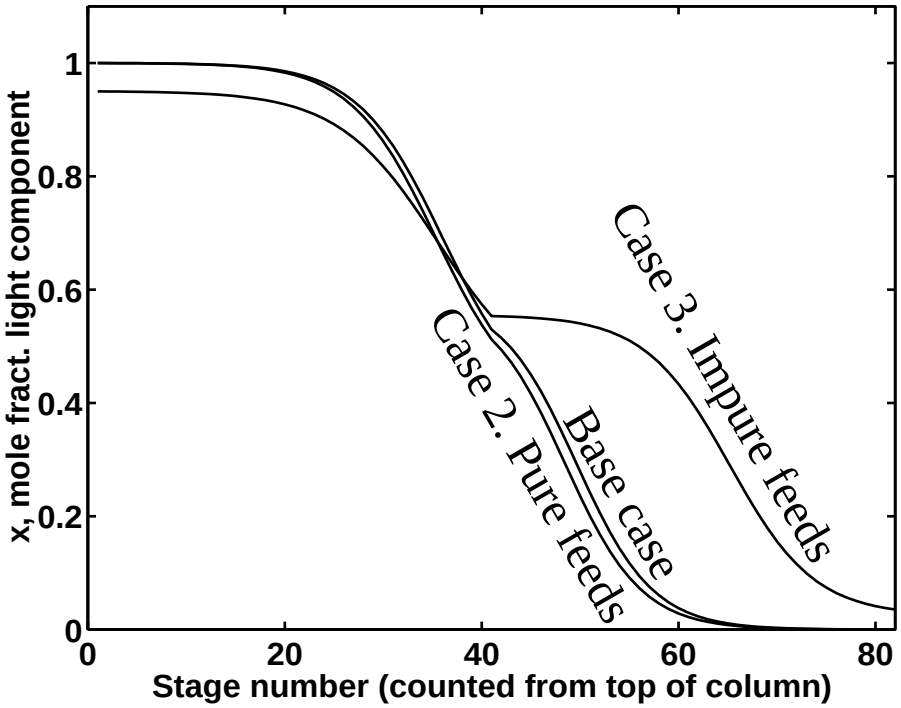


Figure 5.8: Comparison of concentration profiles

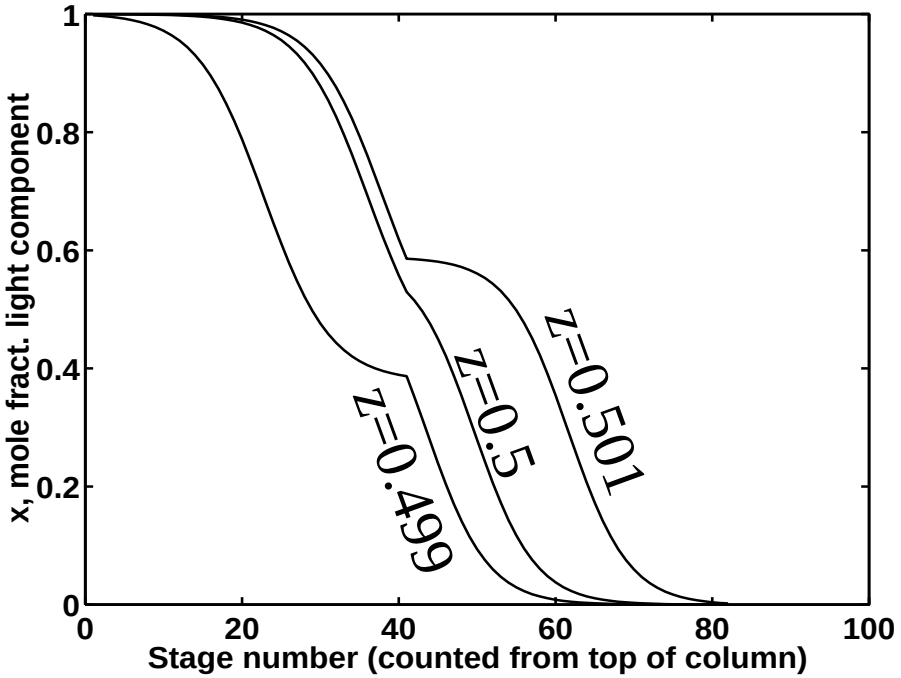


Figure 5.9: Sensitivity of concentration profiles

leads to very large changes in the concentration profile. The changes are largest near tray 35 and 49—the accumulation points.

## 5.4 Discussion

### Relation to a state space point of view

Above, we have examined cascade systems with one very small eigenvalue, which results in very large time constants. In this subsection, we discuss this in relation to a state space point of view, and try to make a connection between steady state sensitivity and the dynamic behavior of such systems. We argue that the dynamic behavior of the system is essentially one-dimensional.

In order to formulate the argument, we define the gain of a matrix, say $G$, in the input direction $u$ to be: $gain = \frac{||Gu||}{||u||}$. In this expression, we define the direction of $u$ to be an input direction, and the direction of $Gu$ to be the corresponding output direction. In this sense, we talk of gains and directions for any matrix–not only transfer functions.

Consider a stable system described by a state space model on the form:

$$\dot{x} = Ax + Bu \tag{5.10}$$

We assume that the $A$-matrix has one real Left Half Plane eigenvalue very close to zero; the other eigenvalues are much faster. Note that this is the case for the interconnected cascades described in this paper; these have one very long time constant, the others are fast.

From the definition of the slow eigenvalue, $\lambda_{slow}$, we get:

$$Ax_{slow} = \lambda_{slow}x_{slow} = very \quad small \tag{5.11}$$

which means that the gain of $A$ is very small in the input direction corresponding to the slow eigenvector, $x_{slow}$. Turning things around, this implies that the gain of **the inverse**, $A^{-1}$, is very **large** in the **output** direction corresponding to the direction of the slow eigenvector. Since the steady state gain of **the system** is given by

$$x = -A^{-1}B \cdot u \tag{5.12}$$

this implies that small changes in the inputs, $u$, will typically cause large changes in the states, $x$, in the direction of the slow eigenvector. Hence, the steady state gain is typically very much aligned with the slow dynamics. In other words, the dynamics is essentially **one-dimensional**; that is, the state tends to stay on a line $x = p \cdot x_{slow}$, where $p$ is a scalar parameter. However, exceptions may occur if a weak output directions of the $B$-matrix is aligned with the weak output directions of the $A$-matrix, in which case the situation may be different.

One might conjecture that this one-dimensional behavior exists also in the non-linear case, that is, for large inputs, $u$, in the nonlinear cascade models. Locally–that is, reasonably close to steady state–one would expect the slow eigenvector of the linearized system to be the tangent of a one-dimensional slow manifold, say $x = x(p)$, where $p$ is a scalar parameter. The state, $x$, would then tend to stay on this slow manifold under varying inputs, resulting in essentially one-dimensional behavior.

### "All trays have the same response"

Having realized that one mode is slow, Skogestad and Morari (1987) derived very accurate formulaes for the slow time constant of binary distillation columns, based on the assumption that all trays in a column have the same response. That is, they assumed that the change in mole fraction of light component at tray $j$ may be expressed as $\Delta x_j(t) = a_j f(t)$, where $a_j$ represents the amplitude at tray $j$ and $f(t)$ is the response– the same for all stages.

In essence, this is an assumption of one-dimensional (linear) behavior. In the light of the previous subsection, the good results obtained by Skogestad and Morari may therefore not come as a great surprise.

### Nonlinearities

In this paper, we have essentially used linear tools for the analysis of the dynamics of the binary distillation column. In doing this, we have omitted certain aspects of the dynamics that are important. Such an aspect is, for example, assymetric dynamics (e.g. Hwang, 1991). The time required to reach a new steady state after a step in an input, depends on the direction of the step. In particular, the time constant is large for a transition to a steady state where the purity of the product is high. Such nonlinearities may, to a large extent, be removed by an algebraic transformation of variables; for example, it often helps to introduce a logarithmic transformation of the compositions (Skogestad and Morari, 1988).

Hwang (1991) discusses what he denotes as composition shock waves in distillation columns. The idea is that a composition "wave" travelling through the column may be self-sharpening, and thus behave similar to a shock wave. The self-sharpening effect is due to the nonlinearities.

## 5.5 Conclusion

In this paper, we have analyzed the dynamics of binary distillation columns. By numerical experiments, we demonstrated that the time constants of such columns may increase exponentially with the number of stages in the column.

We then made use of an analogy to diffusion in plug flow. The analogy is transparent, and it is thus possible to estimate its time constant, which does indeed increase exponentially with the number of stages (or, more correctly, length of pipe, which is analoguous to the number of stages in a binary distillation column). Similar analogies have also been presented by previous workers (e.g. Rosenbrock, 1962).

By using concepts from the plug flow analogy—such as equivalent velocity and diffusivity—the dynamics of binary distillation was illustrated. The analogy provides a visualization of the dynamics of the column.

## Notation

| | |
|---|---|
| $D$ | distillate flow rate |

| | |
|---|---|
| $F$ | feed flow rate |
| $K$ | slope of vapor-liquid equilibrium line |
| $L$ | liquid molar flow rate |
| $M$ | molar holdup on tray |
| $N$ | number of trays in column |
| $s$ | Laplace variable |
| $t$ | time |
| $u$ | equivalent velocity |
| $V$ | vapor molar flow rate |
| $x$ | liquid mole fraction of light component |
| $y$ | vapor mole fraction of light component |
| $z$ | space coordinate; or feed mole fraction of light component |

Greek

| | |
|---|---|
| $\alpha$ | constant relative volatility |
| $\phi$ | flux of chemical species |
| $\nu$ | diffusivity |
| $\tau$ | time constant |

Subscripts

| | |
|---|---|
| $i$ | index over stages in column |
| $j$ | index over stages in column |
| $N$ | last stage in column |

# References

[1] Celebi, C and E.H. Chimowitz, 1985. Analytic Reduced-Order Dynamic Models for Large Equilibrium Staged Cascades. AIChE J., 31, 12, pp. 2039-2051

[2] Cho, Y.S and B. Joseph, 1983. Reduced-Order Steady State and Dynamic Models for Separation Processes. AIChE J., 29, 2, p. 261-276

[3] Croockewit, P., C. C. Honig and H. Cramers, 1955. Chem Eng Sci, 1955, 4, p 111

[4] Fuentes, C. and W.L. Luyben, 1983. Control of High-Purity Distillation Columns. Ind. Eng. Chem. Proc. Des. Dev., 22, pp. 361-366

[5] Haagensen, A.J and F.P. Lees, 1966. The Frequency Response of a Plate Gas Absorbtion Column. Chem. Eng. Sci., 21, pp. 77-86

[6] Hwang,Y.L., 1990. Dynamics of continuous countercurrent mass-transfer processes - IV. Multicomponent waves and assymetric dynamics.Chem. Eng. Sci., 45, pp. 2907-2915

[7] Hwang,Y.L., 1991. Nonlinear Wave Theory for Dynamics of Binary Distillation Columns. AIChE J. 37, pp. 705-723

[8] Kapoor, N. and T.J. McAvoy, 1986a. An Analytical Approach to Approximate Dynamic Modeling of Distillation Towers. Ind. Eng. Chem. Res., 26, 12, pp. 2473-2482.

[9] Kapoor, N. and T.J. McAvoy, 1986b. Effect of Recycle Structure on Distillation Tower Time Constants. AIChE J., 32, 3, pp. 411-418

[10] Kienle A. and W. Marquardt, 1992. Nonlinear Waves in Counter-Current Separation Processes Involving Highly Nonideal Multicomponent Mixtures. AIChE J., 1992

[11] Kim, C. and J.C. Friedly, 1974. Approximate Dynamic Modeling of Large Staged Systems. Ind. Eng. Chem. Proc. Des. Dev., 13, 2, pp. 177-181

[12] Lapidus, L. and N.R. Amundson, 1950. Ind. Eng. Chem., 42, p. 1071

[13] Levy, R.E., A.S. Foss and E.A. Grens, 1969. Response Modes of a Binary Distillation Column. IEC Fund., 8, 4, pp. 765-776

[14] Marquardt, W., 1990. Traveling waves in chemical processes. Ind.Chem.Eng., 30, pp. 585-606

[15] Montroll, E.W and G.F. Newell, 1952. Unsteady-State Separation Performance of Cascades. J. of Appl. Physics, 23, 2, pp. 184-194

[16] Osborne, A., 1971. The calculation of Unsteady State Multi-component Distillation Using Partial Differential Equations. AIChE J., 17, 3, pp. 696-703

[17] Rademaker, O., J. E. Rijnsdorp and A. Maarleveld, 1975. Dynamics and Control of Continuous Distillation Units. Elsevier, Amsterdam, 1975

[18] Rosenbrock, H.H., 1960. A Theorem of "Dynamic Conservation" for Distillation Columns. Trans. Instn. Chem. Engrs. 38, pp. 279-287

[19] Rosenbrock, H.H., 1962. The Transient Behavior of Distillation Columns and Heat Exchangers. A Historical and Critical Review. Trans. Instn. Chem. Engrs. 40, pp. 376-384

[20] Skogestad, S. and M. Morari, 1987. The Dominant Time Constant for Distillation Columns. Comput. Chem. Engng., 11, 6, pp. 607-617

[21] Skogestad, S. and M. Morari, 1988. Understanding the Dynamic Behavior of Distillation Columns. Ind. Eng. Chem. Res., 27, pp. 1848-1862

[22] Tabrizi, M.H.N., 1990. An investigation into the dynamics of the distillation column, Search for a wave effect. IEEE Proc., pp. 599- 602

[23] Williams, T.J., 1963. The Status of Studies of the Dynamics of Mass-transfer Operations—A review and Commentary. Chem. Eng. Progr. Symp. Ser. 59, 46, pp. 1-8.

[24] Wong, K.T. and R. Luus, 1980. Model Reduction of High-Order Multistage Systems by the Method of Orthogonal Collocation. The Canadian J. of Chem. Eng., 58, pp. 382-388

[25] Wong, S.K.P. and D.E. Seborg, 1986. Low-order Nonlinear, Dynamic Models for Distillation Columns. Proceedings ACC 86, Seattle.

## Appendix A. Slow time constant of pipe analogy for distillation

We are deriving the expression for the slow time constant for the pipe analogy in section 5.2.2:

$$\tau \approx \frac{\nu e^{\frac{ul}{\nu}}}{u^2} \quad when \quad \frac{ul}{\nu} >> 1 \tag{5.13}$$

The pipe system is shown in Fig. 5.2. We consider only half of the pipe, $z \in [0, l]$, since the system is symmetric about $z = l$.

The starting point for the derivation is the mass balance equation for the impurity, $x$:

$$\frac{\partial x}{\partial t} + u\frac{\partial x}{\partial z} = \nu\frac{\partial^2 x}{\partial z^2} \tag{5.14}$$

with boundary conditions:

$$x(0) = 0 \quad and \quad \phi(l) = [ux - \nu\frac{\partial x}{\partial z}]_{z=l} = 0 \tag{5.15}$$

The first of these boundary conditions states that there is pure fluid at the inlet of the pipe; the other that the flux, $\phi$, of impurity across the middle of the pipe ($z = l$) is zero.

To find the slow eigenvalue, we take the Laplace transform of the mass balance, eq. 5.14:

$$\nu x'' - ux' - sx = 0 \tag{5.16}$$

where $s$ is the Laplace variable. The general solution of this equation is on the form:

$$x = Ae^{\lambda_1 z} + Be^{\lambda_2 z} \tag{5.17}$$

where the parameters are still to be determined.

Substituting this solution into the boundary conditions yields:

$$x(0) = 0 \quad \Rightarrow \quad A + B = 0 \tag{5.18}$$

$$\phi(l) = [ux - \nu\frac{\partial x}{\partial z}]_{z=l} = 0 \quad \Rightarrow \quad A(u - \nu\lambda_1)e^{\lambda_1 l} + B(u - \nu\lambda_2)e^{\lambda_2 l} = 0 \tag{5.19}$$

These two equation for the boundary conditions may be put in matrix form as:

$$\begin{pmatrix} (u - \nu\lambda_1)e^{\lambda_1 l} & (u - \nu\lambda_2)e^{\lambda_2 l} \\ 1 & 1 \end{pmatrix} \begin{pmatrix} A \\ B \end{pmatrix} = 0 \tag{5.20}$$

For this matrix equation to have non-trivial solutions, the determinant of the matrix has to be zero:

$$0 = det \begin{pmatrix} (u - \nu\lambda_1)e^{\lambda_1 l} & (u - \nu\lambda_2)e^{\lambda_2 l} \\ 1 & 1 \end{pmatrix} = (u - \nu\lambda_1)e^{\lambda_1 l} - (u - \nu\lambda_2)e^{\lambda_2 l} \tag{5.21}$$

which may be written (divide by $e^{\lambda_2 l}$):

$$(u - \nu\lambda_1)e^{(\lambda_1 - \lambda_2)l} - (u - \nu\lambda_2) = 0 \tag{5.22}$$

Solving this equation for the pole, $s$, closest to zero, yields the desired result. However, we must first find approximations for the terms in this equation. First, the $\lambda's$ are given by the characteristic equation:

$$\nu\lambda^2 - u\lambda - s = 0 \tag{5.23}$$

which yields:

$$\lambda_1 = \frac{u + \sqrt{u^2 + 4\nu s}}{2\nu} \quad \lambda_2 = \frac{u - \sqrt{u^2 + 4\nu s}}{2\nu} \tag{5.24}$$

from which we may find the following approximations for small $s$ (Taylor series around $s = 0$):

$$u - \nu\lambda_1 \approx -\frac{s\nu}{u} \quad u - \nu\lambda_2 \approx u + \frac{s\nu}{u} \tag{5.25}$$

Moreover, we may find the following approximation (Taylor series):

$$e^{(\lambda_1 - \lambda_2)l} = e^{\frac{\sqrt{u^2+4\nu s}}{\nu} l} \approx e^{\frac{ul}{\nu}}(1 + \frac{2sl}{u}) \tag{5.26}$$

Inserting this into eq. 5.22, neglecting second order terms in $s$ and solving for $s$, yields:

$$s = -\frac{u^2}{\nu(1 + e^{\frac{ul}{\nu}})} \tag{5.27}$$

from which the desired formula for the slow time constant may be found:

$$\tau = -1/s = \frac{\nu}{u^2}(1 + e^{\frac{ul}{\nu}}) \approx \frac{\nu}{u^2} e^{\frac{ul}{\nu}}; \quad for \quad \frac{ul}{\nu} >> 1 \tag{5.28}$$

Thus, we have found the approximation for $\tau$.

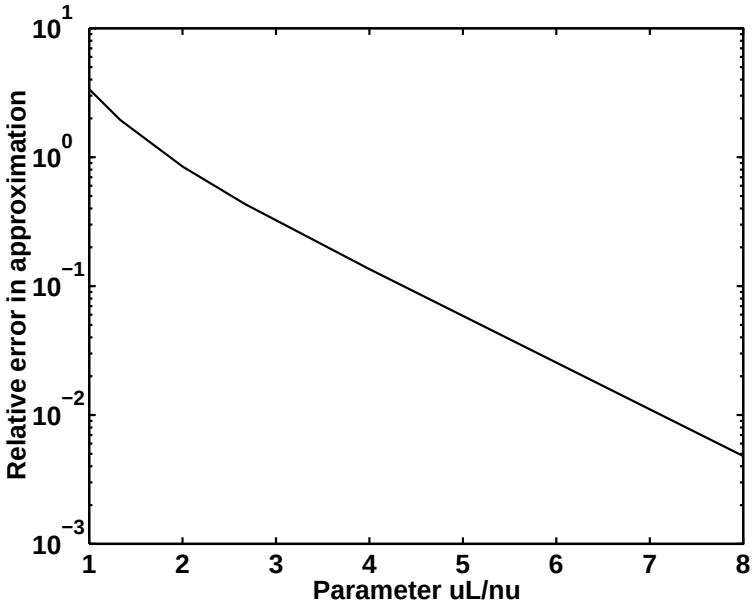


Figure 5.10: Relative error in the approximate formula, eq. 5.28, as function of $\frac{ul}{\nu}$

In order to check how large $\frac{ul}{\nu}$ has to be for this approximation to be valid, we calculated the relative error in $\tau$ as a function of $ul/\nu$, using MATLAB (i.e. numerically). The resulting plot is shown in Fig. 5.28. As can be seen, the relative error is less than about 10% for $ul/\nu > 4$ and less than about 1% for $ul/\nu > 7$.

# Chapter 6

# The Dynamics of Chemical Reactors with Heat Integration

John Morud and Sigurd Skogestad*
Chemical Engineering
University of Trondheim - NTH
N-7034 Trondheim, Norway

Presented at
AIChE Annual Meeting, St. Louis, USA, November 1993

**Abstract**

The starting point for this study was an incident in an industrial ammonia synthesis plant in Germany. A fixed bed reactor became unstable such that the reactor temperatures oscillated with amplitudes of up to $\pm 160^oC$ (limit cycles).

The reactor with its preheater may be viewed as a positive feedback system, and for such systems it is usually assumed in chemical engineering that the response becomes slower as the feedback gain is increased, and that instability occurs as a real pole (system eigenvalue) cross the origin in the complex plane. However, a linear analysis of the reactor system in the vicinity of an operating point reveals that instability occurs as a pair of complex conjugate poles cross the imaginary axis (Hopf bifurcation), and that the system starts oscillating when instability occurs. This somewhat unusual behavior can be explained by the presence of right half plane zeros in the linearized transfer function of the reactor beds.

*Address correspondence to this author. Fax: 47-73594080, E-mail: skoge@kjemi.unit.no

## 6.1 Introduction

Although reactor stability and control has been an active area of research for at least 40 years, incidents such as reactor instability happen frequently in commercial plants. It is important to be able to predict such phenomena, as they may be fatal to a plant, and hazardious to the plant personnel.

The starting point of this work was an incident in an industrial ammonia synthesis plant in Germany. A fixed bed ammonia synthesis reactor—operated without feedback control—suddenly became unstable, such that the recorded temperatures in the reactor started oscillating with a period of about 7 minutes, and a maximum amplitude of about 160 $^0C$ (Naess *et al.*, 1993). A typical such temperature recording is shown in Fig. 6.1. The purpose of this paper is to provide an explanation of this sort of reactor behavior.

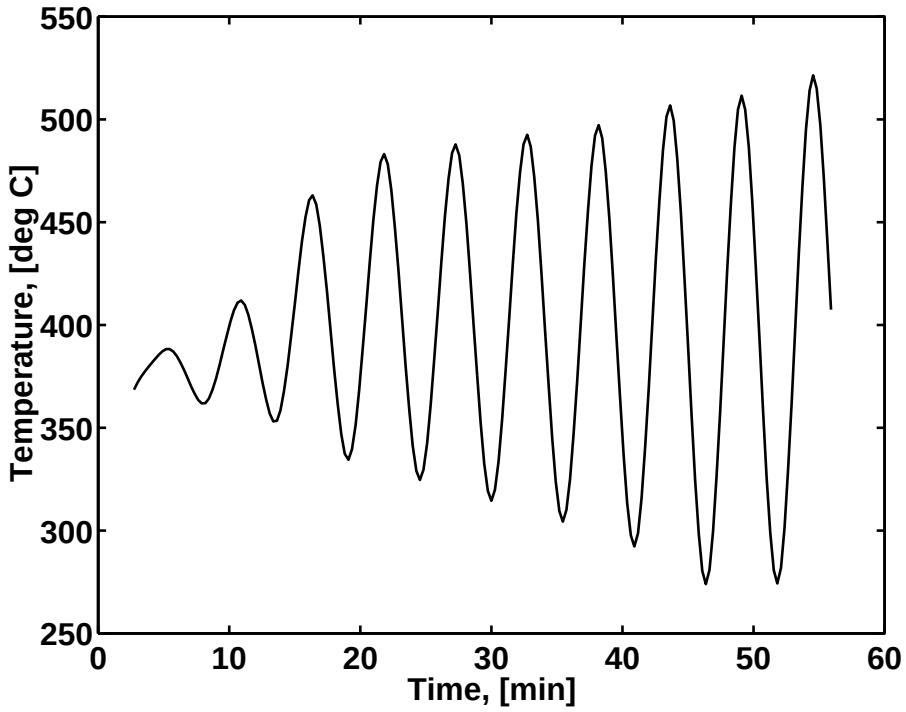


Figure 6.1: Typical temperature recording in the ammonia synthesis reactor (close to the reactor outlet).

We give a brief outline of the paper: First, we present a mathematical model of the ammonia synthesis reactor—describing the concervation of mass and energy. Simulations using this model reproduce the temperature oscillations observed in the industrial plant. We then perform a steady state analysis similar to that of van Heerden (1953), which proves to be inadequate. We therefore proceed with a linear dynamic analysis close to an operating point, which reveals that the instability occurs as a pair of complex conjugate poles cross the imaginary axis in the complex plane (Hopf bifurcation). Finally, we discuss the implications for operation and control of such reactors.

The rest of this Introduction is devoted to reviewing previous work. General work on reactor stability, modeling and control is abundant. Crider and Foss (1968) refer to Nusselt (1927) and independently Schuman (1929) as the first to present a thermal analysis of packed beds. Van Heerden (1953) and Aris and Amundson (1958) analyzed the stability of the steady states of autothermal reactors. Limit cycle behavior in autothermal reactors was presented by Reilly an Schmitz (1966,1967) and Pareja and Reilly (1969). Stephens and Richards (1973) performed a steady state and dynamic analysis of an ammonia synthesis plant and notice that steady state stability criteria are not sufficient for stability. The fixed bed reactor is discussed extensively in the survey of Schmitz (1975) and in the further survey of Ray (1972), Eigenberger (1976) and Jørgensen (1986). Silverstein and Shinnar (1982) discuss the stability of the heat integrated fixed bed reactor. Vakil *et al.* (1973), Wallmann *et al.* (1979), Foss *et al.* (1980) and Wallman and Foss (1981) study the use of multivariable controllers for the control of fixed bed reactors.

### 6.1.1 A simple model of the reactor

Models for fixed beds are abundant in the literature (see e.g. Eigenberger, 1976). The main purpose of our model is **not** to reproduce the industrial case with great numerical accuracy, but rather to yield qualitative insight into the observed phenomenon. Our model is therefore kept as simple as possible.

Fig. 6.2 indicates the simplified system, consisting of three beds in series with quench using fresh feed between the beds and preheating of the feed with the effluent. A material and energy balance yields two partial differential equations:

$$u_w \frac{\partial c}{\partial z} = \frac{C_p}{C_{pc}} r(T,c) \tag{6.1}$$

$$\frac{\partial T}{\partial t} + u_w \frac{\partial T}{\partial z} = \frac{-\Delta H_{rx}}{C_{pc}} r(T,c) + \Gamma \frac{\partial^2 T}{\partial z^2} \tag{6.2}$$

where:

| | | |
|---|---|---|
| $t$ | Time | [sec.] |
| $z$ | Position in reactor | [-] |
| $T$ | Particle temperature | [K] |
| $c$ | Ammonia concentration | [kg NH3/kg gas] |
| $u_w$ | Migration velocity of temperature wave | [1/sec.] |
| $-\Delta H_{rx}$ | Heat of reaction | [J/kg.NH3] |
| $C_{pc}$ | Heat capacity of catalyst and gas | [J/kg cat.K] |
| $C_p$ | Heat capacity of gas | [J/kg.K] |
| $r(T,c)$ | Reaction rate | [kg NH3/kg cat.sec.] |
| $\Gamma$ | Dispersion coefficient due to finite heat transfer | [1/sec.] |

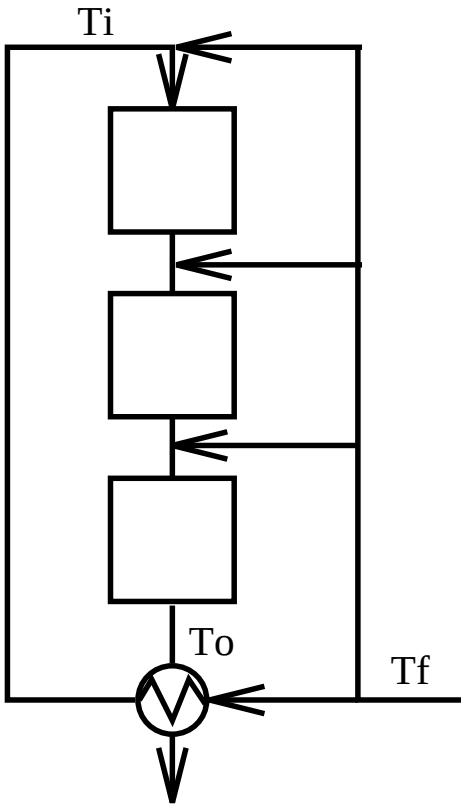


Figure 6.2: Sketch of reactor system with three beds and preheater.

The model was discretized using a finite difference method, and integrated using a standard Runge-Kutta method.

The feed-effluent heat exchanger was modeled with an $\epsilon - NTU$ model (without dynamics for simplicity), which yields a relationship of the form:

$$T_i = \epsilon T_o + (1 - \epsilon) T_f \tag{6.3}$$

where $T_i$ is the reactor inlet temperature and $T_o$ the reactor outlet temperature (see Fig. 6.2) and the heat exchanger efficiency $\epsilon \in [0 \quad 1]$ is a constant independent of temperature.

Appendix A contains numerical values for the parameters as well as a more detailed description of the model.

### 6.1.2 Linearized model

For later analysis, the model of the reactor (without the heat exchanger) was linearized numerically about an operating point (feed temperature 234.8 $^oC$), yielding a standard linear state space model with 30 states on the form:

$$\frac{dx}{dt} = Ax + Bu, \quad y = Cx \tag{6.4}$$

where the state vector $x$ consists of temperatures along the bed; $u$ is the inlet temperature to the first bed, $T_i$ (before the quench; quench temperature $T_f$ was assumed constant); and $y$ is the outlet temperature of the third bed. The transfer function $g(s)$ for the reactor is then $g(s) = C(sI - A)^{-1}B$. The model was analyzed using MATLAB.

### 6.1.3 Simulations of limit cycle behavior

Simulations using the nonlinear model reproduce the observed temperature oscillations in the industrial plant and confirm that the oscillations originates in the reactor/preheating system.

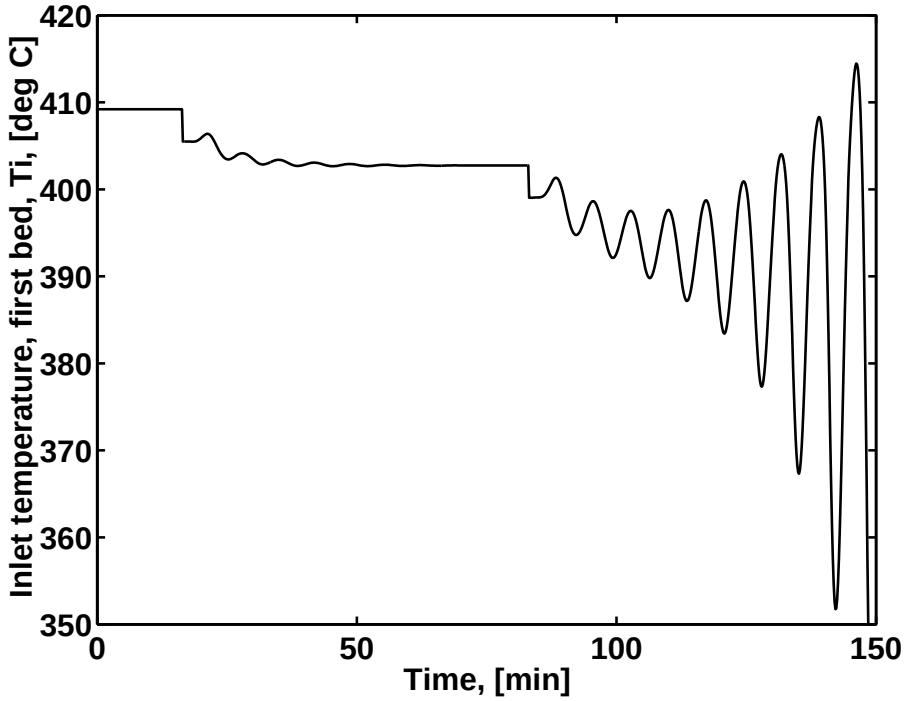


Figure 6.3: Stepping down the feed temperature

A typical simulation result is shown in Figure 6.3, showing the inlet temperature to the first reactor bed as a function of time. The system is disturbed by reducing the feed temperature, $T_f$, by 10 $^oC$ every 4000 seconds, starting from $T_f = 250^oC$. As long as the feed temperature is sufficiently high, the system is stable; however, when the feed temperature drops below some critical value ($T_{f,crit} = 234.8^oC$), the system becomes unstable and exhibit limit cycle behavior (oscillations). If the feed temperature is kept constant after the onset of instability, the long term behavior looks like Figure 6.4, showing sustained oscillations.

We have just looked at the temperature of a fixed position—the first bed inlet—as a function of time. To understand qualitatively what happens in the reactor, we now consider temperature profiles through the reactor at fixed times. Figures 6.5a to 6.5f show several such temperature profiles during one period of the sustained oscillations.

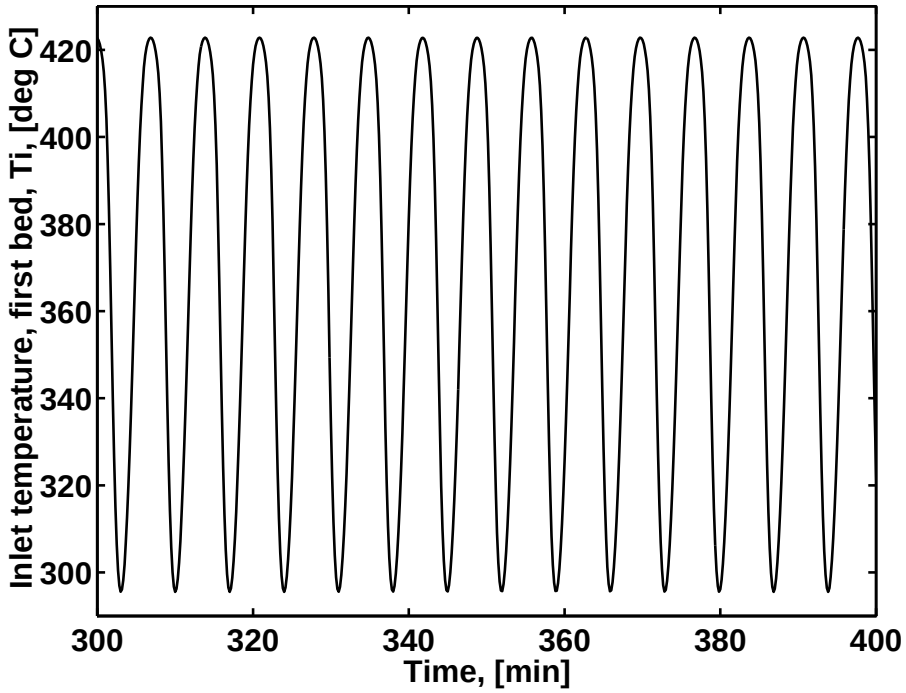


Figure 6.4: Sustained oscillations in temperature

On the horizontal axis, $x = 0$ corresponds to the inlet of the first bed and $x = 1$ to the outlet of the last bed. On the vertical axis is the reactor temperature (range 250 $^oC$-550 $^oC$). The discontinuities in the figures are due to the quenching.

One should note the wavelike bump to the left in Figure 6.5a. 70 seconds later, see Figure 6.5b, the bump has moved a little to the right, growing in size. The wave may be traced through Figures 6.5c-f, where it induces a new wave by heat exchange with the reactor feed, resulting in the sustained temperature oscillations.

## 6.2 Analysis

The objective of this section is to explain the above results. We first start with a simple steady-state analysis which proves to be inadequate. We then perform a conventional linear stability analysis which is found to be consistent with the nonlinear simulations. Finally, we explain why the initial steady-state analysis was inadequate in this case.

### 6.2.1 Simplified steady-state analysis

We first perform a simplified analysis based on steady-state information, similar to that of van Heerden (1953). Consider Figure 6.6, where the steady state characteristics of the reactor and heat exchanger are shown. The plot shows the relationship between the temperatures $T_o$ versus $T_i$ (see Figure 6.2) for the reactor (S-shaped curve) and the heat exchanger (straight line). It is implicitly assumed that other quantities are

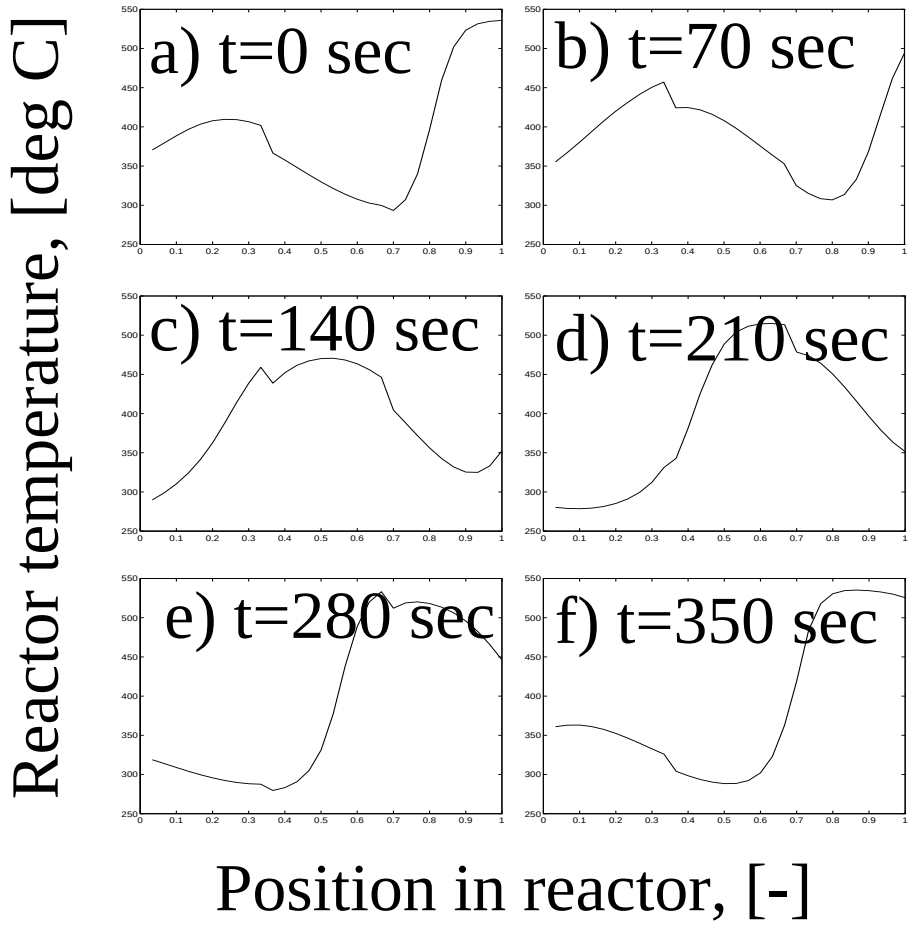


Figure 6.5: Sustained oscillations in temperature

held constant (Flow rates, feed temperature etc.). The heat exchanger characteristic gives the relation between $T_o$, which is considered an input to the exchanger, and $T_i$, which is considered an output. Similarly, the reactor characteristic gives the relation between reactor inlet temperature, $T_i$, and reactor outlet temperature, $T_o$. The plot is very similar to the classical van Heerden plot (van Heerden, 1953).

The steady state operating points are points where the two curves intersect. For the conditions given in Figure 6.6 there are three possible steady state solutions, and the desired one, in which we operate, is the upper one with the highest temperature. Van Heerden (1953) showed that steady states solutions where the reactor characteristic is steeper than the heat exchanger characteristic are always unstable; thus the middle solution in Figure 6.6 is unstable (Note that with control, it is possible to stabilize any operating point).

Now consider the stability of the upper (desired) operating point. Van Heerden (1953) claimed that points where the heat exchanger characteristic is steeper than the reactor characteristic are stable. To induce instability one may reduce the feed temperature as done in the previous section, which corresponds closely to translating the two characteristics in Figure 6.6 in such a way as to bring the two curves closer to

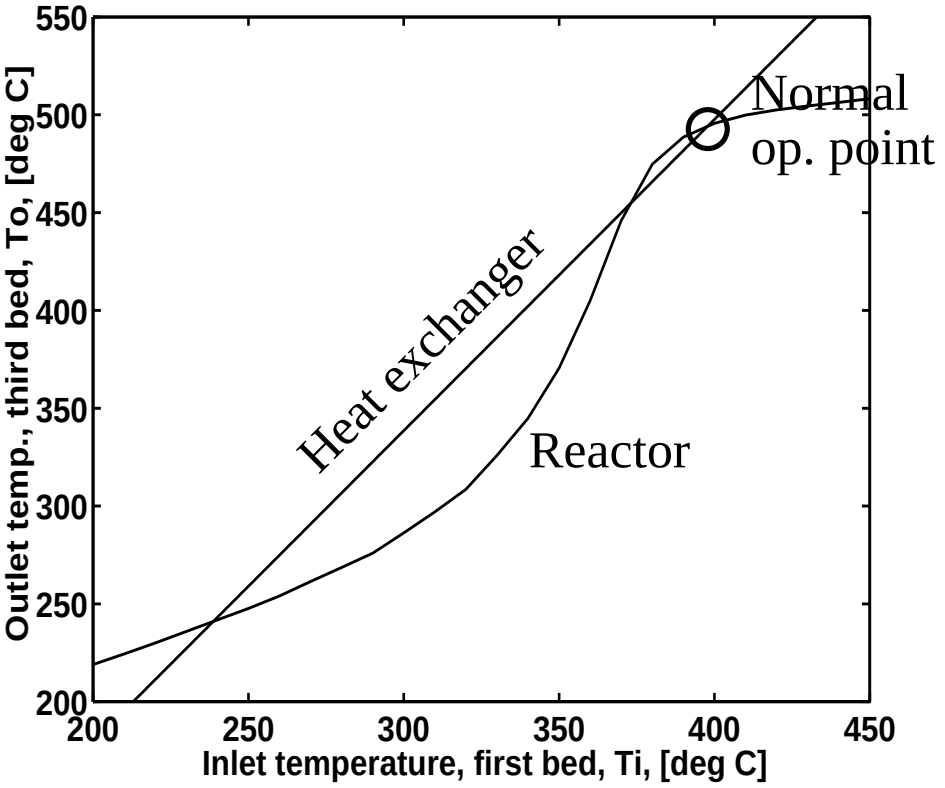


Figure 6.6: Steady state characteristics of reactor (S-shaped curve) and heat exchanger (straight line).

tangency (such that the middle and upper solutions coincide). From the interpretation of van Heerden (1953) one would expect instability to occur exactly when the two curves touch each other. However, the simulations indicate that the oscillatory behavior begins just **before** the curves become tangents to each other. At first this was believed to be caused by nonlinearity or numerical errors, but as we show below a more careful analysis shows that the simulations are indeed correct, and that the upper solution may be unstable, demonstrating that a steady-state analysis is insufficient (Aris and Amundson, 1958).

### 6.2.2 Linear stability analysis

Close to an operating point, the dynamics of a system is well described by its linearized model. The reactor system in fig. 6.2 may hence be represented by the block diagram with positive feedback shown in Figure 6.7, where $k = \varepsilon$ is the steady state gain of the heat exchanger and $g(s)$ the transfer function of the reactor. A linear stability analysis based on computing the eigenvalues (given by the zeros of $1 - g(s)k = 0$) confirmed that the instability occurred at the point found in the nonlinear simulations. Below we consider a root locus analysis and the Nyquist plot to understand what happens.

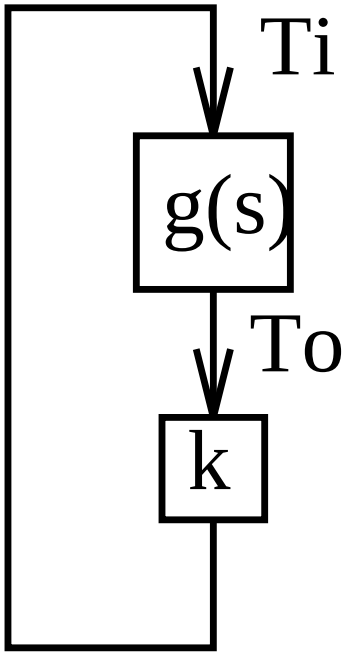


Figure 6.7: Block diagram

### Analysis of reactor model

An analysis of the transfer function of $g(s)$ shows that it has several RHP (right half plane) zeros. Such RHP-zeros generally correspond to inverse responses, and this is confirmed by Figure 6.8 which shows the outlet temperature, $T_o$ in response to a step increase in the inlet temperature, $T_i$. The above response is for the linear model, and similar responses were found for the nonlinear model.

### Root locus analysis

To see how these zeros affect the system stability, assume that $k$ is varied from zero to infinity, corresponding to changing the heat transfer area in the heat exchanger. This yields the root locus plot shown in Figure 6.9. When $k = 0$, the poles of the system are equal to the poles of the system without the heat exchanger (marked with 'X' on the figure). As $k$ is increased towards infinity (corresponding to increased heat transfer area), the poles which stay finite approach the zeros of $g(s)$ (marked with 'O'). Due to the presence of the **right half plane zeros**, the first pole to cross the imaginary axis is **not** the real pole crossing the origin, but a pair of complex conjugate poles.

### Nyquist plot analysis

The stability of the system may be analyzed using the standard Nyquist criterion: For **positive feedback** with a stable $g(s)$, the system is unstable if and only if a plot of the loop transfer function $g(j\omega)k$ encircles the $1 + j0$ point (not -1 point) in the complex plane as the frequency $\omega$ is varied from $-\infty$ to $+\infty$ (Or—which is equivalent—if $g(j\omega)$

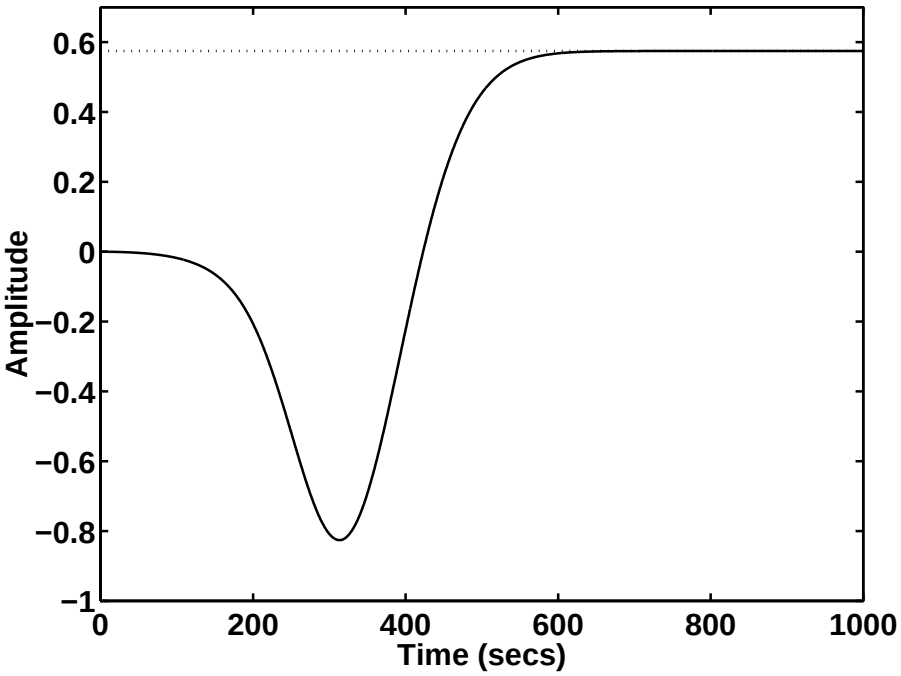


Figure 6.8: Step response of g(s) (reactor without preheating)

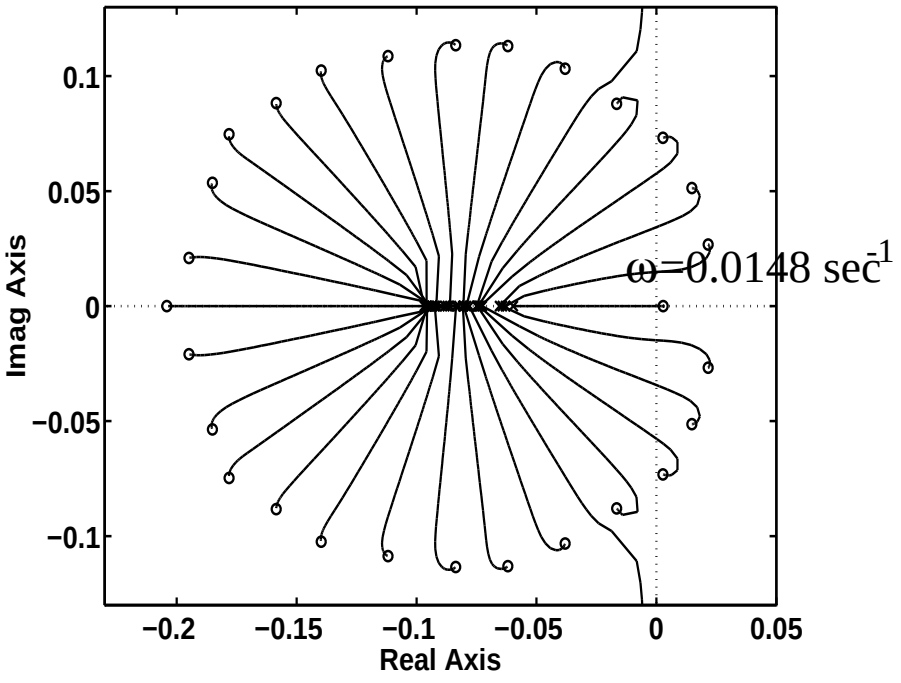


Figure 6.9: Root locus plot of system

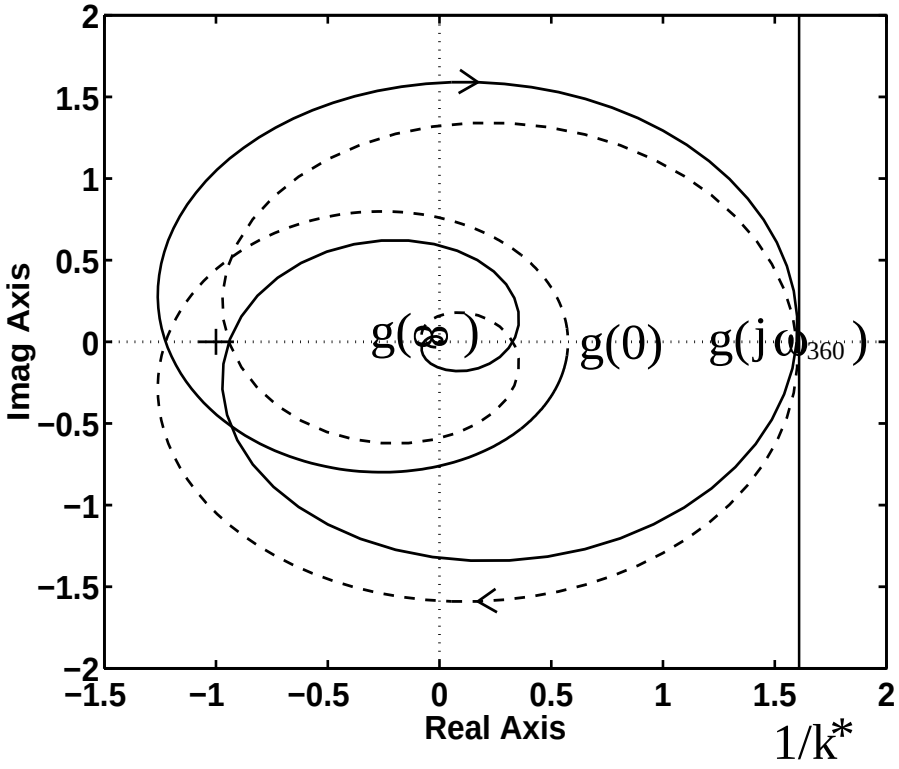


Figure 6.10: Nyquist plot of g(s)

encircles the $1/k + j0$ point).

Consider first the stability of the middle operating point in Fig. 6.6. The reactor steady state gain, $g(0)$, is the slope of the reactor characteristic, and the heat exchanger gain, $k$, is the inverse of the slope of the heat exchanger characteristic. It then follows that the steady state loop gain $g(0)k$ is the ratio of the two slopes, which is larger than one at this operating point since the reactor characteristic is steeper than the heat exchanger characteristic. Since $g(j\omega)k = 0$ at $\omega = \pm\infty$, encirclement of the $1 + j0$ point is unavoidable, and the system is therefore unstable at the middle operating point.

Normally, one will with positive feedback expect that the closed-loop system is stable when $g(0)k$ is less than one. The reason is that the gain $|g(j\omega)k|$ normally decreases with frequency, such that $g(j\omega)k$ never cross the real axis to the right of $g(0)k$ and hence never to the right of $1 + j0$. This implies no encirclement, and thus stability. However, in our case there are right half plane zeros in $g(s)$ which increase the loop gain and at the same time yield a negative phase shift, and make this assumption invalid. This is seen from the Nyquist plot of $g(j\omega)$ in Figure 6.10. There is a point of $g(j\omega)$ crossing the real axis to the right of $g(0)$ at some frequency $\omega_{360}$. As stated above, the Nyquist stability condition tells that the system will be unstable if this curve encircles the point $1/k$. The system is stable for small values of $k$ (corresponding to little heat integration), and is unstable if $k > k^*$, where the critical gain $k^*$ is

given by $k^* = 1/g(j\omega_{360})$. As can be seen, this gain, $k^*$, is a little lower than the one corresponding to the instability of the steady state, $k = 1/g(0)$, i.e. the instability will occur when the heat exchanger characteristic in fig 6.6 is a little **steeper** than the reactor characteristic. The fact that the instability occurs at a nonzero frequency, also shows that the onset of the instability corresponds to a Hopf bifurcation, which is consistent with the observed limit cycles in the nonlinear simulations.

## 6.3 Discussion

### 6.3.1 Physical explanation for the inverse response

The reason why the reactor instability manifests itself as oscillations—and not the more common runaway without any oscillations—is the inverse response behavior of the reactor. A physical explanation for this inverse response is therefore of interest.

Consider a fixed bed where an exothermic reaction is taking place, and suppose we make a sudden decrease in the inlet temperature (step change). This will affect the bed outlet by two mechanisms: by the migration of temperature waves in the bed, which is a slow process; and by changes in the concentration of chemical species, which is a relatively fast process. Now, the initial effect of the decrease in inlet temperature is normally a decrease in the reaction rate in the first part of the bed. Since the temperature waves are slow, the initial effect on the last part of the bed is only to make the reactant concentration higher, such that the outlet temperature **increases**. Eventually, there is a loss of conversion in the whole reactor and the outlet temperature decreases. Such **inverse response** characteristics are well known (Silverstein, 1982), and indicate **right half plane zeros** in the linearized transfer function of the bed. Right half plane zeros are of fundamental importance when discussing control, as they limit the achievable control performance of any control system.

### 6.3.2 Effect of pressure in the synthesis loop

In this paper, we have shown that the ammonia synthesis reactor may become unstable when the feed temperature drops below a critical value. It is important to note that this critical value is pressure dependent, such that the instability may just as well be initiated by a sudden drop in pressure in the synthesis loop, which was how the instability was induced in the industrial case.

### 6.3.3 "Positive feedback yields slow responses"

In the Nyquist plot analysis above, it was shown that the reason for oscillatory instability in the ammonia synthesis reactor could be attributed to the shape of the reactor transfer function, $g(j\omega)$. The plot of this transfer function crosses the real axis at a point, $g(j\omega_{360})$, to **the right** of the steady state point, $g(0)$.

However, for most chemical engineering systems, there is no such point of $g(j\omega)$ crossing the real axis to the right of $g(0)$. When the positive feedback gain, $k$, is increased, the instability will then occur as a pole moves through the origin. This has

made many authors make statements like: "Positive feedback in a plant makes the response of the plant slow, and the sensitivity to slow disturbances high". Since there are systems where this is not the case, as demonstrated above, such statements should be used with care.

### 6.3.4 Control of reactors with heat integration

Although there has been a lot of work on the control of fixed bed reactors, many reactors in the industry are left uncontrolled. When a processing unit can be operated safely without control, this is to be preferred, as it is wanted to keep the complexity of a plant to a minimum.

Two important issues which have to be considered for the ammonia synthesis reactor in question are extinction and limit cycle behavior. Extinction of the reactor—which corresponds to operation at the lower operating point in Fig. 6.6—may occur if the reactor temperature becomes sufficiently low. When this happens, the reactor can not resume normal operation without external addition of heat, which necessitates special startup procedures. The other important issue, limit cycle behavior induced by heat feedback through the heat exchanger, may lead to material damage in the reactor, as well as deterioration of the catalyst.

Even a very simple controller will get rid of the possibility of the limit cycle behavior caused by preheating the reactor feed by the effluent. For example, consider using the quench valve before the first bed to control the temperature at the first bed inlet. This may be done using a simple PI-controller. Since there is no RHP-zero in this control loop, the controller may be made quite fast (compared to the overall reactor response time of about 7 min). Thus, the feedback path through the controller will dominate compared with the positive feedback through the heat exchanger, and thus the reactor with controller will behave approximately as a reactor without feed-effluent heat exchange. That is, the reactor will exhibit a dynamic behavior similar to a reactor with an independent preheater.

This controller will of course not eliminate the possibility of reactor extinction, which may or may not be a problem. To avoid extinction, one may make sure that gas temperature at the first bed inlet—the set point of the controller—is sufficiently high, e.g. with a safety margin of $10^oC$ or so. Alternatively, one might specify that the quench valve in question should have a specified margin from fully closed or fully open, and cascade a (relatively slow) controller on top which sets the safety margin accordingly. It is important that this last controller is not too fast, as the reactor transfer function has inverse response behavior.

One may ask whether the observed RHP-zeros will limit the performance of the reactor. The answer is that this will only be the case if one wants to control the reactor outlet temperature $T_o$ (or some other internal temperature in the reactor) using a quench further upstream in the reactor (and thus adjusting the inlet temperature to an upstream bed). Probably, it is not critical that the outlet temperature is tightly controlled, and the RHP-zero will not present a serious limitation. Also, as already noted, there is no RHP-zero when controlling the inlet temperature using the inlet quench, so stabilization is not limited by RHP-zeros.

### 6.3.5 Comparison with previous work

That ammonia synthesis reactors may exhibit limit cycle behavior, has also been noted by Stephens and Richards (1973) (possibly because of an incident in an ICI plant?). However, their paper does not contain any dynamic analysis, and leave the impression that the authors did not really understand what is happening.

However, the very general paper by Silverstein and Shinnar (1982) contains a generic analysis of reactor systems with feed-effluent heat exchange and a combustion chamber. In their analysis, which is based on Linear Systems Theory, they explain the conditions for reactor stability. Although these authors did not specifically mention ammonia synthesis reactors, one may consider ammonia synthesis to be a special case of their analysis.

### 6.3.6 Effect of plant integration on the dynamics of plants

From a general point of view, introducing heat integration in a plant may be thought of as moving the poles and zeros of the plant. Generally, the introduction of feedback paths moves poles, parallel paths move zeros. Feedback paths introduced by heat integration may therefore destabilize an otherwise stable plant.

For control, the zero locations of a plant may be more important than the pole locations. A controller may be considered to be an approximate inverse of the plant. Right half plane zeros of the plant will therefore limit the bandwidth of the control system, since they will end up as unstable poles in the controller if the bandwidth is too high. Parallel paths introduced by heat integration may move plant zeros into the right half plane, and hence introduce fundamental limitations in achievable control performance. However, as noted above the RHP-zero may not affect stabilization if there are measurements available for which the RHP-zero does not appear.

Positive feedback paths in plants will often make a pole go through the origin as the loop gain of the feedback path is increased towards 1. This will the make the response of the plant slow, and the sensitivity to slow disturbances high. For fixed bed reactors, this is not what is happening.

## 6.4 Conclusion/Summary

An industrial case has been analyzed. A fixed bed autothermal ammonia synthesis reactor became unstable, such that the recorded temperatures in the reactor oscillated heavily. Such oscillations may damage the reactor.

A mathematical model of the reactor reproduces the phenomenon. The oscillatory behavior (limit cycles) occurs in the simulations when the reactor feed temperature or the operating pressure is too low. The phenomenon is best described as a temperature wave migrating through the reactor, being fed back through the heat exchanger.

A linear analysis close to the steady state operating point shows that for given operating conditions in the reactor, the phenomenon occurs when the heat exchanger area becomes sufficiently high. From a linear point of view, the phenomenon may be explained using root locus techniques. Right half plane zeros in the reactor bed transfer

functions attract poles as the "gain" of the heat exchanger is increased. The instability occurs as a pair of complex conjugate poles cross the imaginary axis in the complex plane.

Even a simple controller may eliminate the possibility of limit cycle behavior. E.g. fixing the temperature at the entrance of the first bed using a PI-controller will do this. To avoid extinction, one could e.g. cascade a slow controller on top.

# References

[1] Aris,R. and Amundson, N.R.(1958). An analysis of chemical reactor stability and control. Ch.Eng.Sci, vol 7,no 3, pp 121-155.

[2] Barkelew, C.H. (1959). Stability of chemical reactors. Chem. Prog. Symp. ser. 55, 25, pp 37-46

[3] Crider, J.E. and Foss, A.S. (1966). Computational studies of transients in packed tubular reactors. AIChE J. 12, pp 514-522

[4] Crider, J.E. and Foss, A.S. (1968). An analytic solution for the dynamics of a packed adiabatic chemical reactor. AIChE J. 14, 1,pp 77-84

[5] van Doesburg, H. and de Jong, W.A. (1976). Transient behavior of an adiabatic fixed bed methanator. Chem. Eng. Sci 31, pp 45-51 and 53-58

[6] Eigenberger, G. (1985). Dynamics and stability of chemical engng. processes. Int. Chem. Eng. v 25, no 4, pp. 595-610

[7] Eigenberger, G. and Schuler, H. (1989). Reactor stability and safe reaction engineering. Int. Chem. Eng. 29, 1, pp 12-25

[8] Foss, A.S. *et al.* (1980). Multivariable control system for twobed reactors by the characteristic locus method. Ind. Eng. Chem. Fund. 19, 1, pp 109-117

[9] Gilles, E.D. (1976). Reactor models. Chem. Reaction Engng, 4th Int. Symp., Heidelberg, DECHEMA, Frankfurt, pp. 459-486

[10] Gilles, E.D. *et al* (1978). Relaxation oscillations in chemical reactors. AIChE J. 24, pp. 912-920

[11] Gusciora, P.H. and Foss, A.S. (1989). Detecting and avoiding unstable operation of autothermal reactors. AIChE J. v 35, no 6, pp 881-890

[12] Jorgensen, S.B. (1986). Fixed Bed Reactors and Control - a review. DYCORD-86, pp. 11-21

[13] Kreith, F. and Bohn, M.S. (1986). Principles of heat transfer. Harper and Row, 1986, ISBN 0-06-350369-7

[14] Naess, L., Mjaavatten, A. and Lie, J.O. (1992) Using Dynamic Process Simulation from Conception to Normal Operation of Process Plants. ESCAPE 1, May 24-28 1992, Elsinore, Denmark

[15] Naess, L., Mjaavatten, A. and Lie, J.O. (1992) Using Dynamic Process Simulation from Conception to Normal Operation of Process Plants. Comp. Chem. Eng., v 17, no 5/6, pp 585-600

[16] Pareja, G. and Reilly, M.J. (1969). Dynamic Effects of Recycle Elements in Tubular Reactor Systems. IEC Fund. 8, 442.

[17] Reilly M. J. and Schmitz, R. A. (1966) AIChE J. 12, 153.

[18] Reilly M. J. and Schmitz, R. A. (1967) AIChE J. 12, 153.

[19] Ray, W.H (1972). 2nd ISCRE, Amsterdam, A8-2

[20] Schmitz, R.A. (1975). Advan. Chem. Ser. 148,156

[21] Silverstein, J.L. and Shinnar, R. (1982). Effect of design on the stability and control of fixed bed reactors with heat feedback. Ind. Eng. Chem. Fund. 21, pp. 241-256

[22] Stephens, A.D. and Richards, R.J. (1973). Steady State and Dynamic Analysis of an Ammonia Synthesis Plant. Automatica, vol. 9, pp 65-78

[23] Vakil, H.B. *et al.* (1973). Fixed bed reactor control with state estimation. Ind. Eng. Chem. Fund. 12, 3, pp. 328-335

[24] van Heerden, C. (1953). Autothermic Processes. Properties and Reactor design. Industr. Engng. Chem. (Industr.), 45, 1242

[25] Wallmann, P.H. and Foss, A.S. (1979). Multivariable integral control for fixed bed reactors. Ind. Eng. Chem. Fund. 18, 4, pp 392-399

[26] Wallmann, P.H. and Foss, A.S. (1981). Experiences with dynamic estimators for fixed bed reactors. Ind. Eng. Chem. Fund. 20, 3, pp. 234-239

# Appendix A. Data for the simple model

Reaction rate (kg $NH_3$/kg catalyst.hr) as a function of temperature and concentration (interpolation was used for the computations):

| | Mole % ammonia | | | | | | | |
|---|---|---|---|---|---|---|---|---|
| Temp $^oC$ | 4 | 8 | 12 | 16 | 20 | 24 | 28 | 32 |
| 200 | 4.21E-03 | 1.99E-03 | 1.24E-03 | 8.60E-04 | 6.30E-04 | 4.80E-04 | 3.80E-04 | 3.00E-04 |
| 225 | 1.09E-02 | 4.94E-03 | 2.990E-03 | 2.03E-03 | 1.47E-03 | 1.10E-03 | 8.50E-04 | 6.60E-04 |
| 250 | 2.82E-02 | 1.22E-02 | 7.180E-03 | 4.78E-03 | 3.40E-03 | 2.52E-03 | 1.91E-03 | 1.47E-03 |
| 275 | 7.16E-02 | 2.99E-02 | 1.707E-02 | 1.113E-02 | 7.77E-03 | 5.66E-03 | 4.23E-03 | 3.21E-03 |
| 300 | 0.17460 | 7.09E-02 | 3.95E-02 | 2.52E-02 | 1.73E-02 | 1.24E-02 | 9.07E-03 | 6.77E-03 |
| 325 | 0.39791 | 0.16031 | 8.73E-02 | 5.45E-02 | 3.66E-02 | 2.56E-02 | 1.84E-02 | 1.34E-02 |
| 350 | 0.82238 | 0.33626 | 0.18008 | 0.10986 | 7.20E-02 | 4.91E-02 | 3.42E-02 | 2.39E-02 |
| 375 | 1.5253 | 0.63940 | 0.33894 | 0.20208 | 0.12851 | 8.44E-02 | 5.57E-02 | 3.60E-02 |
| 400 | 2.4752 | 1.0914 | 0.57462 | 0.33355 | 0.20325 | 0.12507 | 7.43E-02 | 3.91E-02 |
| 425 | 3.7000 | 1.6802 | 0.87489 | 0.48855 | 0.27687 | 0.14894 | 6.51E-02 | 6.19E-03 |
| 450 | 5.1418 | 2.3640 | 1.1988 | 0.62469 | 0.30373 | 0.10701 | -2.40E-02 | -0.11790 |
| 475 | 6.7532 | 2.9962 | 1.4717 | 0.66174 | 0.19777 | -9.31E-02 | -0.29030 | -0.43510 |
| 500 | 8.4343 | 3.6015 | 1.5726 | 0.46305 | -0.19270 | -0.61340 | -0.90480 | -1.1228 |
| 525 | 10.1174 | 3.9467 | 1.3117 | -0.19340 | -1.1162 | -1.7242 | -2.1527 | -2.4758 |
| 550 | 11.660 | 3.8427 | 0.41310 | -1.6289 | -2.9469 | -3.8436 | -4.4824 | -4.9621 |
| 575 | 12.771 | 3.0260 | -1.4267 | -4.2211 | -6.1385 | -7.5211 | -8.5284 | -9.2748 |
| 600 | 13.233 | 1.2188 | -4.5484 | -8.4020 | -11.188 | -13.156 | -14.872 | -16.198 |
| 625 | 12.847 | -1.9064 | -9.2383 | -14.312 | -18.284 | -21.444 | -23.951 | -25.502 |
| 650 | 10.3176 | -6.3544 | -15.151 | -21.402 | -26.502 | -30.877 | -34.666 | -37.880 |
| 675 | 6.8883 | -12.151 | -22.775 | -30.364 | -36.450 | -41.802 | -46.647 | -51.112 |
| 700 | 2.5073 | -19.668 | -32.737 | -42.303 | -49.995 | -56.491 | -62.140 | -67.143 |
| 725 | -2.9827 | -29.206 | -45.366 | -57.381 | -67.103 | -75.337 | -82.506 | -88.864 |
| 750 | -9.7330 | -41.084 | -61.085 | -76.100 | -88.278 | -98.587 | -107.56 | -115.50 |
| 775 | -17.889 | -55.623 | -80.337 | -98.986 | -114.10 | -126.86 | -137.93 | -147.70 |
| 800 | -27.577 | -73.145 | -103.580 | -126.58 | -145.17 | -160.81 | -174.30 | -186.16 |

Table 6.1: Reaction rate, r [kg NH3/kg catalyst.hr] as function of temperature and ammonia concentration

The reaction is $N_2 + 3H_2 \rightleftharpoons 2NH_3$ and the feed is stochiometric.

Gas heat capacity, $C_{pg}$ 3500 $J/kg.K$

| | |
|---|---|
| Heat capacity of catalyst, $C_{pc}$ | 1100 $J/kg.K$ |
| Heat of reaction $-\Delta H_{rx}$ | $2.7 \cdot 10^6$ $J/kg\ NH_3$ |
| Migration velocity, bed 1, $u_{w1}$ | 0.0111 $bed\ lenghts/sec.$ |
| Migration velocity, bed 2, $u_{w2}$ | 0.0092 $bed\ lenghts/sec.$ |
| Migration velocity, bed 3, $u_{w3}$ | 0.0067 $bed\ lenghts/sec.$ |
| Dispersion coefficient, bed 1, $\Gamma_1$ | $5.6 \cdot 10^{-4}$ $(bed\ lenghts)^2/sec.$ |
| Dispersion coefficient, bed 2, $\Gamma_2$ | $4.6 \cdot 10^{-4}$ $(bed\ lenghts)^2/sec.$ |
| Dispersion coefficient, bed 3, $\Gamma_3$ | $3.3 \cdot 10^{-4}$ $(bed\ lenghts)^2/sec.$ |

Typical operating conditions:

| | |
|---|---|
| Mass flow through heat exchanger, $\dot{m}_c$ | 127 $tons/hr$ |
| Quench 1. bed, $Q_1$ | 58 $tons/hr$ |
| Quench 2. bed, $Q_2$ | 35 $tons/hr$ |
| Quench 3. bed, $Q_3$ | 32 $tons/hr$ |

| | |
|---|---|
| Inlet mole fraction $NH_3$ (stochiometric feed) | 0.04 |
| Reactor pressure | 200 $bar$ |
| Typical inlet gas feed temperature, $T_f$ | 240 $^oC$ |

Heat exchanger:

| | |
|---|---|
| Heat transfer coefficient, $U$ | 536 $W/m^2.K$ |
| Heat exchanger area, $A$ | 283 $m^2$ |
| Calculated heat exchanger efficiency, $\epsilon$ | 0.6285 |

Data not needed for simple model (needed for more rigorous models):

| | |
|---|---|
| Volume, bed 1 | 6.69 $m^3$ |
| Volume, bed 2 | 9.63 $m^3$ |
| Volume, bed 3 | 15.2 $m^3$ |
| Bed void fraction, $\alpha$ | 0.33 |
| Catalyst/gas heat transfer coefficient, $ha$, bed 1 | $5.3 \cdot 10^5$ $W/m^3.K$ |
| Catalyst/gas heat transfer coefficient, $ha$, bed 2 | $4.4 \cdot 10^5$ $W/m^3.K$ |
| Catalyst/gas heat transfer coefficient, $ha$, bed 3 | $3.3 \cdot 10^5$ $W/m^3.K$ |
| Catalyst bulk density | 2200 $kg/m^3$ |
| Typical gas density | 50 $kg/m^3$ |

## Mathematical model of quench points

The mixing of streams at quench points were modelled as:

$$T_{mix} = \frac{\dot{m}_F}{\dot{m}_F + \dot{m}_q} T_F + \frac{\dot{m}_q}{\dot{m}_F + \dot{m}_q} T_q \tag{6.5}$$

$$c_{mix} = \frac{\dot{m}_F}{\dot{m}_F + \dot{m}_q} c_F + \frac{\dot{m}_q}{\dot{m}_F + \dot{m}_q} c_q \tag{6.6}$$

where subscript q, F and $mix$ refer to the quench stream, the reactor flow before the quench, and the reactor flow after the quench respectively. Here $T$ is temperature, $c$ is concentration of ammonia and $\dot{m}$ is mass flow rate.

## Model for the heat exchanger

The model for the heat exchanger is a standard $\epsilon - NTU$ model for a countercurrent heat exchanger (see e.g. Kreith and Bohn, 1986):

$$C^* = \dot{m}_{cold} / \dot{m}_{hot} \tag{6.7}$$

$$NTU = \frac{UA}{\dot{m}_{cold} C_{pg}} \tag{6.8}$$

$$\epsilon = \frac{1 - e^{-NTU(1-C^*)}}{1 - C^* e^{-NTU(1-C^*)}} \tag{6.9}$$

$$Q = \epsilon \dot{m}_{cold} C_{pg} (T_{hot,in} - T_{cold,in}) \tag{6.10}$$

$$T_{hot,out} = T_{hot,in} - \frac{Q}{\dot{m}_{hot} C_{pg}} \tag{6.11}$$

$$T_{cold,out} = T_{cold,in} + \frac{Q}{\dot{m}_{hot} C_{pg}} \tag{6.12}$$

where:

| | | |
|---|---|---|
| $A$ | Heat transfer area | $[m^2]$ |
| $C^*$ | Ratio of flow rates | [-] |
| $C_{pg}$ | Gas heat capacity | $[J/kg.K]$ |
| $\dot{m}_{cold}$ | Mass flow, cold stream | $[kg/s]$ |
| $\dot{m}_{hot}$ | Mass flow, hot stream | $[kg/s]$ |
| $NTU$ | Number of transfer units | [-] |
| $Q$ | Heat transfer rate | [W] |
| $T_{cold,in}$ | Temperature of cold stream entering exch. | $[K]$ |
| $T_{cold,out}$ | Temperature of cold stream leaving exch. | $[K]$ |
| $T_{hot,in}$ | Temperature of hot stream entering exch. | $[K]$ |
| $T_{hot,out}$ | Temperature of hot stream leaving exch. | $[K]$ |
| $U$ | Heat transfer coefficient | $[W/m^2.K]$ |
| $\epsilon$ | Heat transfer efficiency | [-] |

## Numerical solution method

The model equations, eq. 6.1 and 6.2 , may be solved as follows: The reactor beds are discretized, with grid spacing $\Delta z$.

1. First, consider the energy balance, Equation 6.2. This equation has the following form:

$$\frac{\partial T}{\partial t} + u\frac{\partial T}{\partial z} = f(T,c) + \Gamma\frac{\partial^2 T}{\partial z^2} \tag{6.13}$$

   By Taylor series expansion to 2. order, we get the following finite difference approximations for the space derivatives:

$$\frac{T_j - T_{j-1}}{\Delta z} = \frac{\partial T}{\partial z} - \frac{\Delta z}{2}\frac{\partial^2 T}{\partial z^2} + O(\Delta z^2) \tag{6.14}$$

$$\frac{T_{j+1} - 2T_j + T_{j-1}}{\Delta z^2} = \frac{\partial^2 T}{\partial z^2} + O(\Delta z^2) \tag{6.15}$$

   Introducing these into eq. 6.13 yields:

$$\frac{\partial T_j}{\partial t} = f(T_j, c_j) - u\frac{T_j - T_{j-1}}{\Delta z} + (\Gamma - \frac{u\Delta z}{2})\frac{T_{j+1} - 2T_j + T_{j-1}}{\Delta z^2} \tag{6.16}$$

   In order not to introduce numerical instabilities, it is advisable to ensure that the coefficient of the last term stays positive:

$$\frac{\partial T_j}{\partial t} = f(T_j, c_j) - u\frac{T_j - T_{j-1}}{\Delta z} + max[(\Gamma - \frac{u\Delta z}{2}), 0]\frac{T_{j+1} - 2T_j + T_{j-1}}{\Delta z^2} \tag{6.17}$$

2. Next, consider the mass balance, eq. 6.1. This is an **ordinary** differential equation in the space coordinate, and may be integrated at a given time using whatever method, e.g. improved Euler.

The system is now reduced to a system of ordinary differential equations for the temperatures $T_j$, and may be integrated in time using any numerical method.

# Appendix B. Discussion on the choice of mathematical model

The purpose of this Appendix is to counter possible objections to the choice of mathematical model, numerical method, discretization etc. used in the chapter. This is done by comparing the numerical results with similar results obtained using a more rigorous model, a different numerical method and by using a large number of discretization points for this rigorous model. In doing this, the relation between the current simplified model and the "rigorous" model should also become transparent.

The outline of the Appendix is as follows: First, we present a more rigorous model, consisting of three hyperbolic partial differential equations for each reactor bed. We then argue why the current simplified model may be viewed as a simplified version of this more rigorous model. Then, the numerical method for the rigorous model is presented; and finally, simulation results of the two methods are compared.

## Description of the "rigorous" model

The equations used to describe the reactor beds are:

Energy balance for catalyst phase (neglecting internal heat conduction in the pellets):

$$\frac{\partial T_c}{\partial t} = \frac{(-\Delta H_{rx}) r(T_c, c)}{C_{pc}} - \frac{ha}{(1-\alpha)\rho_c C_{pc}}(T_c - T_g) \tag{6.18}$$

Energy balance for the gas:

$$\frac{\partial T_g}{\partial t} + u\frac{\partial T_g}{\partial x} = \frac{ha}{\alpha \rho_g C_{pg}}(T_c - T_g) \tag{6.19}$$

Mass balance:

$$\frac{\partial c}{\partial t} + u\frac{\partial c}{\partial x} = \frac{(1-\alpha)\rho_c}{\alpha \rho_g} r(T_c, c) \tag{6.20}$$

where:

| | | |
|---|---|---|
| $c$ | Ammonia concentration | [kg NH3/kg gas] |
| $C_{pc}$ | Heat capacity of catalyst | [J/kg cat.K] |
| $C_{pg}$ | Heat capacity of gas | [J/kg.K] |
| $ha$ | Heat transfer coefficient | [W/m3.K] |
| $r(T_c, c)$ | Reaction rate | [kg NH3/kg cat.sec. ] |
| $t$ | Time | [sec.] |
| $T_c$ | Catalyst temperature | [K] |
| $T_g$ | Gas temperature | [K] |
| $u$ | Interstitial velocity of the gas | [reactor lenghts/sec.] |
| $x$ | Position in reactor | [-] |

| | | |
|---|---|---|
| -$\Delta H_{rx}$ | Heat of reaction | [J/kg.NH3] |
| $\alpha$ | Bed void fraction | [-] |
| $\rho_c$ | Catalyst density | [kg/m3] |
| $\rho_g$ | Gas density | [kg/m3] |

The heat exchanger and quench models for this model was the same as for the simple model (Appendix A).

## Simplification of the "rigorous" model

In this section, we perform an order of magnitude analysis, which will make it possible to simplify the "rigorous" model.

First, we argue why the time derivatives $\frac{\partial T_g}{\partial t}$ and $\frac{\partial c}{\partial t}$ are negligible compared to the other terms in the balance equations for the gas. When the heat transfer coefficient is high, the gas temperature, $T_g$, follows the catalyst temperature, $T_c$, closely; which implies that $\frac{\partial T_g}{\partial t} \sim \frac{\Delta T_c}{7min}$, where $7min$ is a typical time scale of the temperature wave and $\Delta T_c$ is a typical temperature amplitude. On the other hand, the convective term in the energy equation, $u\frac{\partial T_g}{\partial x}$, is of the order $\frac{\Delta T_c}{10\,sec}$, where $10sec$ is the order of the gas residence time. The convective term is thus much larger, which means that the time derivative, $\frac{\partial T_g}{\partial t}$, may be neglected in the energy balance of the gas. By a similar reasoning, the time derivative, $\frac{\partial c}{\partial t}$, in the mass balance for the gas may also be neglected.

Next, we approximately solve the energy balance for the gas, eq. 6.19, and express the gas temperature as a function of the catalyst temperature. Defining $H = \frac{ha}{\alpha \rho_g C_{pg}}$, which may be interpreted as the inverse of the time constant of a fluid particle, the solution of the gas energy balance (eq. 6.19) may be approximated as a convolution integral (far from the bed entrance compared to the length $u/H$):

$$T_g = \int_0^\infty e^{-\frac{H}{u}\eta} \cdot \frac{H}{u} \cdot T_c(x-\eta) \cdot d\eta \tag{6.21}$$

Now, if the length scale of the gas temperature change, $u/H$, is much smaller than a typical length scale of the catalyst temperature profile, the catalyst temperature profile in this integral may be approximated by a Taylor series:

$$T_c(x-\eta) = \sum_{n=0}^{\infty} \frac{(-\eta)^n}{n!} \frac{\partial^n T_c}{\partial x^n}|_x \tag{6.22}$$

Substituting this into the convolution integral and integrating yields the following approximation to the gas temperature:

$$T_g = \sum_{n=0}^{\infty} (\frac{-u}{H})^n \frac{\partial^n T_c}{\partial x^n} \tag{6.23}$$

Dropping terms after the second order and substituting into eq. 1 gives:

$$\frac{\partial T_c}{\partial t} + \beta u \frac{\partial T_c}{\partial x} = \frac{(-\Delta H_{rx}) r(T_c, c)}{C_{pc}} + \frac{u^2 \beta}{H} \frac{\partial^2 T_c}{\partial x^2} \tag{6.24}$$

where $\beta = \frac{\alpha \rho_g C_{pg}}{(1-\alpha)\rho_c C_{pc}}$.

Finally, we rewrite the gas mass balance by multiplying by this $\beta$ on each side:

$$\beta u \frac{\partial c}{\partial x} = \frac{C_{pg}}{C_{pc}} r(T_c, c) \tag{6.25}$$

Equations 6.24 and 6.25 now constitute our simplified model, if we identify $u_w = \beta u$ and $\Gamma = \frac{u^2 \beta}{H}$. Before comparing numerical solutions, we present the numerical method used for the simulation of the "rigorous" model.

## Numerical solution of the "rigorous" model

The equations to be solved, eqs. 6.18-6.20, are hyperbolic and may be solved by the method of characteristics. The system has the following structure:

Gas phase:

$$\frac{\partial \psi}{\partial t} + u \frac{\partial \psi}{\partial x} = f(\psi, \chi) \tag{6.26}$$

Catalyst phase:

$$\frac{\partial \chi}{\partial t} = g(\psi, \chi) \tag{6.27}$$

where $\psi = [T_g, c]'$ is a vector of gas temperature and concentration, and $\chi = T_c$ is the catalyst temperature. The characteristic lines of these equations are $x = u\ t + constant$ and $x = constant$ respectively. Along the characteristic lines, the partial differential equations degenerate into the ordinary differential equations

$$\frac{d\psi}{dt} = f(\psi, \chi) \tag{6.28}$$

$$\frac{d\chi}{dt} = g(\psi, \chi) \tag{6.29}$$

$x$ and $t$ are discretized as $x_i = i \cdot \Delta x$ and $t^k = k \cdot \Delta t$. Now, if we choose $\Delta t = \frac{\Delta x}{u}$, the discretized equations become: (Improved Euler):

predictor:

$$\psi_{i,pred}^{k+1} = \psi_{i-1}^{k} + f(\psi_{i-1}^{k}, \chi_{i-1}^{k}) \cdot \Delta t \tag{6.30}$$

$$\chi_{i,pred}^{k+1} = \chi_{i}^{k} + g(\psi_{i}^{k}, \chi_{i}^{k}) \cdot \Delta t \tag{6.31}$$

corrector:

$$\psi_i^{k+1} = \psi_{i-1}^k + \frac{1}{2}[f(\psi_{i-1}^k, \chi_{i-1}^k) + f(\psi_{i,pred}^{k+1}, \chi_{i,pred}^{k+1})] \cdot \Delta t \tag{6.32}$$

$$\chi_i^{k+1} = \chi_i^k + \frac{1}{2}[g(\psi_i^k, \chi_i^k) + g(\psi_{i,pred}^{k+1}, \chi_{i,pred}^{k+1})] \cdot \Delta t \tag{6.33}$$

## Numerical results/Comparison of rigorous and simplified model

The simplified and "rigorous" models may now be compared. For this comparison, we use 760 discretization points for the "rigorous" model.

We step down the feed temperature to the reactor by steps of 10 $^oC$, starting from 250 $^oC$ as before. Fig 6.11 shows the inlet temperature to the first bed, $T_i$ (before the quench), as a function of time for the rigorous model; and the corresponding figure for the simplified model is shown in Fig 6.3. As with the simplified model, the instability starts when the feed temperature drops from 240 $^oC$ to 230 $^oC$. However, the rate at which the amplitude increases when the system goes unstable is somewhat larger for the rigorous model than for the simplified model. This may not be very surprising when it is noted that this rate of increase is critically dependent on the difference between the actual feed temperature, $T_f$ (230 $^oC$) and the critical feed temperature, say $T_{f,crit}$, where the system is marginally stable. The critical feed temperatures of the two models differ somewhat, which explains the different rates of increase.

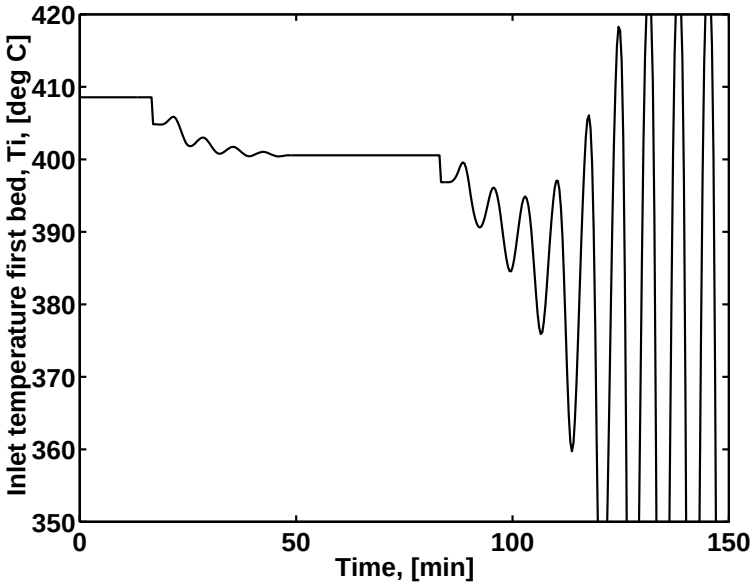


Figure 6.11: Stepping down the feed temperature

Fig. 6.12 compares temperature profiles through the reactor at a given (large) time for the two models. The profiles compares as well as could be expected considering the assumptions made in the modeling.

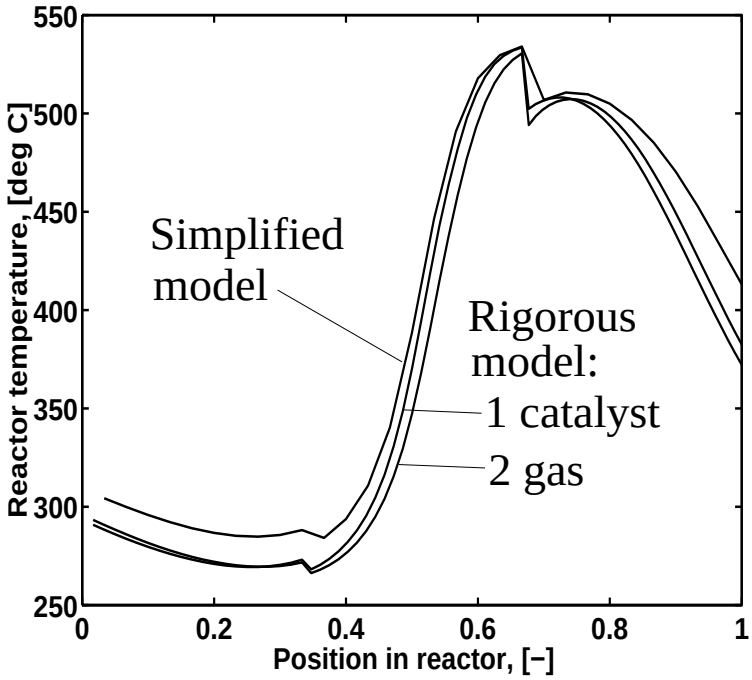


Figure 6.12: Comparing temperature profiles in the reactor. Simple and "rigorous" model

Numerical comparison thus suggests that the simplifications made are reasonable.

# Appendix C. Physical explanation of why the gain is larger at a phase lag of $2\pi$ than at steady state

In the chapter, it was shown that the transfer function of a reactor bed has a larger gain at a phase lag of $2\pi$ than at steady state. The purpose of this appendix is to shed some light on this phenomenon, using a somewhat different perspective on the dynamics of a reactor bed.

Consider a reactor bed where the feed temperature is given a sinusoidal perturbation:

$$\delta T_{inlet} = \delta T_0 \cdot cos(\omega t) \tag{6.34}$$

The period of this signal is $\tau = \frac{2\pi}{\omega}$ and the wavelenght in the reactor bed is $\lambda = u_w \cdot \tau = \frac{2\pi u_w}{\omega}$ (the distance travelled by the wave during one oscillation period, $\tau = \frac{2\pi}{\omega}$).

The propagation of this disturbance through the bed may be considered to be caused by two different effects:

1. By migration of temperature waves through the bed, which is a slow process, and
2. by changes in the concentration of the flowing gas, which has a very short residence time compared to the temperature waves, and thus is a fast process.

To really see the wave nature of the temperature waves, it is convenient to look at the phenomenon as seen in a moving coordinate frame following the wave as it propagates through the bed.

The energy equation of a reactor bed is:

$$\frac{\partial T_c}{\partial t} + u_w \frac{\partial T_c}{\partial z} = f(T_c, c) + \Gamma \frac{\partial^2 T_c}{\partial z^2} \tag{6.35}$$

Take the velocity of the moving coordinate frame to be $\frac{dz}{dt}|_{obs} = u_w$. The energy equation then becomes:

$$\frac{\partial T_c}{\partial t} + \frac{dz}{dt} \cdot \frac{\partial T_c}{\partial z} = f(T_c, c) + \Gamma \frac{\partial^2 T_c}{\partial z^2} \tag{6.36}$$

or by using the chain rule of differentiation:

$$\frac{dT_c}{dt}|_{obs} = f(T_c, c) + \Gamma \frac{\partial^2 T_c}{\partial z^2} \tag{6.37}$$

This is a very simple equation describing the change in catalyst temperature as seen by an observer moving through the bed, following the moving coordinate frame. It is seen that the rate of increase of the catalyst temperature as seen by this moving

observer is caused by two effects; production of heat by the reaction and transport of heat by the diffusion term.

Now, in order to find the transfer function gain of the bed during sinusoidal inputs, consider the following thought experiment (Think of a surf-rider): An observer starts moving at the bed inlet on the top of a temperature wave, and moves through the bed with the migration velocity of the temperature waves. After a while, he leaves the bed outlet, and notes the change in wave height—or amplitude. The gain of the bed transfer function is then simply the ratio of final to initial amplitudes—or ratio of final to initial height of the temperature wave on which he rides.

To see the relation to phase lag, assume that we compare two different cases:

1. Very low frequency (small $\omega$), i.e. wavelenght >> reactor lenght. This corresponds approximately to steady state operation of the reactor; hence the phase lag is virtually zero.

2. Medium range frequency, i.e. wave lenght = reactor length. In this case, the phase lag of the bed from input to output is $2\pi$

Now, in case 2, the top of the wave—which the observer follows—is followed by a wave valley where the conversion is low. As the gas residence time of the reactor is low, the observer senses this almost instantly, and has fresher gas around him in case 2 than he has in case 1. As the reaction rate term, $f(T_c, c)$ in eq. 6.37, is a decreasing function of the ammonia concentration, $c$, the rate of temperature increase, $\frac{dT_c}{dt}|_{obs}$, is thus larger in case 2 than in case 1. The final amplitude—and hence the gain—is thus larger for case 2, i.e. for a phase lag of $2\pi$, than in case 1, i.e. for zero phase lag. This explains the peak in the transfer function of the bed.

As a final comment, note that the damping effect caused by the dispersion term, $\Gamma\frac{\partial^2 T_c}{\partial z^2}$, will dominate at sufficiently high frequencies—corresponding to very short wavelenghts ($\lambda = u_w \cdot \tau = \frac{2\pi u_w}{\omega}$). This follows from an order of magnitude analysis:

$$\Gamma\frac{\partial^2 T_c}{\partial z^2} \sim \Gamma\frac{\Delta T_c}{\lambda^2} = \Gamma(\frac{\omega}{2\pi u_w})^2 \cdot \Delta T_c \tag{6.38}$$

Since this is increasing as the **square** of the frequency, $\omega$, this dispersion term is important for the roll-off of the bed transfer function at high frequencies (Of course, the assumptions made in the derivation of the model eventually break down as the frequency becomes very large).

# Chapter 7

# Allowable Operating Regions of Integrated Distillation Arrangements

John Morud and Sigurd Skogestad*
Chemical Engineering
University of Trondheim - NTH
N-7034 Trondheim, Norway

Presented at
AIChE Annual meeting, San Francisco, USA, Nov. 13-18 1994

**Abstract**

The steady state behavior of an integrated three-product distillation column known as the Petlyuk column is examined. When four of the outlet compositions from the column are specified, the steady state solutions have a rather strange nature, including multiplicity. Our explanation to this behavior is based on the solutions of the system when only three of the outlet compositions are specified. These solutions were computed numerically using an arclenght continuation method, and their nature is explained in physical terms. Based on the solutions, the effect of adding the fourth specification is explained.

*Address correspondence to this author. Fax: 47-73594080, E-mail: skoge@kjemi.unit.no

## 7.1 Introduction

Traditionally, the separation of three or more components has been achieved by arranging distillation columns in series. There exist several different alternatives, e.g. the direct and indirect sequences. For these arrangements, two columns are necessary in order to separate a three component mixture.

Approximately 50 years ago, Wright (1949), proposed a clever arrangement to separate a three component mixture in one single shell. The idea was to insert a vertical wall in the shell, and thus achieve what is effectively a prefractionator connected to a distillation column. This column arrangement is now better known as the Petlyuk column after Petlyuk *et al.* (1965), who studied it theoretically. Subsequent studies indicate that the Petlyuk column typically may save 30 % energy compared to traditional column arrangements [17]. Hence, the Petlyuk column has the potential to combine low investment costs with low energy requirements.

In spite of its potential, very few Petlyuk columns are presently in operation. One reason for this may be that the tight integration between the column sections makes the column rather complex and therefore more difficult to design and operate than traditional arrangements. The column may, for example, exhibit multiple steady state solutions for certain sets of specifications (e.g. [3], [17]).

The starting point for this work is the paper by Wolff *et al.* (1993,1994), who study such multiplicities. As the Petlyuk column has five degrees of freedom, they considered using four of these to control four of the outlet compositions from the column, and using the remaining fifth degree of freedom to minimize the energy consumption. They found that the (steady state) energy consumption as a function of the remaining degree of freedom does not have a nice convex shape - as might be expected - but exhibits a strange behavior with two solution branches and a "hole" in the operating range (i.e. there is a range of values for the remaining degree of freedom where no steady state solutions exist). The purpose of this paper is to provide an explanation of the steady state behavior found by Wolff *et al.*

The strategy chosen in order to provide such an explanation is as follows: First, we find all steady state solutions for a case with three outlet compositions specified, and interpret the solutions as geometrical surfaces. These surfaces can be linked to our physical understanding of the column. Then, the effects of adding/changing a fourth specification may be viewed geometrically in terms of the surfaces.

A brief outline of the paper: First, we define some terminology and explain the strange steady state behavior of the column when four outlet compositions are specified. We then describe the mathematical model and the numerical methods. After presenting the computed solution surfaces, we explain their shapes by physical arguments. We then draw a larger picture in terms of these solution surfaces in order to explain the effect of adding/changing specifications on the shape/nature of the solutions. Finally, we discuss the relevance to operation and control.

For readers unfamiliar with the Petlyuk column, we use the rest of this introduction to give a brief review of previous work. The review follows that of Wolff *et al.* (1993,1994).

In 1939, Brugma (1939) proposed a column design similar to the Petlyuk column,

but with a reboiler and a condenser also in the prefractionator. This design has been denoted a pseudo-Petlyuk design by previous workers (e.g. Wolff *et al.*, 1994).

The Petlyuk column was originally proposed by Wright (1949), who patented the idea. The column got its name from Petlyuk *al.* (1965), who studied the column theoretically.

Stupin an Lockhardt (1971) study the use of Fenske-Underwood equations for the design of Petlyuk columns.

Tedder and Rudd (1978) examine the energy requirement of various separation arrangements, including the pseudo-Petlyuk column.

Fidowski and Krolikowski (1986) compare the energy requirement of the Petlyuk column to other designs, such as the direct and indirect sequences.

Glinos and Malone (1988) derive analytical expressions for various column designs, including the Petlyuk column.

Chavez *et al.* (1986) study multiplicity in Petlyuk columns. They have an explanation of the multiplicity in terms of "matching specifications in interlinked columns".

Faravelli *et al.* (1989) examine the resilience of the steady states of the Petlyuk column to changes in the internal flows. Their work is based on the work by Chavez *et al.*

Triantafyllou and Smith (1992) give an overview over the design of Petlyuk columns. They explain how the Petlyuk column may be approximated - from a design point of view - by a regular distillation column and two side strippers.

The only report of an industrial application of a Petlyuk column is from BASF in Germany, as reported by Rudd (1992).

## 7.2 The Petlyuk column

The purpose of this section is to describe the column, describe the problem at hand and to introduce some terminology needed for the subsequent discussion.

### The column

The Petlyuk column separates a three component mixture of light ($A$), intermediate ($B$) and heavy component ($C$). Fig. 7.1 shows the system, consisting of a prefractionator and a main column.

The main column resembles an ordinary distillation column in that there is a reboiler at the bottom, producing a vapor flow rate, $V$, and a condenser at the top, yielding a liquid reflux, $L$. The prefractionator, however, does not have a separate reboiler and condenser. Instead it takes a fraction, $R_V \equiv V_2/V$, of the vapor stream, $V$, from the main column to use as boilup, and it takes a fraction, $R_L \equiv L_1/L$, of the liquid stream, $L$, to use as reflux.

The feed to the system, $F$, is placed at the middle of the prefractionator. The products are withdrawn from the main column: the light component in the distillate flow, D; the intermediate component in the side draw, $S$; and the heavy component from the bottom, $B$.

Figure 7.1: Petlyuk column

Note that *in practice* the prefractionator and the main column may be built in a single shell using a dividing wall.

### Degrees of freedom and operating objectives

It is assumed that the holdups (condenser level, reboiler level and pressure) are already controlled. The system then has five degrees of freedom, which may be represented by the parameters given above: $L$, $V$, $S$, $R_L$ and $R_V$. Possible objectives (specifications) for the operation of the column might be to control the compositions of the outlet streams and to minimize the energy consumption.

If the relative volatilities are reasonably large, there will be almost no heavy component at the top of the main column, and almost no light component at the bottom; it is therefore unnecessary to specify these two quantities. Hence, we need only one degree of freedom to control each of the top and bottoms compositions, and two for the side composition (possibly one if we don't care whether the impurity is light or heavy), a total of four (three) degrees of freedom. The remaining degree of freedom (two degrees) could then be used to minimize the energy consumption. For subsequent discussion we distinguish between two different sets of specifications:

1. *Three compositions specified.* In this case three degrees of freedom are used to specify one concentration in each outlet stream, i.e. $x_{A,top}$, $x_{B,side}$ and $x_{C,bottom}$. The remaining two degrees of freedom are used for energy minimization.

2. *Four compositions specified.* In some cases the side product may be specified - not in terms of the purity of the intermediate (B), $x_{B,side}$ - but rather in terms

of both a maximum amount of light impurity (A) and a maximum amount of heavy impurity (C). Specifying these two impurities is equivalent to specifying, in addition to the three specifications above, the ratio of light to heavy impurity in the side stream, $x_{A,side}/x_{C,side}$. In this case, there is only one degree of freedom left for energy minimization.

#### Solutions and solution manifolds

We define a *solution* to be an operating point which satisfy the specifications on the compositions, not taking the energy minimization into account. Since there are remaining degrees of freedom there will be a family of solutions; we will denote such a family a *solution manifold.*

For the first specification set above, "Three compositions specified", there are two degrees of freedom left (five degrees of freedom minus three specifications). Hence, the solution manifold is twodimensional, i.e. a surface. For the second specification set, "Four compositions specified", there is one degree of freedom left, i.e. the solution manifold is a curve. Note that, in general, the solution manifold does not have to be connected; it may consist of several parts, or branches.

Observe that the solution manifold of the second specification set is part of the solution manifold of the first set. Hence, by calculating the solution manifold of the first specification set, we have also calculated the solution manifold of the second.

#### A typical solution manifold

It is not always easy to predict what type of solutions to expect, not even qualitatively. For example, consider the second specification set, with four compositions specified. One might intuitively think that the energy consumption as a function of the remaining degree of freedom, $X$ say, would be a nice convex function with a well defined minimum. However, as was shown by Wolff *et al.* [17], the numerical solution typically looks like the curve shown in Fig 7.2, exhibiting two solution branches and a hole in the operating range. In the figure, the remaining degree of freedom, $X$, is the vapor split fraction, $R_V$. Other choices of $X$ yield similar results. Before explaining why the energy consumption as a function of the remaining degree of freedom has such a shape, we describe the simple mathematical model and the numerical methods used to support our arguments. We compute all solutions of the model for the case with three specifications.

## 7.3 Mathematical model and numerical solution

### 7.3.1 Model of the column

The model is simplified as much as possible to reveal some essential features of the Petlyuk column. It is assumed (Fig. 7.1):

- Eight equilibrium stages in the prefractionator, sixteen in the main column;

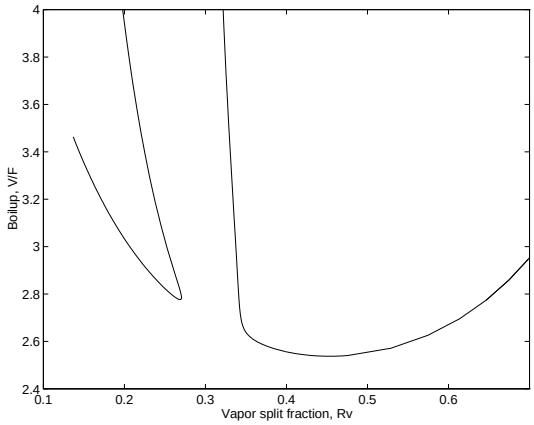


Figure 7.2: Energy consumption, $V/F$, as function of $R_V$. Four compositions specified.

- Constant relative volatilities 4:2:1;
- Constant molar flows;
- Total condenser; and
- Reboiler taken as one equilibrium stage.

The mass balances for equilibrium stage "$i$" are taken as:

$$L \cdot x_{c,i+1} - V \cdot y_{c,i} = L \cdot x_{c,i} - V \cdot y_{c,i-1} \tag{7.1}$$

where $L$ and $V$ are the liquid and vapor molar flows through the stage; $x_{c,i}$ and $y_{c,i}$ are the liquid and vapor mole fraction of component "c", where "c" refers to any of the three components $A$, $B$ or $C$.

The vapor mole fraction of component "c", $y_{c,i}$, is given by the vapor equilibrium:

$$y_{c,i} = \frac{\alpha_c x_{c,i}}{\sum_{c=A,B,C} \alpha_c x_{c,i}} \tag{7.2}$$

The mixer and splitter models mix or split either liquid or vapor. The mass balance for liquid becomes:

$$\sum_{in} F_{in} x_{c,in} = \sum_{out} F_{out} x_{c,out} \tag{7.3}$$

where the $F$'s are molar flows and "in" and "out" are indices over the inlet and outlet streams. This expression determines a mixer; for a splitter more specifications are needed: the split fraction of the outlet flow rates, i.e. $R_L$ or $R_V$, and that the outlet flows have the same composition. The mass balance for vapor is the same as for liquid when $x$ is replaced by $y$.

The reboiler model is taken as an equilibrium stage with the vapor flow rate specified. The condenser is supposed to be a total condenser, i.e. the condenser model simply converts vapor to liquid with no change in compositions.

Now that the models of the column elements - the stages, mixers, splitters, reboiler and condenser - are established, we describe how these were combined to an equation system.

### 7.3.2 The equation system

The model described in the previous section was solved using the equivalent of McCabe-Thiele stepping: The vapor and liquid compositions at the middle of the prefractionator and the main column are guessed, and the system is solved stage by stage towards the top and the bottom of the column. Of course, the guess is in general wrong, so there will be a mismatch - residuals - in the splitters at the top and bottom of the prefractionator, as well as in the reboiler and in the condenser. One may consider this stage-by-stage procedure to be equivalent to an equation system $f(z) = 0$, where:

- z : unknowns consisting of five degrees of freedom - $L$, $S$, $V$, $R_L$, $R_V$ - and eight guesses (four streams times two mole fractions), a total of 13 unknowns.
- f : function values consisting of three specifications and eight mismatches (four locations times two mole fractions), a total of eleven function values.

It is seen that there are two more unknowns than equations, which means that there exists a two-parameter family of solutions, i.e. a *two-dimensional surface.*

To find the solution surface, a continuation method was used.

### 7.3.3 A simple continuation scheme

Continuation methods are well established; therefore the method used will only be briefly discussed here. An easily accessible book on the subject is the book by Seydel, 1988 ([12]). The method used here is not particularly sofisticated and was chosen for its simplicity.

The equation system to be solved is on the form $f(z) = 0$ with two more variables than equations, i.e. the solutions form a surface. Since a surface may be constructed from the curves lying in it, a family of such solution curves are found. The overall procedure is:

1. First find an initial solution $z_0$ (with flow splits $R_{L,0}$, $R_{V,0}$).
2. Temporarily make an additional specification to get only **one** more variables than unknowns. The choice of additional specification is almost arbitrary; here, we fix the ratio

   $(R_L - R_{L,0})/(R_V - R_{V,0})$.
3. Solve the resulting equation using arclength continuation to find a solution curve lying in the solution surface.
4. Repeat for various values of the ratio

   $(R_L - R_{L,0})/(R_V - R_{V,0})$, each time starting at $z_0$.

5. Construct the solution surface from the computed curves.

The arclength continuation method used in this procedure is as follows: We are to solve $f(z) = 0$, now with only one unknown more than the number of equations. Assume that we have already calculated a set of points $z_0, z_1 \cdots z_n$ on the solution curve, and that we desire to find a point $z_{n+1}$ a distance approximately $\delta$ from $z_n$. First linearize to get the equation for the tangent of the solution curve: $0 = J \cdot \Delta z$, where $J \equiv \frac{\partial f}{\partial z^T}$ is the Jacobian of $f$. It is seen that any deviation, $\Delta z$, on the tangent is in the *null space* of the Jacobian. The hyperplane orthogonal to the tangent is spanned by the *row space* of the Jacobian. This suggests the following two step procedure:

1. A prediction of the next point $z_{n+1}$ is found by taking a small step, $\delta$, in the direction of the nullspace of the Jacobian, $\mathcal{N}(J_n)$ (tangent direction). The Jacobian was computed numerically, using central differences.

2. A correction is made iterating in the row space of the Jacobian, $\mathcal{R}(J_n^T)$, by Newton-Rapson like iterations using the pseudoinverse of the Jacobian, $J_n^+$, evaluated at the previous point, $z_n$:

$$z_{n+1}^{k+1} = z_{n+1}^k - J_n^+ \cdot f(z_{n+1}^k), \quad k = 1, 2, 3 \cdots \tag{7.4}$$

### 7.3.4 Numerical results

As the solutions forms a two parameter family - i.e. a surface - one may parametrize it by almost any two variables. Here, we use the liquid and vapor split fractions, $R_L$ and $R_V$, as parameters. Any other quantity, Q say, may thus be considered a function of these two parameters, formally $Q = Q(R_L, R_V)$.

Figs. 7.3 and 7.4 show a typical result as a function of the parameters, $R_L$ and $R_V$. Fig. 7.3 shows the calculated energy requirement, represented by the boilup $V/F$; Fig. 7.4 shows the calculated ratio of light to heavy component in the side stream, $x_{A,side}/x_{C,side}$. As can be seen, the energy surface is a nice convex function with a well defined energy minimum, whereas the ratio of light to heavy component in the side stream has the shape of a saddle.

## 7.4 Discussion of results

In this section we first make a physical argument as to why the surfaces ought to have the shape they have. We then explain the connection between the shape of these surfaces and the effect of specifying e.g. the ratio of side stream impurities.

#### Shape of the energy surface

First, consider the calculated energy requirement as a function of the liquid and vapor split fractions, $R_L$ and $R_V$, Fig. 7.3. The energy surface looks as we might intuitively expect, with a well defined minimum. Any excursion from the minimum point costs in terms of energy. Too high $R_L$ and $R_V$ means that we use all the vapor and liquid in

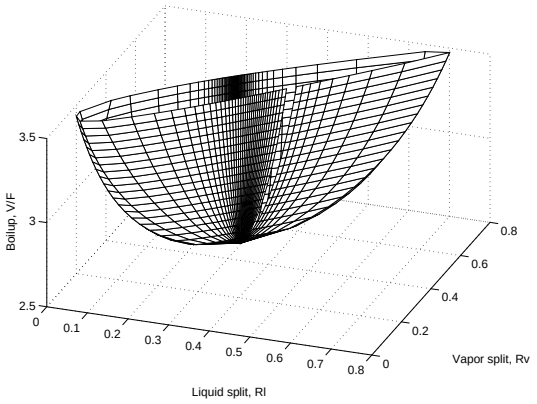


Figure 7.3: Calculated energy consumption, $V/F$, as a function of $R_L$ and $R_V$. Three compositions specified.

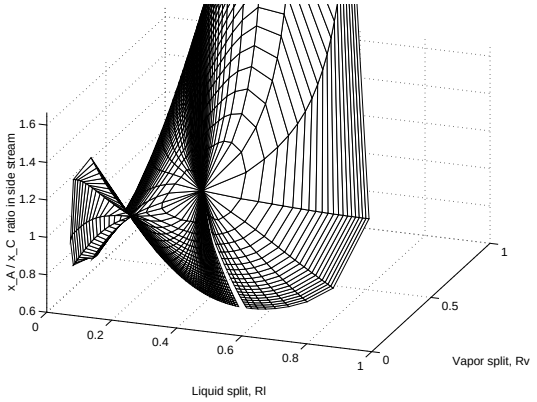


Figure 7.4: Calculated ratio of light to heavy impurity in side stream. Three compositions specified.

the prefractionator, not leaving much to the main column, which is stupid. A similar argument applies to low $R_L$ and $R_V$, not leaving much for the prefractionator. High $R_L$ and low $R_V$ means that the liquid to vapor ratio is too high in the prefractionator and too low in the main column, again stupid. A symmetrical argument applies to low $R_L$ and high $R_V$.

### Shape of the $x_{A,side}/x_{C,side}$ surface

Next, consider Fig. 7.4 showing the calculated ratio of light to heavy component in the side stream, $x_{A,side}/x_{C,side}$ as a function of the liquid and vapor split fractions, $R_L$ and $R_V$.

A change in one of the split fractions has an effects on both the prefractionator and the main column. For example, consider a *decrease* in the liquid split fraction, $R_L$ (while keeping $R_V$ and the other three product compositions constant). This affects the purity of the sidestream in two ways:

1. By degrading the separation in the prefractionator: The liquid to vapor ratio, $L/V$, in the prefractionator *decreases*, and if it becomes sufficiently low, there is a breakthrough of heavy component, $C$, at the top of the prefractionator into the main column. This heavy component ends up in the side stream, *reducing* the ratio of light to heavy component in the side stream, $x_{A,side}/x_{C,side}$.

2. By improving the separation in the main column: The liquid to vapor ratio, $L/V$, in the main column *increases*, which by itself increases the concentration of light component, $A$, in the side stream, and decreases the concentration of heavy component, $C$, in the side stream, and thus *increases* the ratio of light to heavy component in the side stream, $x_{A,side}/x_{C,side}$.

The two effects are thus *competing*, indicating that the ratio $x_{A,side}/x_{C,side}$ may have a *maximum* along a line of constant $R_V$. This is indeed the case and may be explained as follows: If $R_L$ is decreased towards zero starting from a relatively high value, then the ratio $x_{A,side}/x_{C,side}$ will first *increase* due to the second effect, but a further reduction of $R_L$ will *decrease* $x_{A,side}/x_{C,side}$ due to the first effect (breakthrough of heavy component). A similar argument along a line of constant $R_L$ (varying the vapor split fraction, $R_V$) yields a *minimum* along this direction.

To summarize: The $x_{A,side}/x_{C,side}$ surface has a maximum along a line of constant $R_V$ and a minimum along a line of constant $R_L$, that is, the surface has the shape of a *saddle*.

### Combining the surfaces

Now that the general shape of the solution surfaces has been established, we explain what this means in terms of specifying e.g. the $x_{A,side}/x_{C,side}$ ratio. Consider Fig. 7.5, showing an *idealized* picture of the solution surfaces (functions of the liquid and vapor split fractions, $R_L$ and $R_V$). Fig 7.5c shows the $x_{A,side}/x_{C,side}$ ratio, while Fig 7.5b shows the energy consumption. The two surfaces have been placed above each other on purpose, to emphasize that points on the two surfaces that have the same arguments $R_L$ and $R_V$ correspond to each other. In other words, corresponding points on the two surfaces are placed *above* one another.

Specifying the $x_{A,side}/x_{C,side}$ ratio is equivalent to finding the intersection of the saddle, Fig 7.5c, with a horizontal plane. Since the surface is a saddle, this intersection yields *two* branches of intersection curves (marked with 'O' in the figure). The corresponding branches on the energy surface are found by projecting these two curves upward onto the energy consumption surface, Fig 7.5b. The original figure with a "hole" in the operating range, Fig. 7.5a, is found by projecting the branches onto the $R_V - V/F$ plane.

This explains the effect of adding the fourth specification on the outlet composition. It can be seen geometrically the effect of changing the value of the fourth specification; this corresponds to translating the horizontal plane upwards or downwards. Thus we have obtained a qualitative picture of the effect of the fourth specification.

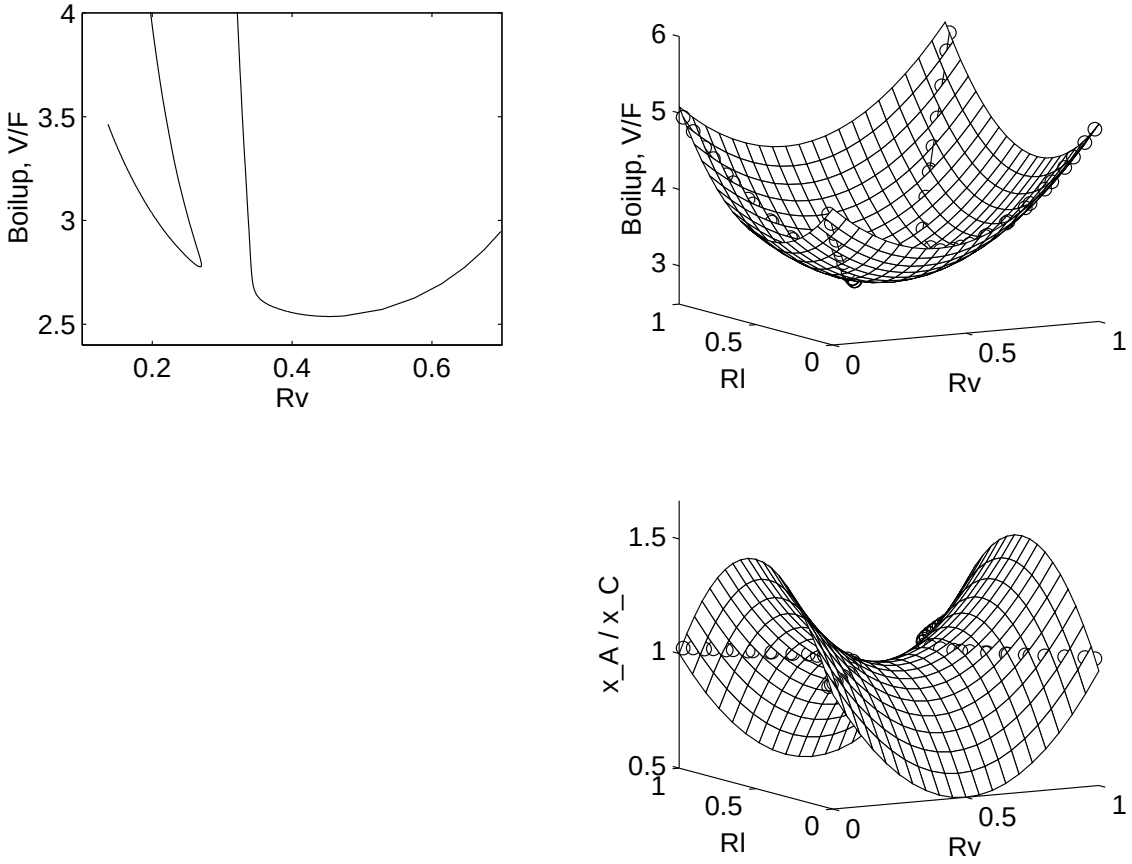


Figure 7.5: Relation between three specifications and four specifications. Note: surfaces have been idealized.

## 7.5 General discussion

### A comment on the saddle shape

Since the flow split fractions $R_L$ and $R_V$ represent some sort of trade-off between the column sections - i.e. larger internal flows in one column section means less in another - it should not come as a surprise to find maxima or minima along lines of constant $R_L$ or lines of constant $R_V$. Also, since the Petlyuk column has a near top-bottom symmetry, one would expect $R_L$ to have a similar effect on the $x_{A,side}/x_{C,side}$ ratio as $R_V$ has on the *resiprocal* of this quantity, i.e. $x_{C,side}/x_{A,side}$. This indicates strongly that the $x_{A,side}/x_{C,side}$ ratio as a function of $R_L$ and $R_V$ has the shape of a saddle; at least it should not be very surprising. One may conjecture that such saddle shapes should be quite common in integrated column arrangements. Adding a specification on a saddle-like quantity would then imply multiple solution branches and complex multiple solutions.

### Operation and Control

As shown by Wolff *et al.* (1993,1994), it is relatively easy to control the Petlyuk column for the case with three compositions specified, but the fourth specification complicates matters. It is not obvious how to design a good feedback control system in this case. However, systems with more manipulated variables (in our case, the degrees of freedom) than outputs (in our case, the outlet concentrations) normally do not have fundamental limitations in achievable control performance (i.e. bandwidth limitations). Since there is one excess degree of freedom when four outlet compositions are specified, we do not expect any fundamental limitations in the achievable performance in this case. The design of such controllers is an area of future research.

### A comment on thermodynamics

In this work, we have used a very simple model with constant relative volatilities; still, this system exhibits a rather complex steady state behavior. More rigorous thermodynamics yield similar results (Wolff *et al.*, 1993, 1994). However, it should be noted that more complex thermodynamics might complicate the steady state behavior even further.

## 7.6 Conclusion

Complex steady state behavior of Petlyuk columns - with multiple solutions and a "hole" in the operating range - was explained by physical/geometrical arguments. The numerical method used for supporting the arguments was an arclength continuation method applied to a simple mathematical model of a Petlyuk column.

The nature of the solutions is similar to what is obtained by more rigorous models.

# References

[1] Brugma, A.J., 1937, Dutch Patent No. 41, 850 (October 15, 1937)

[2] Cerda, J. and A.W. Westerberg, 1981, "Shortcut Methods for Complex Distillation Columns. 1. Minimum Reflux", *Ind. Eng. Chem. Process Des. Dev*, 20, p. 546-557.

[3] Chavez, C.R., J.D. Seader and T.L. Wayburn, 1986, "Multiple Steady-State Solutions for Interlinked Separation Systems", *Ind. Eng. Chem. Fundam.*, 25, p. 566-576.

[4] Faravelli, T., M. Rovaglio and E. Ranzi, 1989, "Dynamic Analysis and Stability of Interlinked Multicomponent Distillation Columns", *Dechema Monographs*, 116, p. 229-236.

[5] Fidowski, Z. and L. Krolikowski, 1986, "Thermally Coupled System of Distillation Columns: Optimization Procedure", *AIChE J.*, 32, 4, p. 537-546.

[6] Glinos, K. and F. Malone, 1988, "Optimality Regions for Complex Column Alternatives in Distillation Systems", *Chem. Eng. Res. Des.*, 66, p. 229-240.

[7] Jacobsen, E.W. and S. Skogestad, 1991. "Multiple Steady States in Ideal TwoProduct Distillation". *AIChE Journal*, vol 37, No. 4., pp 499-511.

[8] Jacobsen, E.W., 1994, "Dynamics of systems with input multiplicity with binary distillation as an example", Lecture at Chem. Eng. Dept, NTH, Trondheim, March 11, 1994.

[9] Jacobsen, E.W. and S. Skogestad, 1994, "Instability in Distillation Columns". AIChE Journal. In press.

[10] Petlyuk, F.B., V.M. Platonov and D.M. Slavinskii, 1965, "Thermodynamically optimal method for separating multicomponent mixtures", *Int. Chem. Eng.*, 5, 3, p. 555-561.

[11] Rudd, H., 1992, "Thermal Coupling for Energy Efficiency", *Chemical Engineer* (Distillation Supplement), 27. august 1992.

[12] Seydel, R., 1988, "From equilibrium to chaos. Practical bifurcation and stability analysis". Elsevier Science Publishing Co. 1988.

[13] Stupin, W.I. and Lockhart, F.I., 1971, "", Paper 64th Annual AIChE Meeting, San Fransisco

[14] Tedder, D.W. and D.F. Rudd, 1978, "Parametric Studies in Industrial Distillation: Part 1. Design Comparisons", *AIChE J.*, 24, 2, p. 303-315.

[15] Triantafyllou, C. and R. Smith, 1992, "The Design and Optimisation of Fully Thermally Coupled Distillation Columns", *Trans IChemE*, 70, p. 118-132.

[16] Wolff, E.A., S. Skogestad and K. Havre, 1993, "Dynamics and Control of Integrated Three-product (Petlyuk) Distillation Columns". AIChE annual meeting, St.Louis, November, 1993.

[17] Wolff, E.A., S. Skogestad and K. Havre, 1994, "Dynamics and Control of Integrated Three-product (Petlyuk) Distillation Columns". ESCAPE'4, Dublin, March 28-30, 1994.

[18] Wright, R.O., 1949, U.S. Patent No. 2,471,134 (May 24, 1949).

## Nomenclature

| | |
|---|---|
| $B$ | Bottoms flow rate [mole/time] |
| $D$ | Distillate flow rate [mole/time] |
| $f(z)$ | equation system of Petlyuk column |
| $F$ | Feed flow rate [mole/time] |
| $J$ | Jacobian matrix of $f(z)$ |
| $L$ | Liquid reflux flow rate in top of main column [mole/time] |
| $L_1$ | Liquid flow rate in top of prefractionator [mole/time] |
| $R_L$ | Liquid split fraction at top of prefractionator, $L_1/L$ [-] |
| $R_{L,0}$ | $R_L$ in the vector $z_0$ [-] |
| $R_V$ | Vapor split fraction at bottom of prefractionator, $V_2/V$ [-] |
| $R_{V,0}$ | $R_V$ in the vector $z_0$ [-] |
| $S$ | Side stream flow rate [mole/time] |
| $V$ | Vapor flow rate from reboiler [mole/time] |
| $V_2$ | Vapor flow rate in bottom of prefractionator [mole/time] |
| $x$ | Liquid mole fraction [-] |
| $y$ | Vapor mole fraction [-] |
| $z$ | unknown vector in equation system $f(z)$ |
| $z_0$ | Starting value of $z$ for continuation algorithm |

Greek

| | |
|---|---|
| $\alpha$ | relative volatility [-] |

Subscripts

| | |
|---|---|
| *bottom* | indicates bottoms flow |
| $c$ | index over component A (light), B (intermediate), C (heavy) |
| *in* | index over inlet streams |
| *out* | index over outlet streams |
| *side* | indicates side stream |
| *top* | indicates distillate flow |

# Chapter 8

# Optimizing Control of Process Plants

John Morud and Sigurd Skogestad*
Chemical Engineering
University of Trondheim - NTH
N-7034 Trondheim, Norway

Unpublished

**Abstract**

Control systems for chemical process plants are often built in a hierarchical manner, with regulatory control at the lowest level; a supervisory control level above; and an optimizing control level on top. In this paper, we study the selection of controlled outputs at the regulatory control level; specifically, we examine the possibility of choosing controlled outputs, whose optimal set points are insensitive to disturbances at steady state. As a measure of sensitivity, we use the worst case deterioration of an objective function under disturbances. With this measure of sensitivity, the output selection problem becomes a minimax problem, where the outputs and their set points are chosen to minimize the worst case loss in this objective.

In order to gain some insight into the output selection problem, and facilitate its solution, we simplify the problem by means of second order Taylor series expansions of the process model and the objective function which is to be minimized. Using these expansions, we formulate a procedure for output selection, and apply it to a simple process example.

*Address correspondence to this author. Fax: 47-73594080, E-mail: skoge@kjemi.unit.no

## 8.1 Introduction

Control systems for chemical process plants are often built in a hierarchical manner, with regulatory control at the lowest level; a supervisory control level above; and an optimizing control level on top [9]. The optimizing level finds optimal—or good—set points for the control levels below. This situation is schematically shown in Fig. 8.1.

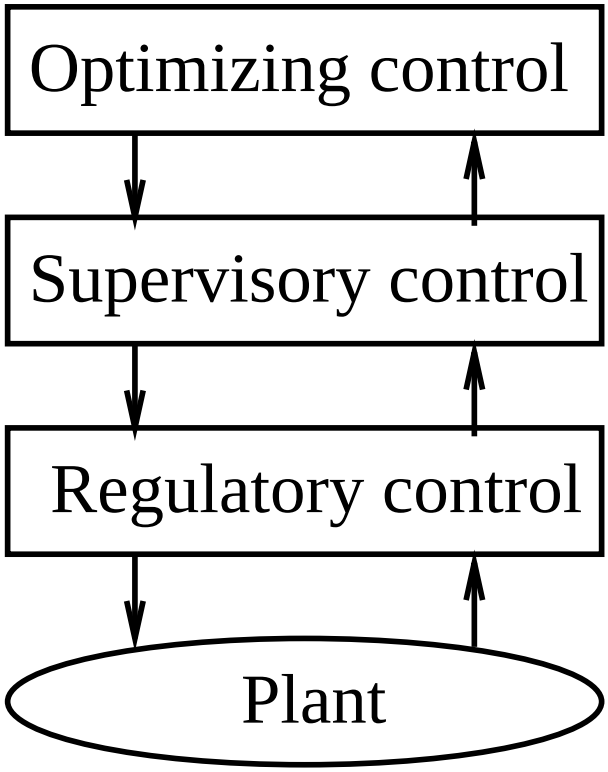


Figure 8.1: Hierarchical control system.

A question that arises is how to design the different control levels so that the overall system performs well under uncertainty. In an ideal world, the optimizing control level could simply compute optimal manipulated inputs from a model of the process and then implement those on the real plant. Such a controller may be denoted an open loop implementation of the optimizing controller. In practice, such a controller may often yield poor performance, since there is always a mismatch between the plant and the model; there are unmeasured disturbances entering the process; the measurements are noisy and biased; and the computed inputs are not accurately implemented.

To combat the uncertainty, it is customary to implement the optimization in a feedback manner, where certain output variables are kept at set points using the manipulated variables. The optimizing control level then chooses the set points for these output variables.

Two distinct questions then arises; the first is how to choose which outputs to be kept at set points—this is what we study in the paper; the second is how to find optimal set points for these outputs. Fortunately, the questions are often easy to answer.

In many cases, the optimum may be very flat (i.e. insensitive to the manipulated variables), and the important disturbances known or measured. In such cases the precision at which the optimal set points are computed and implemented is not crucial; the system yields most of the potential profit anyway (Maarleveld and Rijnsdorp, 1970). In other cases, the optimum is known to be at the intersection of process constraints, in which case so called constraint control may be used [8]. One then regulates the plant so that it stays on the active constraints. For example, if the optimum operating point of, say, a reactor is at its maximum allowable temperature, using a simple PI-controller to keep the reactor at that temperature may be a good solution.

What we have in mind in this paper are situations where it is not that simple; the optimum is neither on constraints nor is flat. One specific example is energy minimization of Petlyuk columns, which was the topic in the previous chapter. Even though the Petlyuk column may save 30 % energy compared to conventional distillation arrangements, it is easy to imagine that it is also possible to waste enormous amounts of energy if the column is operated poorly.

To make the design of the optimizing control level a simple task, there are at least three properties we would like the control system to have:

- We would like the objective function to be as flat as possible as seen from the optimizing level. This means that the system performance should not deteriorate too much if the set points are not accurately computed and implemented.

- We would like the measurement or estimation of controlled outputs to give reliable information for the optimization. Some measurement devices are more accurate than others; moreover, some measurements yield more information about the optimization objective than others.

- We would like the optimal set points to be insensitive to disturbances entering the process. Such insensitivity to disturbances reduces the need for frequent changes of set points, and makes the task of searching for the optimum set points less noisy, and hence easier. In some cases, there may even be no need for set point changes as soon as the optimal set points have been found the first time, eliminating the need for an optimizing control level.

In the paper, we restrict ourselves to studying the third point, insensitivity to disturbances. In order to see the importance of making the optimal set points insensitive to disturbances, it is convenient to consider a concrete example. Consider baking a cake. The optimization objective is then to make a cake which is neither raw, nor burned; that is, there is an optimal value of heat input and cooking time, which will make the optimal cake. Now, if we had never done this before, and if we were to construct the stove ourselves, we might consider regulating the heat input to the stove. The optimizing control level—i.e. the person making the cake—is then left to choose the optimal set point for the heat input. Needless to say, this would probably be a frustrating experience, since the optimal heat input depends on external disturbances, such as the room temperature, or the opening of the door of the stove. Moreover, as the stove temperature would probably increase with time, the result would probably

be sensitive to the cooking time; for instant, the cake would probably be burned if the cooking time is a little too long. In other words, the optimum is not flat with respect to cooking time. An alternative to regulating the heat input, which is the one adopted in practice, is to regulate the temperature in the stove using a simple thermostat as a controller. In this case, the sensitivity of the optimal temperature to external disturbances is very small, which means that the predetermined set point—the temperature given by the recipy in the cook book—is much more likely to yield near optimal results.

The purpose of this paper is thus to investigate how to choose outputs at the regulatory control level, such that the optimal set points for these outputs are insensitive to plant disturbances at steady state. This means that the scope of our analysis is restricted; we do not consider, for instant, how to choose the outputs in order to make the optimum flat with respect to the set points, nor how to deal with bias in some of the plant measurements. Such issues are important, and need further work.

We give a brief outline of the paper. First, we define some notation for the process model and the objective function to be minimized; and proceed by defining a criterion for selecting regulated outputs at the regulatory control level. The criterion chosen, is to minimize the worst case deterioration in performance by not taking disturbances into account when optimizing the set points of the selected outputs. As this problem is rather complex, we turn to simplifications—although the original problem may be solved numerically in specific cases. The simplifications consists of using second order Taylor series expansions of the process model and the operating objective around the nominal optimum. Using this simplified Taylor series analysis, we then formulate a procedure for output selection, and apply the procedure to a simple process example.

The rest of this introduction is devoted to reviewing some previous work.

The basic ideas in this paper are inspired by the work by Morari *et al.*, 1980a, which is a part of a series of papers studying synthesis of control structures for chemical process plants. In their paper, Morari *et al.* study how to decompose a plant for the purpose of control system synthesis; how to classify control objectives into regulatory and optimizing control; and how to analyze optimizing control structures.

Maarleveld and Rijnsdorp (1970) study constraint control of distillation columns. When optimizing pressure in distillation columns, the optimal column pressure varies with varying throughput. However, in a certain operating range, this optimum corresponds to maximum allowable pressure drop in the stripping section of the column. Hence, by measuring this pressure drop, and regulating it at the maximum allowable value, the column follows the optimum operating point as the throughput varies. In other words, the optimal set point of the controlled output—the pressure drop—is insensitive to the disturbance—the throughput. In their paper, a control scheme is proposed, which also handles situations where there are switches in active constraints, i.e. when active constraints become inactive and *vice versa*.

Tyreus, 1987, discusses the possibility of designing the regulatory control system so as to make the plant behavior as optimal as possible. The idea is that there are several alternative ways of designing a satisfactory regulatory control system. With

this freedom of choice, it is therefore possible to pick the regulatory control system which yields the best performance with respect to the economic objective function.

Kim *et. al.* (1991) present an on-line optimizing control system, which they tested on an experimental distillation column. The plant model was a linear input-output model, which was identified on-line using plant measurements.

We now return to the task of finding outputs at the regulatory control level, such that their optimal set points are insensitive to plant disturbances. Our overall objective is to outline a procedure for selecting the regulated outputs according to this criterion. However, in order to formulate such a procedure, we first need to define some notation, and derive some results.

## 8.2 Problem definition

We consider a plant at steady state, which is to be regulated at some operating point so as to optimize an overall objective. Examples of such overall objectives could be the maximization of profit, or the minimization of energy consumption.

In this section, we define a criterion for selecting outputs at the regulatory control level, such that their optimal set points are insensitive to persisting plant disturbances (at steady state). Examples of such disturbances could be changes in raw materials or feed flow rates, changes in cooling water temperatures, or even weather conditions. Even parametric model uncertainty could be considered a "disturbance", at least for mathematical convenience.

Before we develop the criterion for output selection, we define some notation for the plant and the optimization objective.

### Plant model and objective function

We consider a plant at steady state, given by a plant model:

$$f(x,u,d)=0; \quad y=Cx \tag{8.1}$$

Here, $x$, $u$ and $d$ are the states, the manipulated variables, and the disturbances, respectively; $y$ is the controlled outputs.

The objective which is to be minimized, say $\Phi_1$, is given by:

$$\min_u\{\Phi_1(x,u,d)\} \tag{8.2}$$

subject to the constraints given by the plant model above. For example, this may reflect the wish to minimize energy consumption, maximize yield, etc.

To make the notation simple, we eliminate the states from this objective function, using the plant model, yielding:

$$\min_u\{\Phi_2(u,d)\} \tag{8.3}$$

We make a last notational change. The inputs, $u$, are consumed when regulating the outputs, $y$. Thus, we may rewrite the objective as:

$$\min_r\{\Phi(r,C,d)\} \tag{8.4}$$

where $r$ are the set points for the controlled outputs, and the matrix $C$ represents which outputs—or combinations of outputs—that are regulated.

### Selection of controlled outputs

The choice of outputs to be regulated at the regulatory control level, is equivalent with the choice of the matrix $C$ in the output equation, $y = Cx$. Normally, there will be restrictions in this choice; for example, it may be demanded that the elements of $C$ be restricted to the integers zero or one, meaning that a particular state is an output if the element is one, and not if it is zero. In other cases, combinations of outputs may be regulated, in which case the elements of $C$ can take any value as long as the corresponding output could be measured or estimated.

### A criterion for selecting regulated outputs

If we knew the disturbance, $d$, we could calculate the optimal set points for the outputs as a function of the disturbance; formally $r_{opt}(d)$. This yields a value $\Phi_{opt}(d)$ for the objective function, which is only dependent on the disturbance, $d$, and which is the best achievable value for the objective function by any controller. On the other hand, if we use a fixed set point, $r$, we get a higher (worse) value for the objective function, i.e. $\Phi(r, C, d)$. The loss in objective by not compensating for disturbances, say $\Psi$, is thus the difference between the two:

$$\Psi(r, C, d) = \Phi(r, C, d) - \Phi_{opt}(d) \tag{8.5}$$

A possible criterion for selecting the best outputs to regulate—given by the particular choice of $C$—and the best set point, $r$, for these outputs, could be to minimize the worst case loss, that is:

$$\min_{r \in \mathcal{R}, C \in \mathcal{C}} [\max_{d \in \mathcal{D}} \{ \Psi(r, C, d) \}] \tag{8.6}$$

Here, $\mathcal{R}$ is the set of allowable set points, $\mathcal{D}$ is the set of possible disturbances, and $\mathcal{C}$ is the set of allowable output selections.

By best outputs to regulate, we here refer to outputs, whose optimal set points are as insensitive to the disturbance as possible. If we are lucky, we may in some cases be able to find outputs, whose optimal set points are very little affected by disturbances. Of course, insensitivity of optimal set points is by no means the only important issue; there may be others, according to the particular situation. Thus, it is necessary to regard the results of the minimax problem as candidate sets of controlled outputs, and not final answers.

Note that the minimax problem is not necessarily easy to solve. If the set of allowable outputs, $\mathcal{C}$, is discrete, the problem becomes combinatorical. In practice though, if the number of possible outputs is very small, say less than 15, we could simply search through all combinations of outputs; if the number of outputs is larger, but still relatively small, say less than 100, we could use a branch and bound algorithm.

A second possible difficulty, is that even for a fixed $C$, the optimization problem need not be convex. However, if the disturbance set $\mathcal{D}$ is sufficiently small, the loss

function may be approximated by a quadratic function in $r$ and $d$ close to the nominal optimum (for example by Taylor series expansions to second order), and the problem becomes easy.

Even though we may in many cases solve this problem numerically for given disturbance sets, we now turn to simplifications. Such simplifications may yield important insights into the nature of the output selection problem.

## 8.3 Simplified analysis

In this section, we consider a situation where the disturbances are so small that the loss function, eq. 8.5, may be adequately represented by its second order Taylor series expansion around the nominal optimum. We show how to simplify the minimization of the worst case loss, eq. 8.6, in order to faciliate the solution. As a byproduct, one may get some insight into the controlled output selection problem.

Before we present the method, note that the use of Taylor series expansions on this problem has some limitations. We show below that the first order effect of disturbances on the objective function is independent of the output selection when the process is at the optimum. In fact, if it were, we could change the nominal set point and improve the nominal objective (by nominal we refer to the case of no disturbance). Therefore, in order for the output selection to matter from a steady state point of view, the disturbances have to be so large that the effects of second and higher order terms become important. However, as we truncate the Taylor series to second order and study the second order effects, this Taylor series will have a limited range of validity. This means that the second order term—which is what we try to do something about in the simplified analysis—may not always be representative for the higher order effects of finite disturbances. In the light of such limitations, the results of the procedure proposed below should—in specific cases—be analyzed in more detail before they are accepted as final answers.

### First order effect of disturbances

First, we show that when the process is at the optimum, the first order effect of the disturbances on the objective function is independent on the particular choice of controlled outputs.

Consider the objective function, $\Phi_2(u,d)$. When the outputs are regulated, the inputs are determined by the outputs and the disturbances, formally $u = u(y,d)$; that is, we may write:

$$(\frac{\partial \Phi_2}{\partial d})_y = (\frac{\partial \Phi_2}{\partial u})_d (\frac{\partial u}{\partial d})_y + (\frac{\partial \Phi_2}{\partial d})_u \tag{8.7}$$

However, as $(\frac{\partial \Phi_2}{\partial u})_d = 0$ at the optimum, the relation becomes:

$$(\frac{\partial \Phi_2}{\partial d})_y = (\frac{\partial \Phi_2}{\partial d})_u \tag{8.8}$$

Hence, at the optimum, the output selection does not influence the sensitivity, $(\frac{\partial \Phi_2}{\partial d})_y$, of small disturbances on the objective function.

To minimize the effect of disturbances on the optimal set points, we therefore turn to second order effects.

### A Taylor series expansion

We approximate the loss function, $\Psi \equiv \Phi(r, C, d) - \Phi_{opt}(d)$, by a second order Taylor series expansion around the nominal optimum, i.e. for no disturbances and nominally optimal set points. The idea is to make the optimal set point insensitive to the disturbance, such that we do not have to know the actual disturbance in order to use a precomputed set point for the outputs.

By Taylor series expansion of the loss function to second order, we then get for fixed $r$ and $C$:

$$\delta\Psi = \Psi_d \delta d + \frac{1}{2}\delta d^T \Psi_{dd} \delta d \tag{8.9}$$

Note that the first order term, $\Psi_d \delta d$, is zero at the nominally optimal operating point. This follows from the discussion above, where it was shown that the first order effect of disturbances on the objective function at the optimum is independent of the actual choice of controlled outputs. Thus:

$$\delta\Psi = \frac{1}{2}\delta d^T \Psi_{dd} \delta d \tag{8.10}$$

This implies that if the plant is optimized for the nominal conditions ($d = 0$), it is impossible to do anything further about the first order effects of the disturbance, $\delta d$, on the objective function. The first term in the Taylor series that we can do anything about, is the second order term. However, since the disturbance is finite, this need not necessarily imply that this second order effect is small.

In Appendix A, we show how the Hessian matrix, $\Psi_{dd}$, may be computed numerically.

### A possible disturbance set, and the minimization of the worst case loss

In order to minimize the worst case loss, we need to know the set of possible disturbances. A convenient disturbance set from a mathematical point of view, would be the disturbances covered by an ellipsoid:

$$\delta d^T A^{-1} \delta d < 1 \tag{8.11}$$

An other way of writing this, is:

$$||\delta\tilde{d}|| < 1; \quad where \quad \delta\tilde{d} = D^{-1}\delta d \quad and \quad D = A^{1/2} \tag{8.12}$$

Thus, $\tilde{d}$ could be considered a scaled disturbance, and $D$ could be considered a scaling matrix.

With this notation, the loss function becomes:

$$\delta\Psi = \frac{1}{2}\delta\tilde{d}^T (D^T \Psi_{dd} D)\delta\tilde{d} \tag{8.13}$$

**The worst case loss, then becomes** (to second order):

$$worst\_case\_loss = \frac{1}{2}||D^T \Psi_{dd} D|| \tag{8.14}$$

where the norm $||(.)||$ is the largest singular value. Note this expression, as it is an essential part of the controlled output selection procedure that is presented in the next section.

Since the Hessian of the loss function, $\Psi_{dd}$, depends on the output selection, $C$, the best output selection in the sense of minimizing effects of disturbances becomes:

$$C = \arg \min_{C \in \mathcal{C}} ||D^T \Psi_{dd} D|| \tag{8.15}$$

It is shown in Appendix A that the Hessian of the loss function, $\Psi_{dd}$, may be expressed as:

$$\Psi_{dd} = \begin{pmatrix} -(CB)^{-1}(CE) \\ I \end{pmatrix}^T H_1 \begin{pmatrix} -(CB)^{-1}(CE) \\ I \end{pmatrix} - H_{opt} \tag{8.16}$$

where all matrixes except the output selection, $C$, are constant matrixes for a given nominal optimum. The details are contained in the Appendix.

Thus, using this expression, the Hessian of the loss function, $\Psi_{dd}$, may be evaluated very quickly for various output selections, $C$, thus faciliating the solution of the minimization problem.

## 8.4 A procedure for output selection

We are now in a position to formulate a procedure for generating candidate sets of regulated outputs. These candidates may then be analyzed further to see if they are adequate with respect to other criteria that may be present in a given situation. In the procedure, we use the simplified analysis, using the Taylor series expansions. A similar procedure may be deviced in a more rigorous case, although this may become computationally expensive in practical cases.

The procedure is:

1. Define a plant model, $f(x, u, d) = 0$ and an objective function, $\min_u \Phi_1(x, u, d)$. Also, identify possible disturbances, and define a disturbance set, $\mathcal{D}$, defined by the scaling matrix, $D$, in eq. 8.12. Also define a set of candidate outputs, $\mathcal{C}$, for the output selection.

2. Compute the nominal optimum of the model ($d = 0$) using your favorite optimization method.

3. Define a loss function according to eq. 8.5, and streamline a procedure for evaluating the Hessian of this expression, $\Psi_{dd}$, for different output selections, $C$. One way of doing this is presented in Appendix A.

4. Solve the minimization given by eq. 8.15 for the best output selection, $C$. In practice, it may be better to make a list of good $C$'s, say a top ten list. We could then choose from this list according to other criteria that may be important. In practice, there may be many output selections, $C$, that yield a small worst case loss, $\Psi(r, C, d)$.

5. Analyze the candidates to see if they are adequate. This step includes using common sense to eliminate candidates that are unfeasible for reasons not included in the optimization. Such reasons may depend on the particular situation.

## 8.5 An example, CSTR with chemical reaction

To illustrate the procedure, we examine a continuous stirred tank reactor (CSTR). The example is a slightly modified version of the example of Economou *et al.* (1986). Notation and parameter values for the example are listed in Appendix $B$ (taken from Economou *et al.*, 1986).

Consider a CSTR where a reversible reaction $A \rightleftharpoons B$ takes place according to a reaction rate expression on the form:

$$r = k_1 x_A - k_2 x_B; \quad where \quad k_1 \equiv C_1 e^{\frac{-E_1}{RT}} \quad and \quad k_2 \equiv C_2 e^{\frac{-E_2}{RT}} \tag{8.17}$$

The model for the system is taken as:

Reactant mass balance

$$\frac{dx_A}{dt} = \frac{1}{\tau}(z_A - x_A) - r \quad \equiv f_1(x_A, T); \quad \tau = \frac{M}{F} \tag{8.18}$$

Energy balance

$$\frac{dT}{dt} = \frac{1}{\tau}(T_F - T) + \frac{-\Delta H_{rx}}{\rho C_p} r \quad \equiv f_2(x_A, T) \tag{8.19}$$

This model may be written in a more compact form as:

$$\dot{x} = f(x, u, d) \tag{8.20}$$

where $x = [x_A, T]^T$, $u = T_F$ and $d = [z_A, F]^T$ are the states, the manipulated variable and the disturbances, respectively.

### Outputs, manipulators, disturbances and operating objective

The operating objective is to manipulate the inlet temperature, $T_F$, so as to keep the mole fraction of product, $x_B \equiv 1 - x_A$, as high as possible. Hence, we define the objective function:

$$\Phi_1 = -x_B \equiv x_A - 1 \tag{8.21}$$

We assume that we have measurements of the temperature, $T$, and of the product mole fraction (relatively slow measurement).

There may be disturbances in feed mole fraction, $z_A$, (up to 10 % deviation) and in the feed flow rate, $F$, ($\pm 20\%$). Hence, we scale the disturbance vector, $\delta d = [\delta z_A, \delta F]^T$ with the diagonal matrix $D = diag\{0.1, 0.2\}$ (The absolute values of feed mole fraction and flow rate are $z_A = 1$ and $F = 1$).

### Finding the nominal optimum

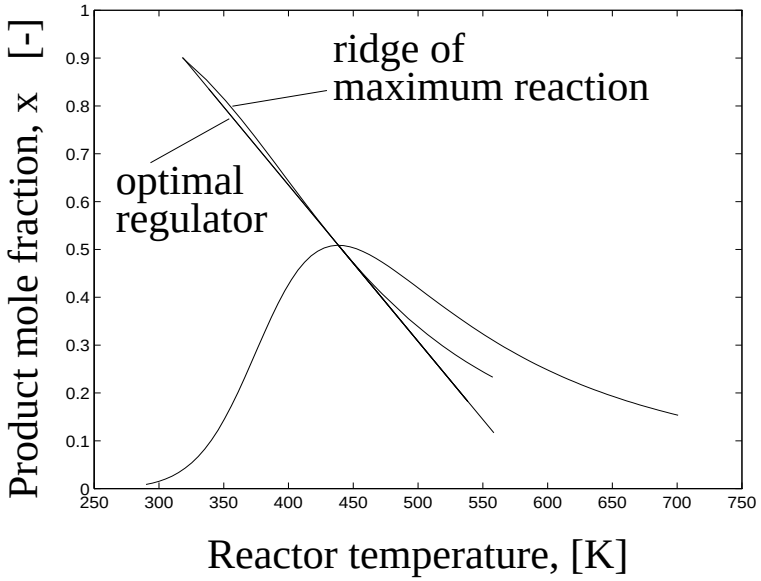


Figure 8.2: Product mole fraction as a function of reactor temperature (bell shape), optimal linear regulator (straight line) and ridge of maximum reaction rate (other curve).

We consider steady state operation.

Calculating the product mole fraction, $x_B$, as a function of reactor temperature for a range of inlet temperatures (when there are no disturbances) yields the bell shaped curve in Fig. 8.2, from which the optimum operating point—the maximum—may be approximately read. This optimum was polished, using Newton-Raphson to solve the first order conditions:

$$L_z = 0 \tag{8.22}$$

where $L = \Phi_1 + \lambda^T f$ is the Lagrangian, and $z \equiv [x^T, u^T, \lambda^T]^T$.

The results of this computation is:

$$x \equiv \begin{pmatrix} x_A \\ T \end{pmatrix} = \begin{pmatrix} 0.49 \\ 438.5 \end{pmatrix}; \quad T_F = 435.9; \quad \lambda = \begin{pmatrix} 9.82 \\ 0 \end{pmatrix} \tag{8.23}$$

which is the nominal optimum.

### Finding outputs to regulate

We are now in a position to illustrate the choice of regulated variables, using minimization of the worst case loss in the objective function. To do this, we compare three candidates for the controlled output:

- Case 1, $C = [1, 0]$. In this case, we regulate the first state variable, which is the mole fraction of reactant.
- Case 2, $C = [0, 1]$. In this case, we regulate the temperature in the reactor.
- Case 3, $C = [cos(\phi), sin(\phi)]$, $\phi \in [0, \pi]$. In this case, we regulate a linear combination of concentration and temperature.

We have performed some computations in order to illustrate how we may discriminate between these cases. For the first two cases, $C = [1, 0]$ and $C = [0, 1]$, we simply evaluated the worst case loss, using equation 8.14. In the third case, $C = [cos(\phi), sin(\phi)]$, we minimized the worst case loss over all angles $\phi$, using equation 8.15. In all cases, the Hessian matrix, $\Psi_{dd}$, was evaluated by the method outlined in Appendix A. The result of this calculation is:

- Case 1, $C = [1, 0]$. $worst\_case\_loss = \infty$
- Case 2, $C = [0, 1]$. $worst\_case\_loss = 0.0022$
- Case 3, $C = [100, -0.33]$. $worst\_case\_loss = 0$

We see that Case 1, where we regulate the concentration, results in an infinite loss in objective **according to the Taylor series approximation**. This is, of course, not very surprising, since the mole fraction of reactant has a minimum at the nominal optimum. It is therefore impossible to regulate this quantity based on a measurement of the mole fraction alone (from a linear point of view).

We see that there is a combination of the measurements, Case 3, that yields a zero value for the worst case loss. This means that the set point of this combination is in fact independent of the disturbances (from a steady state point of view). The situation is shown in Fig. 8.2, where the line $\delta y \equiv C\delta x = 0$ is shown (marked "optimal regulator"). Keeping the output, $y = Cx$, at its optimal set point, corresponds to keeping the system at this straight line. Also plotted is the curve of maximum reaction rate, $\frac{\partial r}{\partial T}|_{x_A} = 0$. Not surprisingly, the two curves turn out to be tangential at the optimum.

However, we see that in Case 2, where the temperature is regulated, the worst case loss in product mole fraction compared to the optimal strategy is only $\Delta x_B = 0.0022$,

under the disturbance set that was postulated (10 % uncertainty in reactant mole fraction, 20 % in feed flow rate). Since this is negligible, we would probably choose this option in practice, even though the combination of measurements, Case 3, had a lower loss.

Fig. 8.3 shows the loss in objective for the different cases when there are **large** disturbances in feed mole fraction of reactant, $z_A$. As can be seen, Case 3, where a combination of states is kept at set point, is near optimal for any feed mole fraction. The largest deviation from optimum occurs at $z_A \approx 0.3$ and is less than $\Delta x_B = 0.001$, which is negligible. That this strategy performs that well for large disturbances, must be considered coincidental, since the strategy was derived from local properties near the optimum. Also plotted in the figure is Case 2, where the reactor temperature is kept constant, and an open loop policy, where the feed temperature is kept constant. In both cases, the loss in objective is relatively small for any reasonable disturbance in feed mole fraction of reactant.

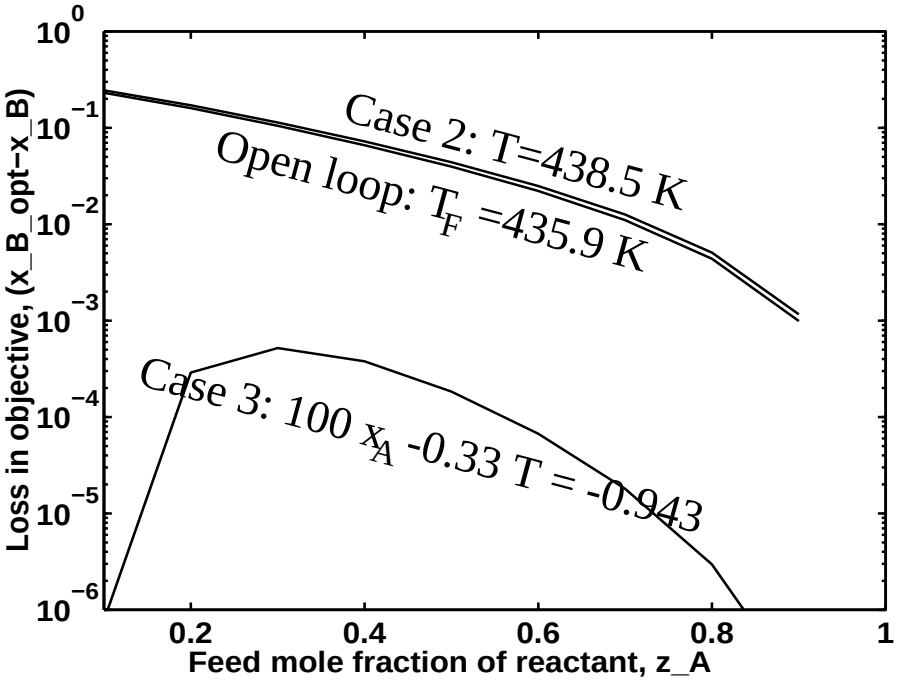


Figure 8.3: Loss in product mole fraction as a function of feed mole fraction of reactant, $z_A$.

## 8.6 Connection to dynamic optimization

It is instructive to analyze the same reactor example (section 8.5) from a dynamic point of view. We demonstrate that keeping the combination of measurements in Case 3 above at its optimal value, is in fact an optimal strategy also in the dynamic case (for small deviations from the optimum).

We assume that the states are close to optimum, but that they have not reached it yet. When there are no disturbances, the dynamic counterpart of the optimization problem presented above is:

$$\min_{u(t)} \int_0^\infty \Phi(x,u)dt \tag{8.24}$$

s.t.:

$$\dot{x} = f(x,u) \tag{8.25}$$

where $\Phi = -x_B$ is the product mole fraction as before, and $\dot{x} = f$ is the CSTR model above.

Close to the nominal optimum, we may approximate this by the LQ problem (see Bryson and Ho, 1969):

$$\min_{u(t)} \int_0^\infty \begin{pmatrix} \delta x^T & \delta u^T \end{pmatrix} M \begin{pmatrix} \delta x \\ \delta u \end{pmatrix} dt \tag{8.26}$$

s.t.

$$\dot{\delta} x = f_x \delta x + f_u \delta u \tag{8.27}$$

Here $M \equiv \begin{pmatrix} L_{xx} & L_{xu} \\ L_{ux} & L_{uu} \end{pmatrix}$ is the Hessian of the Lagrangian $L = \Phi + \lambda^T f$, which is the same Lagrangian as in the steady state case before. Evaluation of this Hessian at the nominal optimum calculated before yields:

$$\begin{pmatrix} L_{xx} & L_{xu} \\ L_{ux} & L_{uu} \end{pmatrix} = \begin{pmatrix} 0 & -0.0262 & 0 \\ -0.0262 & 0.0001 & 0 \\ 0 & 0 & 0 \end{pmatrix} \tag{8.28}$$

Inserting this into the objective function and adding a small penalty on the manipulated input yields:

$$\min_{u(t)} \int_0^\infty \left( \delta x^T Q \delta x + \epsilon \cdot \delta u^2 \right) dt \tag{8.29}$$

where $Q = L_{xx} = \begin{pmatrix} 0 & -0.0262 \\ -0.0262 & 0.0001 \end{pmatrix}$. Note that this matrix violates the common sufficient criterion for stability, $Q \geq 0$, which means that special care must be taken to verify stability of the optimal feedback solution of the problem.

Evaluating the optimal feedback gain, $\delta u = -K\delta x$ for a very small penalty on the states, $\epsilon = e^{-10}$, yields the feedback gain (using MATLAB):

$$K = lqr(f_x, f_u, Q, \epsilon) = -2810 \cdot \begin{pmatrix} 100 & -0.33 \end{pmatrix} \tag{8.30}$$

Thus, there is an enormous negative feedback gain in the state direction $C = \begin{pmatrix} 100 & -0.33 \end{pmatrix}$ (In fact, $\epsilon \to 0 \quad \Rightarrow \quad ||K|| \to \infty$). This means that this feedback very quickly pulls the state vector onto the line, $C\delta x \equiv \begin{pmatrix} 100 & -0.33 \end{pmatrix} \delta x = 0$—a singular arc. After that, the system slides slowly down to the nominal optimum along this line, $C\delta x = 0$. Note that this is the same line as predicted from the steady state analysis (Case 3 above). Hence, in this particular case, the dynamic analysis yields the same result as the steady state analysis. Of course, this need not be the case in general.

## 8.7 Discussion

In the steady state analysis above, we based the selection of controlled outputs solely on the basis of insensitivity of the optimal set points to external disturbances. However, as was mentioned in the introduction, this is not the only issue. We would also like the optimum to be flat, as seen from the optimizing control level, and robust with respect to measurement failure—that is, we would like to choose reliable measurements, that are not failure prone, and that give reliable information about the optimization objective. Moreover, that the set points of the controlled outputs are insensitive to disturbances from a steady state point of view, does not necessarily mean that regulating these outputs yields good regulation from a dynamic point of view. Thus, we need to take such issues into account.

One way of dealing with such issues, could be to use the criterion discussed in this paper to generate a list of possibly good candidate sets of regulated outputs, as opposed to just calculating one single best set. The output sets on this list could then be evaluated by the other criteria, and the best one selected.

Above, we demonstrated that at the nominal optimum, the output selection only affects second and higher order terms in the Taylor series expansion of the objective function. Because of this, one might expect that the loss in objective, $\Psi$, will often be very small for many of the output selections, although there may be some bad selections. Indeed, this was the case in the CSTR example presented above, where choosing temperature as regulated output was almost as good as the optimal strategy from a steady state sensitivity to disturbances point of view. For larger disturbances, the second order Taylor series expansion may not necessarily be an adequate representation of the real loss function around the nominal optimum. However, in many cases one would expect that the removal or suppression of the second order term in the series will often reduce the sensitivity to large disturbances as well.

## 8.8 Conclusion

In this paper, we have considered the problem of selecting regulated outputs at the regulatory control level. The basic idea is choose outputs, whose optimal set points are insensitive to persisting disturbances at steady state. If we can find such outputs, we do not need to know the disturbances in order to choose the optimal set points for the outputs.

Mathematically, the problem becomes a minimax problem, where the outputs are selected so as to minimize the worst case deterioration in performance by not taking disturbances into account. This problem is nonlinear, but may in many cases be solved numerically. However, in order to simplify the problem, and to gain some insight into the output selection, the problem was approximated by second order Taylor series expansions around the nominal optimum. With these approximations, the problem becomes much easier.

The solutions from the minimax problem ought to be considered as candidate sets of controlled outputs, and not final answers. First, the analysis is based on a steady

state analysis. Therefore, the candidates must be analyzed with respect to dynamic performance. Second, if the Taylor series approximation is used, it should be verified that the candidates produced are adequate. The second order Taylor series expansion has a limited range of validity, and if the second order terms are important, one may in specific cases suspect that third- and higher order effects are also in action. However, one might expect that the removal—or suppression—of second order terms may often significantly reduce the sensitivity of the optimal set points to disturbances.

# References

[1] Arkun, Y. and G. Stephanopoulos, 1980. Studies in the synthesis of control structures for chemical processes, Part IV. AIChE J., 26, 6, 975-991

[2] Arkun, Y. and G. Stephanopoulos, 1981. Studies in the synthesis of control structures for chemical processes, Part V. AIChE J., 27, 5, 779-793

[3] Bahri, P.A Bandoni, J.A Barton and G.W.Romagnoli, 1994. Disturbance Economics In Optimising Control: Back-off Calculations for an Industrial Distillation Column. PSE'94, Korea, 1994.

[4] Bryson, A.E. and Y.C. Ho, 1969. Applied optimal control. Waltham, Mass: Blaisdel Publ. Co., 1969

[5] Economou, C., M. Morari and B.O. Palsson, 1986. Internal model control 5. Extensions to nonlinear systems. Ind. Eng. Proc. Dev., 25, 2, 403-411

[6] Ganguly, S. and D.N. Saraf, 1992. On-line optimization: a hierarchical scheme for distillation column control. Chem Eng Proc, 31, 337-347

[7] Kim, Y.H., T.W. Ham and J.B. Kim, 1991. On-line dynamic optimizing control of a binary distillation column. J. Chem Eng of Japan, 24, 1, 51-57

[8] Maarleveld, A. and J.E. Rijnsdorp, 1970. Constraint control of distillation columns. Automatica, 6, 51-58

[9] Morari, M., Y. Arkun, and G. Stephanopoulos, 1980a. Studies in the synthesis of control structures for chemical processes, Part I. AIChE J., 26, 2, 220-232

[10] Morari, M. and G. Stephanopoulos, 1980b. Structural aspects and the synthesis of alternative feasible control schemes, Part II. AIChE J., 26, 2, 232-246

[11] Stengel, R.F., 1994. Optimal Control and Estimation. New York: Dover Publications, ISBN 0-486-68200-5

[12] Sunarto, N., J.A. Bandoni, G.W. Barton and J.A. Romagnoli, 1994. On optimizing control and the effects of disturbances: Application to an industrial gas-tail system. ESCAPE 4, Dublin, 1994.

[13] Tyreus, B.D., 1987. Optimization and multivariable control of distillation columns. Adv. Instrum., 42, 25-44

## Nomenclature

| | |
|---|---|
| $A$ | matrix defining disturbance set |
| $B$ | matrix in linearized process model (Appendix A) |
| $C$ | measurement matrix ($y = Cx$) |
| $C_p$ | heat capacity in example |
| $E$ | matrix in linearized process model (Appendix A) |
| $F$ | feed flow rate |
| $d$ | disturbance vector |
| $\check{d}$ | scaled disturbance vector |
| $D$ | scaling matrix for disturbance vector |
| $f(x,u,d)$ | state space model for the process |
| $H$ | Hessian matrix (Appendix A) |
| $-\Delta H_{rx}$ | heat of reaction in example |
| $I$ | identity matrix |
| $K$ | feedback gain for dynamic optimization |
| $L$ | Lagrangean function |
| $M$ | weight matrix for dynamic optimization; or molar holdup in example |
| $Q$ | weight matrix for states |
| $r$ | reference value for states; or reaction rate in example |
| $T$ | temperature in example |
| $u$ | manipulated variables |
| $x$ | state vector |
| $x_A$ | mole fraction of component $A$ in example |
| $x_B$ | mole fraction of component $B$ in example |
| $y$ | measured outputs |
| $z$ | $= [x^T, u^T, \lambda^T]^T$, augmented vector for use in optimization |
| $z_A$ | feed mole fraction of component $A$ (in example) |

Greek

| | |
|---|---|
| $\epsilon$ | weight on manipulated variable |
| $\Phi$ | objective which is to be minimized |
| $\lambda$ | Lagrange multiplier |
| $\Psi$ | loss in objective compared to the optimum |
| $\rho$ | density in the example |
| $\tau$ | residence time in the example |

Calligraphic

| | |
|---|---|
| $\mathcal{C}$ | represents set of allowable outputs |
| $\mathcal{D}$ | set of possible disturbances |
| $\mathcal{R}$ | set of allowable set points |

Subscripts

| | |
|---|---|
| $1, 2, 3$ | index indicating arguments of objective function |
| *opt* | indicates optimal value |
| $F$ | feed condition in the example |

# Appendix A. Derivation of Taylor series expansion of the loss function

The purpose of this Appendix is to derive an expression for the Hessian of the loss function, $\Psi_{dd}$ in eq. 8.9, at the nominal optimum. For convenience, we repeat the equation for the loss function:

$$\Psi(r, C, d) = \Phi(r, C, d) - \Phi_{opt}(d) \tag{8.31}$$

There are at least two ways of computing the Hessian of this expression. The first, and simplest, is a brute force approach, where the function is differentiated numerically by perturbing the disturbance, $d$, element for element in an outer loop, and evaluating the loss function in an inner loop. This evaluation in the inner loop is straightforward: The first term, $\Phi(r, C, d)$ is simply evaluated without changing the set points; the other term, $\Phi_{opt}(d)$, is evaluated by reoptimizing the plant for the perturbed disturbance.

For completeness, we derive an alternative approach. The advantage with this approach, is that it is only necessary to perform numerical differentiations at the nominal optimum once. After having done that, we may evaluate the Hessian of the loss function for as many output selections, $C$, as we like. The result of the derivation is given by eq. 8.46.

Below, we linearize the process model; derive a relation between the manipulated inputs and the disturbance when the outputs are kept at set points; derive an equation to be used for elimination of states and manipulated inputs; describe a method for finding the nominal optimum; then, finally we derive an expression for the Hessian of the loss function, combining the results of all the other derivations.

### Linearization of the objective function

The objective function, $f(x, u, d) = 0$ may be linearized around the nominal optimum to get:

$$\delta x = B\delta u + E\delta d; \quad where \quad B \equiv -f_x^{-1} f_u; \quad E \equiv -f_x^{-1} f_d \tag{8.32}$$

### A first order condition for the inputs

The controlled outputs, $y = Cx$, are supposed to be kept at fixed set points, $r$; thus:

$$C\delta x = 0 \tag{8.33}$$

Substituting the linearized process model above, we get:

$$\delta u = (-CB)^{-1}(CE)\delta d \tag{8.34}$$

### A relation for elimination of $u$ and $x$

Using the two equations 8.32 and 8.34 we may write:

$$\begin{pmatrix} \delta x \\ \delta u \\ \delta d \end{pmatrix} = M_C \delta d; \quad where \quad M_C = \begin{pmatrix} E - B(CB)^{-1}(CE) \\ -(CB)^{-1}(CE) \\ I \end{pmatrix} \tag{8.35}$$

where $I$ is an identity matrix. Thus, using this equation, we may eliminate the states and the manipulated inputs from any equation to first order in $\delta d$. The subscript $C$ on $M_C$ is placed there as a reminder that the selection of controlled outputs is contained in the matrix.

Note that $M_C$ may be factorized into:

$$M_C = \begin{pmatrix} B & E \\ I & 0 \\ 0 & I \end{pmatrix} \begin{pmatrix} -(CB)^{-1}(CE) \\ I \end{pmatrix} \tag{8.36}$$

This factorization is needed below.

### Finding the nominal optimum

The problem of finding the nominal optimum is:

$$\min_u \{\Phi_1(x,u,d)\} \quad s.t. \quad f(x,u,d) = 0 \tag{8.37}$$

To solve this, one may form a Lagrangian function:

$$L \equiv \Phi_1 + \lambda^T f \tag{8.38}$$

and solve the first order conditions:

$$L_x = 0; \quad L_u = 0 \quad L_\lambda = 0 \tag{8.39}$$

The solution of these equations yields an extremal point, which may be checked to see if it is a minimum.

### Expanding the loss function in a Taylor series

To find a Taylor series expansion for $\Phi_1$, we expand both $\Phi_1$ and $f$ in Taylor series to second order:

$$\delta\Phi_1 \approx \Phi_{1x}\delta x + \Phi_{1u}\delta u + \Phi_{1d}\delta d + \frac{1}{2}\begin{pmatrix} \delta x^T & \delta u^T & \delta d^T \end{pmatrix} H_{\Phi 1} \begin{pmatrix} \delta x \\ \delta u \\ \delta d \end{pmatrix} \tag{8.40}$$

$$0 = \delta f \approx f_x \delta x + f_u \delta u + f_d \delta d + \frac{1}{2}\begin{pmatrix} \delta x^T & \delta u^T & \delta d^T \end{pmatrix} H_f \begin{pmatrix} \delta x \\ \delta u \\ \delta d \end{pmatrix} \tag{8.41}$$

Multiplying the second equation by $\lambda^T$ and adding the first, we get:

$$\delta\Phi_1 \approx L_x\delta x + L_u\delta u + L_d\delta d + \frac{1}{2}\begin{pmatrix} \delta x^T & \delta u^T & \delta d^T \end{pmatrix} H_L \begin{pmatrix} \delta x \\ \delta u \\ \delta d \end{pmatrix} \tag{8.42}$$

where $L = \Phi_1 + \lambda^T f$ as before.

In these equations, $H_{\Phi 1}$, $H_f$ and $H_L$ are the Hessians of $\Phi_1$, $f$ and $L$ with respect to $[\delta x^T, \delta u^T, \delta d^T]^T$.

Now, $L_x$ and $L_u$ are zero at the nominal optimum (first order conditions), hence the expansion may be written:

$$\delta\Phi_1 = L_d\delta d + \frac{1}{2}\begin{pmatrix} \delta x^T & \delta u^T & \delta d^T \end{pmatrix} H_L \begin{pmatrix} \delta x \\ \delta u \\ \delta d \end{pmatrix} \tag{8.43}$$

Note that this equation, which is a second order accurate representation of the objective function around the optimum, contains the Hessian of **the Lagrangian**, $L = \Phi + \lambda^T f$. A common mistake, which was done by Morari *et al.* (1980a) and in the book by Stengel, 1994, is to combine a second order accurate representation of the objective function, $\Phi$, with a first order accurate representation of the process model, $f$. The result of this combination is **not** second order accurate.

Eliminating the states, using eq. 8.35, we get:

$$\delta\Phi_1 = L_d\delta d + \frac{1}{2}\delta d^T(M_C^T H_L M_C)\delta d \tag{8.44}$$

Since this equation only contains $d$, and is a second order accurate representation of the objective function, it has to be equal to the Taylor series expansion of $\Phi(r_{nom}, C, d)$ for fixed $r$ at the nominal optimum, and for a fixed $C$ (uniqueness of Taylor series). Hence, the Hessian of the loss function, eq. 8.31, may be written:

$$\Psi_{dd} = M_C^T H_L M_C - H_{opt} \tag{8.45}$$

which is what we were looking for. Here, $M_C$ is given by eq. 8.35, and $H_{opt}$ is the Hessian of $\Phi_{opt}(d)$ at the nominal optimum. It is possible to derive an expression for this Hessian too, but as it does not depend on the selection of controlled outputs, $C$, we might as well evaluate it numerically.

It is possible to streamline the expression further. Inserting the factorized expression for $M_C$, we get:

$$\Psi_{dd} = \begin{pmatrix} -(CB)^{-1}(CE) \\ I \end{pmatrix}^T H_1 \begin{pmatrix} -(CB)^{-1}(CE) \\ I \end{pmatrix} - H_{opt} \tag{8.46}$$

where:

$$H_1 \equiv N^T H_L N; \quad N \equiv \begin{pmatrix} B & E \\ I & 0 \\ 0 & I \end{pmatrix} \tag{8.47}$$

Using this equation, we may quickly evaluate the Hessian of the loss function, $\Psi_{dd}$, for various output selections, $C$.

# Appendix B. Data for the example.

The data for the example are taken from Economou *et al.*, 1986.

| | |
|---|---|
| $C_1$ | 5000 $L^{-1}s^{-1}$ |
| $C_2$ | $10^6$ $L^{-1}s^{-1}$ |
| $C_p$ | 1000 $cal/kg.K$ |
| $E_1$ | $10^4$ $cal/mole$ |
| $E_2$ | 15000 $cal/mole$ |
| $F$ | 1 $holdup/min$ |
| $R$ | 1.987 $cal/mole.K$ |
| $T_F$ | manipulated var. |
| $z_A$ | 1 |
| | |
| $-\Delta H_{rx}$ | 5000 $cal/mole$ |
| $\rho$ | 1 $kg/L$ |
| $\tau$ | 1 $min$ |

# Chapter 9

# Postscript

## 9.1 Discussion

This thesis has dealt with aspects of the dynamics and operation of integrated chemical process plants. The prime motivation has been a need for understanding how tight couplings between individual process units affect the dynamic and steady state behavior of the overall plant. Such understanding may be valuable, for instant, when designing control systems for integrated plants—or, for instant, when designing plants that are easy to control and operate.

The topics in the thesis range from general considerations of the effects of couplings between process units on plant behavior to the study of specific case studies where such effects are in actions. Examples of such effects are that:

1. An interconnected system of process units may be unstable even though the individual process units are stable by themselves (and *vice versa*).

2. Couplings between process units may introduce new steady states (stable or unstable) even though the individual process units have unique steady states by themselves.

3. Tight integration may make the plant difficult to control.

It is felt that general considerations, which necessarily are rather simplistic in nature, ought to be supported by case studies. Such case studies are more realistic and yield important inputs to the general investigations. The thesis contains two case studies, chapter 6, which deals with the stability of an ammonia synthesis reactor; and chapter 7, which deals with multiple steady states in Petlyuk columns.

Obviously, the results presented in the thesis is not meant to cover every aspect of plant operation and dynamics; the scope of the thesis is restricted. For example, effects of various constraints on plant operation are not considered. Such constraints may in many cases be important, and often need to be taken into account.

Moreover, plants are in general nonlinear. In the thesis, nonlinearities are only taken into account in simulations—not in the analysis. The reason for this is partly pragmatic; we need analysis tools that are conceptually simple, and which can be grasped by the mind. Existing theory for nonlinear systems is complex, and is in practice only practical with the aid of a computer. Of course, some phenomena, such as limit cycles and chaos, are inherently nonlinear, and cannot be understood in terms of linear theory alone, although local linear analysis play an important role in the analysis of nonlinear behavior as well. For instant, the stability of a limit cycle may be analyzed by studying eigenvalues of a linearized Poincaré map.

## 9.2 Conclusions

The main contributions of this thesis are summarized in the points below:

**Chapter 2** discusses the effects of couplings between process units on the dynamic behavior of the overall plant. The idea, which is inspired by Gilliland *et al.* (1964), is to use basic concepts from Linear Systems Theory to shed some light on the dynamic behavior of the plant. Such concepts are, for example, feedback and parallel paths. For linear(ized) systems, feedback changes pole locations and may affect plant stability, whereas parallel paths affect the zero locations and may affect plant controllability. Examples of such feedback and parallel paths are given, such as feed-effluent preheating of a reactor, recycle of unreacted feed etc.

**Chapter 3** . Whereas chapter 2 treats the dynamic behavior of the overall plant, chapter 3 has its focus at individual process units. As in the former chapter, concepts such as feedback and parallel paths are used to shed some light on the dynamic behavior of such process units. However, whereas the interconnections in the former chapter reflect the interconnection structure of the flow sheet, the "interconnections" in this chapter are more loosely defined, and refer to the mathematical structure of the state space model describing the system.

A simple continuous stirred tank reactor (CSTR) is analyzed in detail. Using the linear theory, the effects of various physical phenomena on the stability of the CSTR is investigated. Such physical phenomena include chemical reactions; material recycle; and feed-effluent preheating.

**Chapter 4** treats a special type of interconnected systems, namely cascade interconnections of similar subsystems. Typical examples of such cascades would be the countercurrent separation processes, such as distillation.

By means of Laplace transform techniques, it is shown how the simplest type of cascade systems, scalar cascades of identical subsystems, may be analyzed analytically. The poles of such simple cascades are located at a root locus defined in terms of the subsystem transfer functions. Thus, for simple cascades it is easy to find these pole locations analytically, and thus the dynamic behavior.

It is then shown that interconnection of two such cascade sections may result in very long time constants. Such long time constants have been observed, for example, in high purity distillation columns.

**Chapter 5** . In this chapter, the concentration dynamics of binary distillation columns is considered. A simple model of such a column is analyzed by analogy to plug flow with diffusion in a pipe. By numerical experiments, it is found that the slow time constant of the column increases exponentially with the number of stages (for constant flow rates, feed conditions etc). Using concepts from the analogy, a qualitative description of the column behavior is given.

**Chapter 6** treats a case in more detail. The starting point for the study was an incident in an industrial ammonia synthesis plant in Germany. A fixed bed autothermal ammonia synthesis reactor became unstable, such that the reactor temperature oscillated with large amplitudes (appr. $\pm 160^{o}C$).

The onset of the phenomenon may be analyzed by means of Linear Systems Theory. Using concepts from chapter 2, such as feedback and parallel paths, it is shown how "internal" parallel paths through the reactor beds results in Right Half Plane zeros, and that the feedback from the feed-effluent preheater makes a pair of complex conjugate poles unstable (i.e. in the Right Half Plane). The parallel paths are caused by the combination of two effects in the reactor beds: a disturbance at the bed inlet affects the bed outlet both through the energy balance (migration of temperature waves) and through the mass balance (convection of chemical species). These effects are competing, resulting in inverse response behavior. This inverse response in the time domain, is found in the frequency domain as a peak at very large phase lags, extending well beyond a phase lag of $360^{o}C$. Due to this peak in the frequency response, the feedback from the feed-effluent preheater makes the reactor unstable for some operating conditions.

**Chapter 7** treats another case, this time at steady state. An integrated three-product distillation column known as a Petlyuk column is examined. As shown by Wolff *et al.* (1994), such columns have a rather strange steady state behavior when four outlet compositions are specified. The column may then have multiple steady states at some operating conditions; none at other operating conditions. In the chapter, an explanation to this sort of behavior is given in geometrical terms, supported by numerical computations.

By means of an arclength continuation method, all solutions were computed for a case with three outlet concentrations specified. The result of this computation is geometrical surfaces, whose shape may be explained by physical reasoning. Using these surfaces, the effects of adding or changing a fourth outlet specification is explained. The strange steady state behavior is thus visualized in terms of these surfaces.

**Chapter 8** discusses a problem related to optimizing control of process plants. Such optimizing control systems are often built in a hierarchical manner, with regula-

tory control at the lowest level, and an optimizing control level at the top. In the chapter, the discussion is restricted to the subproblem of choosing which outputs to regulate at the regulatory control level.

Even with this restriction, the problem is still multifacetted; there are a number of aspects to be taken into account, such as dynamic performance/disturbance sensitivity of the system when the selected outputs are regulated. In the chapter, the scope is further restricted to discussing how one may choose controlled outputs, whose optimal set points are as insensitive as possible to disturbances at steady state.

The advantage of choosing outputs in this manner, is that one does not need to know the exact disturbance in order to choose the set points of the controlled outputs. However, as steady state disturbance sensitivity is by no means the only important issue, it is suggested, not to compute a single optimal set of outputs, but rather to make a list of good candidate sets of controlled outputs. By "optimal" and "good" we here refer to the criterion mentioned above—insensitive set points. Having made such a list, one may then choose a set from the list based on other criteria, such as dynamic behavior of the regulated system.

In the chapter, it is shown how the problem of finding controlled outputs, whose optimal set points are insensitive to disturbances at steady state, may be formulated as a minimax problem. It is shown how the analysis may be simplified by means of Taylor series expansions.

## 9.3 Directions for future work

Aspects related to the dynamics and operation of integrated plants have been treated in this thesis. However, as this is a vast subject, one thesis may only scratch the surface of what needs to be done. The following topics could be investigated further:

1. **The dynamics of integrated plants**. In the thesis, Linear Systems Theory was used in order to shed some light on the effects of plant interconnections on the dynamic behavior and controllability of the plant. However, in order to obtain some results, it was necessary to omit certain aspects that are often important, such as constraints and nonlinearities. It is suggested that these aspects be included in future work. It is not obvious how this could be done, but it seems futile to introduce all aspects at once. Rather, it seems reasonable to study restricted classes where such aspects are included. For example, one may study how a particular class of plant constraints, when combined with feedback and parallel paths, affect plant controllability. By "controllability", it is here referred to controllability in a loose sense, i.e. whether the plant is easy or difficult to control.

2. **On-line energy minimization of Petlyuk columns**. Even though Petlyuk columns may save approximately 30% energy compared to conventional arrangements when it is operated properly, it is easy to imagine that it is also possible

to waste enormous amounts of energy in poor operation. Whereas it is straightforward to optimize the energy consumption of a model of such a column, it is not obvious how to perform this optimization on-line, when there is plant-model mismatch, noisy measurements, and impresise actuators.

However, one may hope that there exist certain combinations of outputs that could be kept at set points, such that the optimal values of these set points are relatively insensitive to disturbances at steady state. If, in addition, such outputs could be found, that are adequate also from a dynamic point of view, one could consider half the problem to be solved. In a particular situation, we would also need to find the actual optimal set points. However, one may expect a search for such optimal set points to be possible, as the optimal set points at steady state do not move too much when there are disturbances.

It is suggested that such combinations of outputs may be searched for along the lines of chapter 8.

## 9.4 Final comments

Many aspects of dynamics and multiplicity of chemical engineering systems seem to be related to the structure of the system in question. For example, feedback in nonlinear systems seems to yield multiple steady states in many cases, especially when the output of the open loop system has a maximum or minimum steady state value.

To give a daily life example, consider throwing a ball towards a target. Throwing a ball is a typical example of a system with a maximum; we are only able to throw the ball a certain distance. This maximum distance—considered to be an output—occurs when the angle of departure—the input—has a certain value (near $45^o$). Thus, according to what has been said above, we expect to get multiple solutions when there is feedback. Such feedback could in this case be, for example, to specify a target to hit. That is, we specify the output—the distance to throw. Indeed, in this particular case there are two different angles of departure that makes us hit the target when the target is within our range—none, if the target is out of range. Thus, there exist multiple solutions.

Competing effects in a system may often yield such extrema (maxima, minima, saddle points). A particular case is the Petlyuk column studied in chapter 7, where competing effects between column sections caused the output to lie on a saddle shaped surface; that is, the output has an extremum (the saddle point). Specifying outputs (feedback) resulted in this case to multiple or no steady state solutions, depending on the particular specification.

Considered in connection with what has been written in chapter 2 about the effects of parallel paths (competing effects) and feedback on dynamic behavior, one might conjecture that it ought to be possible to combine this with the steady state multiplicity considerations above in order to formulate a general theory of integrated plants. Formulating such a theory may not be particularly easy, and it is suggested that this be a long term goal of future research.

# References

[1] Gilliland, E.R., Gould, L.A. and Boyle, T.J., 1964. Dynamic effects of material recycle. Preprints JACC, Stanford, California pp 140-146.

[2] Wolff, E.A., S. Skogestad and K. Havre, 1994, "Dynamics and Control of Integrated Three-product (Petlyuk) Distillation Columns". ESCAPE'4, Dublin, March 28-30, 1994.